INSTITUTO SUPERIOR DE ENGENHARIA DO PORTO
MESTRADO EM ENGENHARIA ELECTROTÉCNICA E DE COMPUTADORES



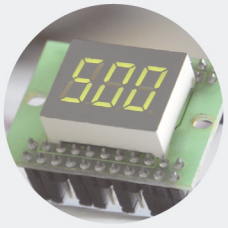


# Resource Management System for Optimizing Production Efficiency in the Wine Sector

**RODRIGO MANUEL PEREIRA BRANQUINHO**
Setembro de 2024

POLITÉCNICO
DO PORTO

Politécnico do Porto
Instituto Superior de Engenharia do Porto

# Resource Management System for Optimizing Production Efficiency in the Wine Sector

**Rodrigo Manuel Pereira Branquinho**

Master in Electrical and Computer Engineering
Specialization Area of Autonomous Systems

ISEP INSTITUTO SUPERIOR DE ENGENHARIA DO PORTO

Departamento de Engenharia Eletrotécnica
Instituto Superior de Engenharia do Porto

September, 2024

*This dissertation partially satisfies the requirements of the Thesis/Dissertation course of the program Master in Electrical and Computer Engineering, Specialization Area of Autonomous Systems.*

**Candidate:** Rodrigo Manuel Pereira Branquinho, No. 1181153, 1181153@isep.ipp.pt

**Scientific Guidance:** Sérgio Filipe Carvalho Ramos, scr@isep.ipp.pt

**Scientific Co-Guidance:** Tiago Campelos Ferreira Pinto, tiagopinto@utad.pt

**Scientific Co-Guidance:** Ana Cristina Briga de Sá, anas@utad.pt

ISEP INSTITUTO SUPERIOR DE ENGENHARIA DO PORTO

Departamento de Engenharia Eletrotécnica
Instituto Superior de Engenharia do Porto
Rua Dr. António Bernardino de Almeida, 431, 4200–072 Porto

September, 2024

*"It always seems impossible until it's done." - Nelson Mandela*

# Abstract

Being agriculture an essential activity sector for the survival and prosperity of humanity, it is fundamental to use sustainable technologies in this field. With this in mind, statistical data is analyzed regarding the food price rise and sustainable development indicators. It is determined that one of the main factors that influences agriculture's success is the soil's characteristics, namely in terms of moisture and nutrients. In this regard, irrigation processes have become indispensable, and their technological management brings countless economic advantages. Like other branches of agriculture, the wine sector needs an adequate concentration of nutrients and moisture in the soil to provide the most efficient results. Given these facts, the use of renewable energies is an important aspect of this study, which also synthesizes the main irrigation methods and examines the importance of evaluating the evapotranspiration of crops. Furthermore, the control of irrigation processes and the implementation of resource management models are of utmost importance to allow maximum efficiency and sustainability in this field.

However, there is a lack of a resource management model that maximizes production efficiency with the largest number of compatible technologies. Therefore, a modular intelligent system is developed, which utilizes data obtained from multiple sources, such as weather conditions, renewable energy and electricity markets. Divided into four key modules, the first module embraces data diversity as an important factor, so the system can adapt to multiple inputs and user definitions. The second module is responsible for determining vineyard water losses through evapotranspiration, and the third one calculates the water requirements for irrigation purposes. The last module uses a supervised machine learning algorithm to achieve optimal energy consumption information. To validate and analyse the model performance, multiple results are provided, considering various realistic scenarios. By adapting the system to a specific vineyard, vital data is acquired and farms can make informed decisions, specially regarding energy and water resources. With a good design and positive results, the system enables a boost in the environmental sustainability of the wine sector operations and enhances productivity of vineyards.

**Keywords**: data processing, evapotranspiration, renewable energies, resource optimization, smart irrigation, sustainable agriculture, vineyard management.

# Resumo

Sendo a agricultura um setor de atividade essencial para a sobrevivência e prosperidade da humanidade, é fundamental a utilização de tecnologias sustentáveis neste campo. Neste sentido, são analisados dados estatísticos sobre o aumento do preço dos alimentos e indicadores de desenvolvimento sustentável. Verifica-se que um dos fatores que influencia o sucesso da agricultura são as caraterísticas do solo, nomeadamente em termos de humidade e nutrientes. Neste sentido, os processos de rega tornaram-se indispensáveis, e a sua gestão tecnológica traz inúmeras vantagens económicas. Tal como outros ramos da agricultura, o sector vitivinícola precisa de uma concentração adequada de nutrientes e humidade no solo para obter resultados mais eficientes. Perante estes factos, a utilização de energias renováveis é um aspeto importante deste estudo, que também sintetiza os principais métodos de rega e analisa a importância da evapotranspiração das plantações. Além disso, o controlo dos processos de rega e a implementação de modelos de gestão de recursos são de extrema importância para permitir a máxima eficiência e sustentabilidade neste campo.

No entanto, não existe um modelo de gestão de recursos que maximize a eficiência da produção com o maior número de tecnologias compatíveis. Assim, é desenvolvido um sistema modular inteligente, que utiliza dados de múltiplas fontes, tais como condições meteorológicas, energias renováveis e mercados de eletricidade. Dividido em quatro módulos, o primeiro considera a diversidade de dados como um fator importante, para que o sistema se possa adaptar a múltiplas entradas e definições. O segundo módulo é responsável por determinar as perdas de água da vinha através da evapotranspiração, e o terceiro calcula as necessidades de água para efeitos de rega. O último módulo utiliza um algoritmo supervisionado para obter informações ótimas sobre o consumo de energia. Para validar e analisar o desempenho do modelo, são fornecidos vários resultados, considerando vários cenários realistas. Ao adaptar o sistema a uma vinha específica, são obtidos dados vitais que permitem tomar decisões informadas, especialmente no que respeita aos recursos energéticos e hídricos. Com um bom *design* e resultados positivos, o sistema permite um aumento da sustentabilidade do setor vitivinícola e melhora a produtividade das vinhas.

**Palavras-Chave**: agricultura sustentável, energias renováveis, evapotranspiração, gestão de vinhas, otimização de recursos, processamento de dados, rega inteligente.

# Contents

# List of Figures

# List of Tables

# List of Acronyms

| | |
|---|---|
| **AC** | Alternating Current |
| **AGDD** | Accumulated Growing Degree Days |
| **API** | Application Programming Interface |
| **CSV** | Comma-Separated Values |
| **DC** | Direct Current |
| **DCC** | Dual Crop Coefficient |
| **DHI** | Diffuse Horizontal Irradiance |
| **DNI** | Direct Normal Irradiance |
| **ET** | evapotranspiration |
| **FAO** | Food and Agriculture Organization |
| **FAO-56** | FAO Irrigation and Drainage Paper 56 |
| **FDR** | Frequency Domain Reflectometry |
| **FFPI** | FAO Food Price Index |
| **GDD** | Growing Degree Days |
| **GHI** | Global Horizontal Irradiance |
| **GIR** | Gross Irrigation Requirement |
| **HAWT** | Horizontal Axis Wind Turbine |
| **IDE** | Interactive Development Environment |
| **IPMA** | *Instituto Português do Mar e da Atmosfera* – Portuguese Institute of the Sea and Atmosphere |
| **ISEP** | *Instituto Superior de Engenharia do Porto* – Polytechnic Engineering Institute of Porto |
| **JSON** | JavaScript Object Notation |

| | |
|---|---|
| **MDPI** | Multidisciplinary Digital Publishing Institute |
| **MEEC** | Master in Electrical and Computer Engineering |
| **NIR** | Net Irrigation Requirement |
| **NOCT** | Normal Operating Cell Temperature |
| **OMIE** | *Operador do Mercado Ibérico de Energia* – Iberian Energy Market Operator |
| **PNG** | Portable Network Graphics |
| **SDG** | Sustainable Development Goal |
| **SPIS** | Solar Powered Irrigation Systems |
| **STC** | Standard Test Conditions |
| **TDR** | Time Domain Reflectometry |
| **TDT** | Time Domain Transmissiometry |
| **VWC** | Volumetric Water Content |

# List of Symbols

| Symbol | Description | Units |
|---|---|---|
| $A$ | area | $\mathrm{m}^2$ |
| $d_r$ | inverse relative distance between earth and sun | 1 |
| $\Delta$ | slope of saturation vapor pressure curve | $\mathrm{kPa}\ {}^\circ\mathrm{C}^{-1}$ |
| $\delta$ | solar declination | rad |
| $E$ | energy | Wh |
| $e$ | vapor pressure | kPa |
| $C$ | energy price | $\mathrm{EUR\,kWh}^{-1}$ |
| $ET$ | evapotranspiration | $\mathrm{mm\,day}^{-1}$ |
| $\eta$ | efficiency | 1 |
| $f$ | factor | 1 |
| $G$ | soil heat flux density | $\mathrm{MJ\,m}^{-2}\,\mathrm{day}^{-1}$ |
| $\gamma$ | temperature coefficient of power | ${}^\circ\mathrm{C}^{-1}$ |
| $\Gamma$ | precipitation | $\mathrm{mm\,day}^{-1}$ |
| $i$ | current | A |
| $I_r$ | solar irradiance | $\mathrm{Wh\,m}^{-2}$ |
| $K_c$ | crop coefficient | 1 |
| $\omega$ | sunset hour angle | rad |
| $P$ | power | W |
| $p$ | pressure | kPa |
| $\phi$ | latitude | rad |
| $\psi$ | psychrometric constant | $\mathrm{kPa}\ {}^\circ\mathrm{C}^{-1}$ |
| $Q$ | flow rate | $\mathrm{L\,s}^{-1}$ |
| $R$ | radiation | $\mathrm{MJ\,m}^{-2}\,\mathrm{day}^{-1}$ |
| $\rho$ | air density | $\mathrm{kg\,m}^{-3}$ |
| $\sigma$ | Stefan-Boltzmann constant | $\mathrm{MJ\,K}^{-4}\,\mathrm{m}^{-2}\,\mathrm{day}^{-1}$ |
| $t$ | time | s |
| $\theta$ | solar zenith angle | rad |
| $u$ | wind speed | $\mathrm{m\,s}^{-1}$ |
| $v$ | voltage | V |
| $z_0$ | surface roughness length | m |
| $\zeta_p$ | turbine power coefficient | 1 |

# Chapter 1

# Introduction

Developed as part of the Thesis/Dissertation Curricular Unit of Master in Electrical and Computer Engineering (MEEC) at *Instituto Superior de Engenharia do Porto* – Polytechnic Engineering Institute of Porto (ISEP), this document covers all the research and work carried out in the field of this project. This chapter provides a brief motivation for the topic under study, explains all the objectives and tasks carried out, and clarifies the structure of the dissertation.

## 1.1 Motivation

Agriculture has always been one of the most important sectors of activity for the survival and prosperity of humanity, becoming one of the main pillars of support for any country. As a field that is constantly evolving, there are various methods and techniques from the primordial times, which end up improving and making this whole activity more efficient [1]. Nowadays, the importance of agricultural resources is becoming increasingly evident, and a considerable impact on this sector triggers a whole negative reaction on a global socio-economic level. However, most of the population mistakenly takes it for granted or does not think about the entire process required to put a product from agriculture on the market [2, 3].

In addition to the human losses and destruction caused by Russia's invasion of Ukraine, also known as the "breadbasket of Europe", several adversities and challenges have complicated the supply of energy and food. These difficulties have ended up further accentuating the vulnerabilities of economic sectors already weakened due

to climate change and the COVID-19 pandemic, and one of the sectors that suffered the most was agriculture [4, 5]. This impact is visible in the graph in Figure 1.1 provided by the Food and Agriculture Organization (FAO), which shows that the FAO Food Price Index (FFPI) has seen a significant increase [6].

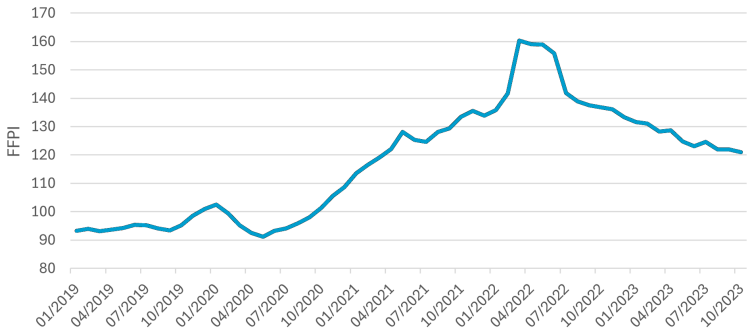


Figure 1.1: FFPI statistical graph from 2019 to 2023, adapted from [6].

Therefore, it is increasingly important to develop systems that make it possible to intensify what is sustainable agriculture to optimize the efficient usage of available resources, in terms of the use of arable land, water, and energy resources [7, 8].

Agriculture turns out to be one of the most intensive activities in terms of land use, with a large percentage of habitable land being used for the production of crops, a figure that continues to increase exponentially over the years [9]. Unfortunately, the agriculture we practice today is destroying the planet. The use of excessive fertilizers, herbicides, and insecticides, which end up being washed into other environments, such as river basins, is a worrying aspect as it causes change and pollution in other ecosystems [10].

Nowadays, the vast majority of the population recognizes that one of the major factors influencing the success of agricultural activity is the existence of adequate moisture and nutrient conditions in the soil. For this reason, agriculture ends up being an activity that requires a great deal of water, and it is expected that, by 2030, this need will increase by 50% due to the constant increase in the world's population. As agriculture is one of the main contributors to water scarcity, it is essential to create appropriate resource management and control systems to make the whole process more efficient and save a valuable asset [11, 12, 13].

These facts also extend to one of the largest parts of the agricultural sector, which is the wine industry. Mankind has been fermenting grapes into wine for centuries, and today, wine is a consumable commodity worldwide. Despite its global popularity, wine production is a fairly exclusive industry, and not all land offers the ideal soil and atmospheric conditions for this activity [14]. In Portugal, a large part of the agricultural plantations are vineyards, making it the 10th country with the highest wine production and 2nd in consumption per capita worldwide [15]. To

maintain this sector as a major contributor to the growth of the national economy, the efficiency of the entire process leading to wine production is of utmost importance [16].

Like other agricultural sectors, the wine sector requires an adequate concentration of nutrients and moisture in the soil [17]. For this reason, the development of systems that allow greater efficiency in this activity's practice is crucial, especially in terms of the irrigation processes that are indispensable for its success [18, 19].

## 1.2 Objectives

With these considerations in mind, this work aims to study solutions and alternatives that will make the entire irrigation system more effective, particularly in the automatic management of resources that will optimize production efficiency in the wine sector.

Given the complexity of the tasks arising, there is a need to dismantle this main objective, obtaining more specific tasks, namely:

- Analysis of the resources needed for successful agricultural activity;
- Study of the most commonly used irrigation methods and their relevance;
- Analysis of existing concepts that make irrigation processes more efficient;
- Identification of effective sensors, actuators, and controllers for these solutions;
- Development of an intelligent optimization model that enables an efficient management of available resources;
- Simulation of real world scenarios to validate the model;
- Critical analysis and discussion of the results obtained.

In a first instance, these specific tasks contribute to the definition and design of the solution, by analysing what are the most important resources for successful agricultural activity, specially in the wine sector. The study of irrigation processes, and how to make them more efficient, is also an indispensable part of the study, since their adaptation to cutting edge technology such as sensors, actuators, and controllers, brings numerous advantages. Concepts like renewable energies, evapotranspiration and resource efficiency, are key points for the development of the intelligent optimization model proposed, and their study helps defining the problem and establishing the solution. The critical analysis of the results obtained through multiple simulations, alongside the carried out study, contributes to the advancement in the area and the identification of new promising paths based on the progress made in this work.

## 1.3 Organization of the Dissertation

Following this introductory chapter, Chapter 2 approaches the literature review of the dissertation theme by firstly contextualizing it in Section 2.1. The chapter also explores the importance of renewable energy sources in agriculture in Section 2.2, and provides information about the irrigation methods most frequently used in Section 2.3. More technically in-depth, Section 2.4 briefly introduces the importance of evapotranspiration in agriculture and Section 2.5 exposes a study regarding some methods to control the irrigation processes. To conclude the literature review, Section 2.6 analyzes existing optimization and resource management models.

Following the literature review, Chapter 3 addresses the methodology implemented in the intelligent optimization model, by explaining the core tenets behind the algorithms developed, with Section 3.1 explaining the architecture of the system. Further detailing of every module of the system is explained, with Section 3.2 and 3.3 exposing how the data processing and specific parameter estimations were carried out. To conclude this chapter, Sections 3.4 and 3.5 clarify the final irrigation and energy models that provide the desirable outputs. As a validation of the optimization model, the achieved results are presented and discussed in Chapter 4, highlighting the main parameters and explaining their importance to the outputs of the system, in parallel with the methodology.

As a conclusion, Chapter 5 summarizes the entire research of this dissertation and exposes the conclusions and contributions drawn from this project, as well as the concepts learned and technical skills implemented.

# Chapter 2

# Literature Review

In order to start developing a project of this size, it was necessary to study the solutions already implemented in the field of sustainable irrigation. From the analysis of system proposals to physical implementations, there are a large number of considerations that must first be analyzed in order to create an efficient optimization model for the management of resources in the wine sector. The following study was published in a special issue of Multidisciplinary Digital Publishing Institute (MDPI) *electronics* journal [20].

## 2.1 Contextualization

In order to start the research in this field, a brief contextualization of the problem must be carried out. According to a statistic search in FAO Aquastat [21] and Eurostat [22] databases, it is evident that the indicators related to water and energy usage in agriculture are increasing, which explains the importance of developing efficient solutions to better manage these resources. Considering the area of implementation of this study, it was decided to place a special focus on Portugal, comparing it with the average values of the European Union.

In Figures 2.1a and 2.1b, one can see an increase in the total percentage of cultivated land and water withdrawal for agricultural purposes relative to the total water collected.

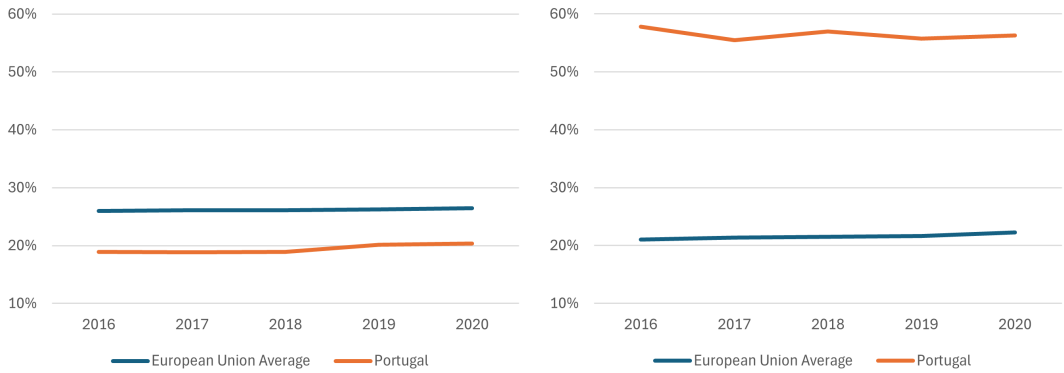


Figure 2.1: Indicators related to land and water usage from 2016 to 2020: (**a**) percentage of total country area cultivated; (**b**) agricultural water withdrawal as a percentage of total water withdrawal (data sources: FAO Aquastat [21] and Eurostat [22]).

One other indicator that is also relevant to this study is the Sustainable Development Goal (SDG) 6.4.1, which tracks the cost per volume of water in cubic meters, by a given economic activity over time. This indicator allows us to assess how economic growth depends on water resources, considering all economic activities, focusing on agriculture, industry, and the service sector. According to the graphic in Figure 2.2, it is clear that the indicator related to the agriculture sector is increasing over the years. The below-average value in Portugal is not surprising, given that there are countries like Denmark where this index is around 267 EUR/$m^3$ or even Luxembourg where it scales exponentially to 1112 EUR/$m^3$.

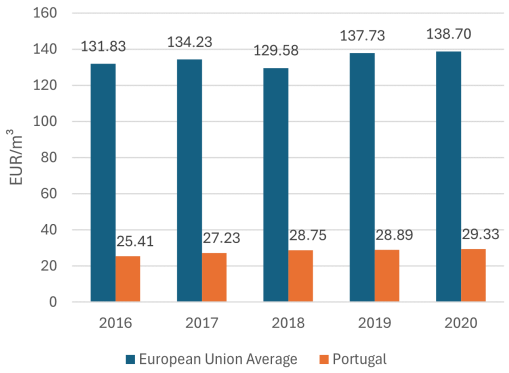


Figure 2.2: SDG 6.4.1 indicator from 2016 to 2020 (data sources: FAO Aquastat [21] and Eurostat [22]).

In terms of energy, the total consumption for agriculture purposes was analyzed, and the percentage of this energy was compared to the total energy used. As seen in Figures 2.3a and 2.3b, both of these indicators also increased during the past years.

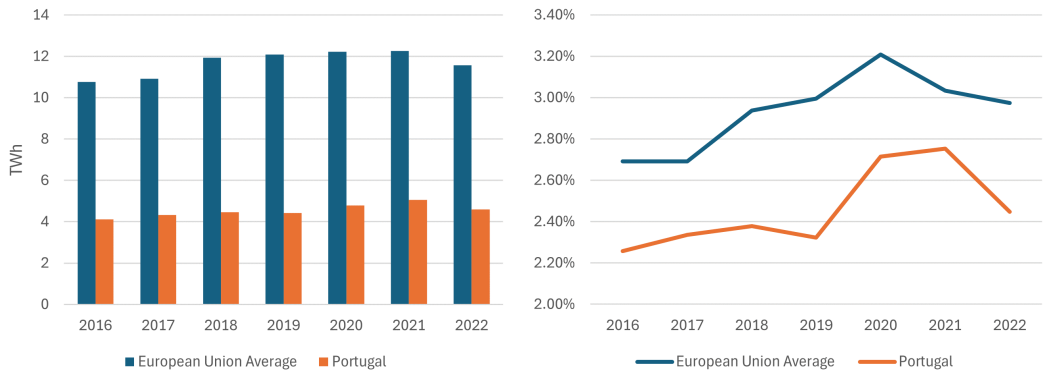


(a) (b)

Figure 2.3: Indicators related to energy usage from 2016 to 2022: (**a**) total energy consumption for agriculture purposes; (**b**) percentage of energy used in agriculture relatively to the total energy used (data sources: FAO Aquastat [21] and Eurostat [22]).

A search in Scopus [23] using the query "renewable energy AND irrigation" until the end of 2023 revealed a total of 1464 documents. This is a very low number of publications considering the importance of renewable energy for efficient and sustainable irrigation management. This gap has been identified by the scientific community, and one can see it is being addressed by the significant increase in related publications since around 2010, as shown in Figure 2.4. Most of these publications – nearly 60 % – refer to journal publications, as highlighted in Figure 2.5, which supports the relevance of the topic. The interest and contribution to the advances in this subject are shared among multiple research and development areas, as shown by Figure 2.6, which include energy, engineering, environmental sciences, among many other complementary fields. The results displayed intentionally cover a broader context considering the exploratory literature review nature of this work.

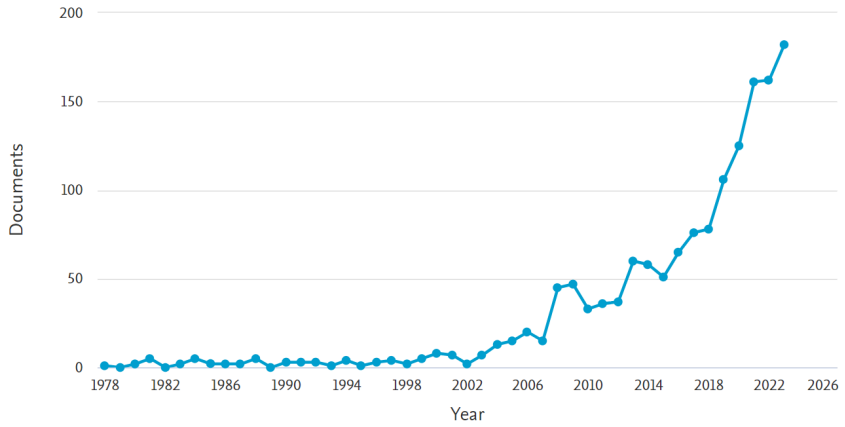


Figure 2.4: Graphical evolution of document publications per year.

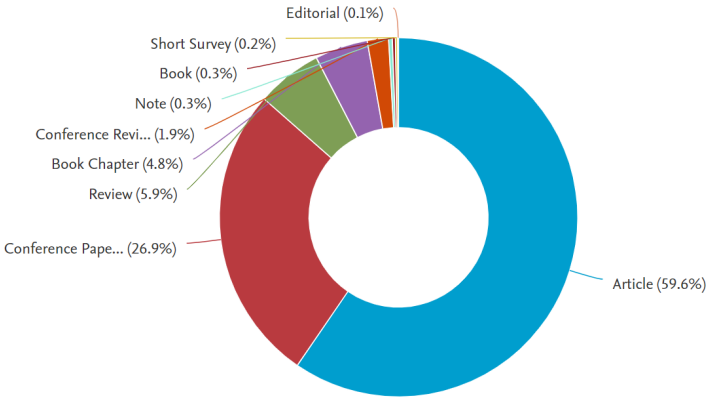


Figure 2.5: Types of work published about the subject.

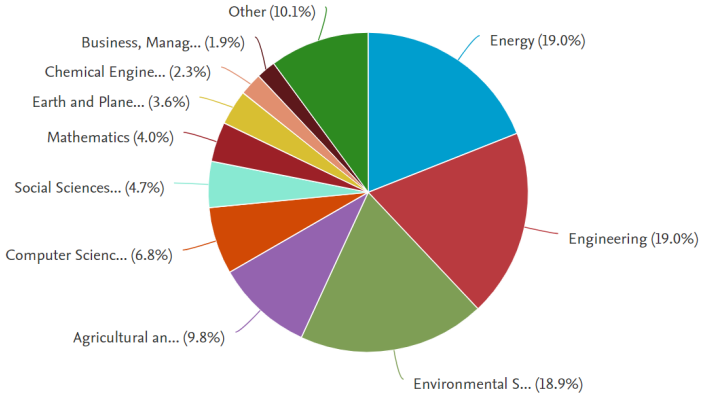


Figure 2.6: Interest and contribution of this subject to the various areas.

Despite all the current systems and solutions which, depending on the availability and need of resources, are successful in increasing the efficiency of irrigation processes, there are still some limitations stemming from the energy and communication dependencies of the equipment used (sensors and actuators).

In certain cases, these limitations can be easily overcome; however, when it comes to land dedicated to wine production characterized by its large scale and adverse characteristics, particularly in terms of terrain accentuation, it is difficult to guarantee that these dependencies can be easily dealt with. In addition, there is also a growing need to make appropriate use of available water and energy resources, which, more than ever, cannot be considered infinite or guaranteed.

One of the main difficulties with irrigation smart systems sometimes lies in the existence of wiring to the sensors or actuators, which can be difficult to implement or damaged by agricultural machinery. A way of overcoming this problem is by implementing wireless-based systems that can be easily applied in any location, with no need to install cables to communicate the data acquired by the equipment [24]. This makes it possible to respond to the main limitation related to the size

and adversity of the terrain, as it is possible to carry out remote communication between the sensors and the system controller. Of course, as the objective is to eliminate the routing of cables across the terrain, the power supply for these sensors and communication modules also has to be provided in another way, namely through batteries (rechargeable or not) and/or photovoltaic cells [25].

## 2.2 Importance of Renewable Energies in Agriculture

With the continuous technological evolution in most economic sectors, agriculture has not escaped the constant innovation that allows the practice of the activity more autonomously and efficiently. However, compared to conventional agricultural activity, modern agriculture ends up requiring a greater energy demand, which very often resorts to fossil fuels [26].

Given the continuous rise in greenhouse gas emissions and consequent climate change, the promotion of renewable energies is increasingly important in all sectors of activity, despite all the challenges that may be imposed [27]. As stated by the European Green Deal, one of the main objectives of its program is to ensure zero net emissions of greenhouse gases by 2050, transforming the European Union into a resource-efficient economy [28].

Achieving sustainable agriculture is not an easy task, but with technological advances, renewable energy sources are becoming increasingly accessible. The decreasing costs of photovoltaic modules, wind technologies, and batteries for storing electricity are increasingly contributing to the implementation of green and sustainable agriculture [29].

The energy used throughout the agricultural production chain can be divided into two main areas: primary energy or energy used directly, namely in lighting, cooling, or heating systems and irrigation processes; and energy used indirectly, such as in the production of fertilizers or agricultural chemicals [26]. As irrigation is one of the most important stages in the success of agricultural activity, it is more than essential to ensure that the energy used by irrigation systems is acquired and used as economically and sustainably as possible.

Within the universe of renewable energies in the agricultural sector, it is important to highlight a few examples, such as solar, wind, hydroelectric, and biomass. Since wind and solar are the most common renewable energies used in this sector, they will be addressed with more focus in the article, although all of them have great potential for ensuring sustainable agriculture.

In addition to all the advantages renewable energies offer, particularly in terms of environmental benefits, sustainability, availability, and security, they are also characterized by their portability and ease of implementation. These turn out to be one of the most important factors about renewable energy sources because not every

place has direct access to an electricity grid and sometimes securing a connection can result in a huge expense, which can make it unfeasible or even impossible [30].

The hillsides have always been the place of choice for growing quality vines, as can be seen in the Douro vineyards in Portugal [31]. Places characterized by rockier, less fertile soil end up producing smaller vines than regions with more fertile soil. This is not necessarily a disadvantage, as smaller vines result in smaller grapes, which offer a higher ratio of concentration and intensity in their extract, producing more unique and exceptional wines. In addition, vineyards grown on slopes have fewer problems with frost and offer natural water drainage, which prevents the land from flooding and consequently destroying the crops [32].

However, the great disadvantage of these lands is their topographical steepness, which immediately makes it difficult to work with agricultural machinery and access the electricity grid due to their remote and adverse nature. With this in mind, implementing an electrical self-production system based on renewable energies is extremely important as it guarantees access to clean, renewable energy, which reduces production costs, taking an important step towards ensuring sustainable agriculture [33, 34].

In addition to all the sensors, actuators, or weather stations that can be placed on agricultural land to measure the many variables that influence irrigation processes, one of the pieces of equipment that can have the greatest energy demand is electric water pumps. Used to direct water from a reservoir to a specific destination, this equipment may be necessary to guarantee the presence of water on agricultural land.

A system made up of electric water pumps powered by photovoltaic panels can become a promising way of watering crops, creating systems often known as Solar Powered Irrigation Systems (SPIS) [35, 36]. As an example, the use of solar-powered electric pumps to extract water from lakes, rivers, or canals is considered a very useful option in Bangladesh, where 35% of them are used purely for irrigation purposes [37, 38].

In SPIS, the energy is generated by a set of photovoltaic panels that are used to power the electric pumps responsible for extracting, lifting, or distributing the water across the terrain [39]. Figure 2.7 shows a schematic of how this type of system is usually implemented.

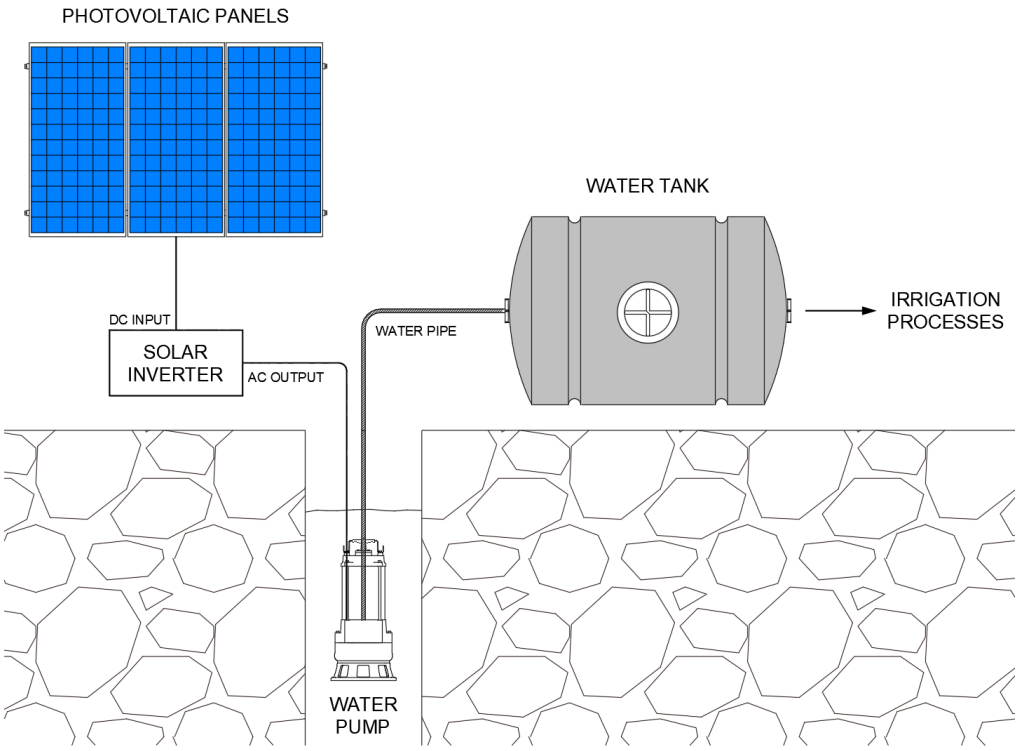


Figure 2.7: Representative diagram of an example SPIS application, adapted from [36].

In addition to the supply of energy obtained from solar power, another type of energy that has also had a major impact is wind power. With the constant increase in investment in this renewable alternative, the goal set by Net Zero is that, by 2050, around 18% of the energy used globally will be supplied by wind. With constant growth every year, wind energy saw a record increase of 273 TWh produced in 2021 compared to the previous year, making it the largest increase among all existing renewable energies [40, 41].

This same principle can also be applied to powering pumps in the agricultural sectors. Instead of conventional photovoltaic panels, a wind turbine can be used to supply energy when the wind is on site, as shown in Figure 2.8.

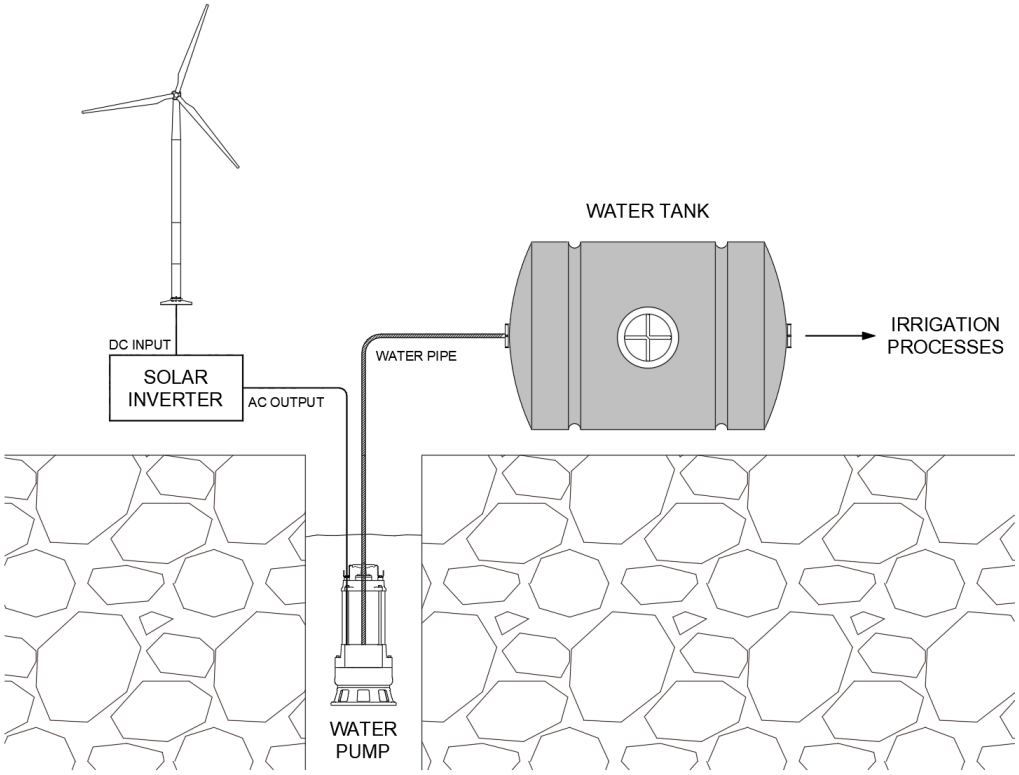


Figure 2.8: Example of using a wind turbine to power electric pumps, adapted from [26].

This type of solution could be viable, for example, in windy steep terraced slopes and dry schist soils, such as the Douro valleys, which are characterized by a range of micro climates and often used for wine production. The so-called northerly winds, which come from the north, can be intense in these regions. However, during the growing season (typically from April to October), the winds are more moderate and are particularly beneficial for the growth of the vines. The existing air currents not only cool and refresh the crops but also prevent disease by ensuring good air circulation. Of course, the extra advantage of these climates is precisely the implementation of wind energy sources that can make the most of the winds in the region [42, 43, 44].

Once the energy supply is guaranteed, the system (both photovoltaic and wind) can be easily integrated with a controller or autonomous model, which manages the irrigation process according to the requirements of the crops or the availability of resources. In addition, the structure that supplies energy can be connected to a battery that guarantees the supply of energy to other equipment on the plantation, namely sensors and actuators associated with the irrigation systems. However, despite the increasingly promising battery developments, they remain considerably expensive and have limited life cycles [45].

An efficient way of avoiding this problem is by storing electrical energy in the form of hydroelectric potential energy, where water is pumped during sunny hours into a tank or reservoir located higher up. Through this reservoir and using the principle of hydroelectric energy production, it is possible to implement a hydroelectric generator made up of turbines that can supply energy in sunless hours. In addition to supplying energy, this water can also be used to irrigate crops, thus playing a major role in the autonomy and efficiency of irrigation processes [46].

## 2.3 Main Irrigation Methods

As previously mentioned, the main purpose of irrigation processes is to supply the amount of water needed by the soil for the proper development of cultivated crops.

Despite all the variables associated with each irrigation method, they all require adequate knowledge of soil characteristics and crop water requirements. One of the main factors to consider when estimating a crop's water needs is evapotranspiration, a concept that results in the integration of the water transpired by the plant itself and the water evaporated [47]. Although the soil itself does not have a direct influence on evapotranspiration, it does influence the calculation of the volume of water to be applied, as well as the actual conduction of water through the soil, which is why it is essential to determine the best irrigation method for the plantation in question.

Within the universe of existing irrigation methods, they can be divided into three categories: surface irrigation, sprinkler irrigation, and localized irrigation [48, 49].

Surface irrigation, where the effect of gravity is the main protagonist, is characterized by the way water runs off the surface of the soil and infiltrates along its path. Used in a large part of the world's irrigated areas because of its simplicity, surface irrigation is distinguished by being a low-tech method that does not need any kind of pumping method, except to place the water on the surface of the land. In this process, water can be applied to the surface of a plot of land in the form of controlled flooding or waterlogging (visible, for example, in rice fields), or it can be applied through the defluence of water through existing channels or strips which guarantee the supply of water to the crops (Figure 2.9).

Figure 2.9: Application of surface irrigation via channels [49].

On the other hand, a more complex system is sprinkler irrigation, where the water is projected onto the crops in the form of rain. Unlike surface irrigation, this method already requires water to be conveyed by pressure along a network of pipes, which requires the implementation of a pumping system with consequent energy consumption. Essentially, sprinkler irrigation systems can be characterized as stationary, where the sprinklers remain in a fixed position, or mobile, where the sprinklers are mounted on moving platforms, as illustrated in Figure 2.10, also known as pivot irrigation.

Figure 2.10: Example of an irrigation pivot in a plantation [50].

Despite the advantages that the previously mentioned methods can bring to the most varied types of crops, particularly in terms of practicality or ease of installation and execution, the irrigation method most used in the wine sector is localized irrigation, also known as micro-watering or drip irrigation.

In this irrigation technique, water is directly applied only to the areas of the soil where plant roots develop and is dispersed slowly and evenly. For this reason, localized irrigation immediately presents a higher efficiency due to the amount of water used to satisfy all crops on a given plantation. This is particularly efficient due to the reduction in water losses as a result of evaporation, which often occurs in previous methods and ends up causing excessive irrigation.

Within the universe of localized irrigation, some specific processes stand out that correspond to distinct hydraulic processes. The micro-sprinkler method, where water is sprayed onto the surface of the soil, ends up being similar to sprinkler irrigation with the difference that small moist areas are created only in the root zone. In drip irrigation, which is one of the most economical options, water is delivered directly to the root area using drippers. Similarly to the previous process, there is subsurface irrigation, where water is applied under the surface of the soil through the implementation of, for example, a buried perforated piping system that discharges water directly to the roots. In Figure 2.11, an example of localized

irrigation is represented, highlighting the difference between surface and subsurface drip irrigation.

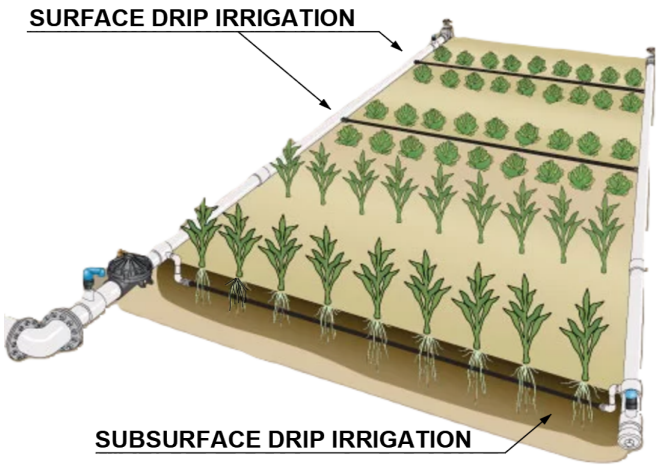


Figure 2.11: Surface and subsurface drip irrigation, adapted from [51].

In general, localized irrigation can contribute to the efficient use of water resources. These types of systems, if planned correctly, reduce the percentage of water waste due to runoff and infiltration into the soil and eliminate almost all losses due to evaporation. In addition to the benefit in production costs, drip irrigation also presents a strong advantage in reducing the growth and appearance of fungi that can cause diseases in the crop and consequent loss of quality in the final product [52].

However, the initial cost of implementing a system of this type ends up being higher compared to other, simpler systems. The value of these systems will always vary depending on the characteristics of the terrain, the composition of the soil, the type of crops, and the source of water used to feed the system. Another disadvantage is that, as they are exposed systems, they can be difficult to combine in plantations where the use of agricultural machinery is frequent, as there may be damage caused to the piping network or to the emitters, a situation that can be overcome with the use of subsurface methods [52].

Despite its disadvantages and expensive implementation, drip irrigation continues to be one of the most used and most economical systems in the long term in the wine sector. Characterized by being the least prone to problems related to soil variability and having the lowest level of difficulties due to the topography of the land, localized irrigation systems are the only ones that can guarantee greater control uniformity in water distribution. For these reasons and when combined with data sensing techniques or optimization models using renewable energies, it is possible to guarantee the highest level of efficiency in wine production [53, 54].

## 2.4 Evapotranspiration Concept

Having determined the best irrigation method for the wine sector, another factor already mentioned and which is extremely important is evapotranspiration (ET), a concept that determines the water needs of a plantation. Generally speaking, vines can grow healthily and efficiently in soils with varying moisture conditions. However, excessive water can result in a wide range of negative impacts on grape production, such as a reduction in the set of flowers and their fruit, abnormal development of the vine trunk, and even dehydration of the grapes [55, 56].

Other studies also revealed that variations in climate and atmospheric conditions largely influence the growth and development of the vine and the consequent yield and quality of the wine produced. In addition to its direct impact, a hotter and drier climate can negatively influence the growth of vines, particularly in terms of increasing soil salinity and, consequently, general soil degradation [57, 58].

Although vines show strong resistance to challenging environmental conditions, estimating trends in soil irrigation needs and requirements, including vine evapotranspiration components under varying soil texture conditions, can be an excellent data source to guarantee sustainable production with guaranteed yield and quality [59].

Evapotranspiration, as the name suggests, is a parameter that defines the amount of water removed from the soil through plant transpiration and direct evaporation. The amount of ET from a plant is not a fixed value and varies depending on geographic location and over time. Some main factors determine its value, namely temperature, relative humidity, wind, solar radiation, and the type of plantation itself [60].

To study plant evapotranspiration, it is important to take into account two essential terms: $ET_0$ (reference or potential evapotranspiration) and $ET_c$ (plantation or crop evapotranspiration). $ET_0$ is a parameter that indicates the ET of a normal lawn under ideal conditions, and $ET_c$ indicates the evapotranspiration of the type of crop. These values are usually represented in the unit mm/day; however, they can be represented in other temporal forms (for example, mm/m, mm/min).

As described in FAO Irrigation and Drainage Paper 56 (FAO-56) [61], the set of methodologies presented below is among the most used to determine the evapotranspiration of a plantation. This approach is frequently applied given its simplicity and robustness, as it requires less input data and provides acceptable ET estimates when compared to other strongly parameterized models or models that take into account measurements via satellite or sensors placed on the ground.

To determine the value of $ET_0$, we can adopt an indirect way that uses the FAO Penman–Moneith method. This method is characterized by having a formula

(Equation 2.1) that allows calculating the value of $ET_0$ using some meteorological data.

$$ET_0 = \frac{0.408\Delta(R_n - G) + \psi\frac{900}{T+273}u_2(e_s - e_a)}{\Delta + \psi(1 + 0.34u_2)} \tag{2.1}$$

where,

$ET_0$ — reference evapotranspiration [mm day$^{-1}$],
$R_n$ — net radiation at the crop surface [MJ m$^{-2}$ day$^{-1}$],
$G$ — soil heat flux density [MJ m$^{-2}$ day$^{-1}$],
$T$ — mean daily air temperature at 2 m height [°C],
$u_2$ — wind speed at 2 m height [m s$^{-1}$],
$e_s$ — saturation vapor pressure [kPa],
$e_a$ — actual vapor pressure [kPa],
$e_s - e_a$ — saturation vapor pressure deficit [kPa],
$\Delta$ — slope of saturation vapor pressure curve [kPa °C$^{-1}$],
$\psi$ — psychrometric constant [kPa °C$^{-1}$].

The equation, despite presenting complex parameters and data, uses simple meteorological records of solar radiation, air temperature, humidity, and wind speed which, as previously mentioned, will directly affect the value of $ET_0$.

Based on the value of $ET_0$ at the plantation location, some approaches allow calculating the value of $ET_c$ through a parameter $K_c$ (crop coefficient). The value of the $K_c$ coefficient is not always the same for the same crop and varies depending on the stage of development the plant is in. To obtain more accurate results, FAO-56 determines two approximations to determine $ET_c$, which are the simple approximation and the Dual Crop Coefficient (DCC) approximation [62, 63].

For the single coefficient used in the simple approximation, the effect of plant transpiration and soil evaporation are combined into a single coefficient $K_c$, obtaining Equation 2.2 for determining $ET_c$.

$$ET_c = K_c \times ET_0 \tag{2.2}$$

On the other hand, the DCC approach separates the single coefficient $K_c$ into a coefficient related to transpiration ($K_{cb}$) and one related to soil evaporation ($K_e$), as can be seen in Equation 2.3. This approach requires additional parameters related to climate, soil, and crop to estimate transpiration and, of course, implies higher computational costs. However, this approach is recommended by FAO-56 when improved estimates of the value of $K_c$ are needed to, for example, schedule accurate daily watering.

$$ET_c = (K_{cb} + K_e) \times ET_0 \tag{2.3}$$

For the purposes of normal planning and management of irrigation processes, the average plantation coefficients obtained by the simple approximation are relevant and more convenient than the $K_c$ calculated by the DCC approximation. However, it is always necessary to analyze the plantation in question and the available resources to determine the best approach.

## 2.5 Control of Irrigation Processes

Taking into account all the previously mentioned concepts, to achieve the status of sustainable agriculture, irrigation processes must be managed in the most intelligent way possible, both in terms of decision-making and in terms of resource use [64]. In this sense, there is a wide range of solutions already implemented that allow intelligent management of irrigation processes and that vary their efficiency depending on their complexity and practicality.

### 2.5.1 Hourly Scheduled Watering

Starting with a more traditional solution that is widely used, the programmed irrigation system appears. These simple systems are relatively developed and continue to make a big contribution in this field, since many irrigation projects still use this technique due to its low price and simplicity. The basic principle most frequently implemented in these systems is the concept of hourly irrigation [65].

Through intelligent programmers that offer a simple interface, the user can define the days and times at which they want to start irrigating a certain area of the land, indicating parameters such as the irrigation time or the percentage of water to be delivered, relative to the available flow rate. With the interconnection of electrovalves that allow the opening or closing of a flow of a given fluid through an electrical drive, the intelligent controller can carry out previously defined irrigation processes by the user, automatically.

### 2.5.2 Solutions Based on Measuring Soil Moisture

One of the solutions implemented for decision-making in irrigation processes are systems that work by obtaining values related to soil moisture in real time. These values can be acquired through the installation of a network of soil moisture sensors at several strategic points on the land, and through intelligent management by an implemented controller, it is possible to define very rigorous irrigation with great savings and less waste [66, 67].

A method used to obtain the value of soil moisture is its gravimetric measurement; however, this process ends up being time-consuming and complex, as it would require the constant removal of several samples from different locations. That being

said, soil moisture sensors are often used to obtain these measurements indirectly, using other soil properties, which can be divided into volumetric sensors, tensiometers, and sensors that measure the electrical resistance of the soil between two probes [68, 69].

Volumetric sensors directly measure the volumetric water capacity in the soil Volumetric Water Content (VWC). This type of sensor is capable of obtaining these readings through the use of neutron probes, heat dissipation sensors, or through the dielectric constant of the soil, which is the most common option. The soil dielectric constant is a property dependent on the soil's moisture content and can be obtained through Time Domain Reflectometry (TDR), Time Domain Transmissiometry (TDT), or electrical capacitance or Frequency Domain Reflectometry (FDR). These volumetric sensors end up being a considerably expensive option (costing more than EUR 100 per unit and around EUR 500 to EUR 1100 for a necessary electronic interpreter); however, they have high precision and allow instantaneous readings, being used mainly in research centers or on plantations with high monetary value, where time and data precision justify the investment [70].

On the other hand, tensiometers are devices capable of measuring soil moisture through the tension with which water molecules are retained by soil particles. When the soil has a high amount of water, the root of a plant does not need to exert much force to absorb it, in the same way that the tensiometer does not need to, so the tension is low. In the opposite case, where there is a low amount of water in the soil, the tension increases. Tensiometers are a cheaper option compared to the previous one, with costs of around EUR 65, and do not require any data interpreter as the values obtained are direct.

Finally, some sensors measure soil moisture through electrical resistance, which is an even cheaper option compared to the previous ones. With costs of no more than EUR 20 (when already incorporated with comparator modules), these sensors have a relatively simple operating mode. Having a shape similar to a fork, this sensor has two conductive probes that act as a variable resistance depending on the water content of the soil. The value of this resistance appears inversely proportional to the value of soil moisture, which means, that the higher the water content in the soil, the better the electricity conduction, meaning the resistance read between the two ends is lower, and vice versa. Through this variable resistance, it is then possible to determine the soil moisture in relative terms (whether it is wetter or drier). As mentioned, it is common to purchase these sensors with comparator modules, which allow obtaining a digital output (by calibrating a potentiometer) or an analog output, both in the form of an electrical voltage.

Through a network of soil moisture sensors properly placed throughout the land, the user can define the ideal minimum and maximum values (threshold) of soil moisture for each zone, making it possible to automate the irrigation process efficiently.

As soon as the controller, through reading the values of a given sensor, detects that the moisture value is below the stipulated minimum, the irrigation of that same area is automatically started. As soon as the maximum value is reached, irrigation is automatically terminated, avoiding excessive watering and maintaining soil moisture values within the stipulated thresholds. With this type of system, as long as it is properly calibrated for the terrain in question (taking into account the type of soil, plantations, or sun exposure), high efficiency is guaranteed, opening up more possibilities for energy and water sustainability [71].

### 2.5.3 Solutions Based on Estimation of Evapotranspiration

As previously mentioned, crop evapotranspiration is directly related to the soil's water needs; therefore, on a day when the plantation's ET value is higher, it is necessary to carry out longer irrigation to compensate for these losses due to evaporation and transpiration [72].

An ET controller automatically adjusts irrigation times according to the land's water needs, based on meteorological evapotranspiration information [73]. Unlike programmed irrigation controllers, in which the user has to constantly update irrigation schedules to avoid excessive or insufficient irrigation, these ET controllers automatically carry out this management [74]. These intelligent controllers can be divided into three distinct categories based on the way they obtain data related to evapotranspiration for each type of plantation: historical, signal-based, or terrain sensors [75].

ET controllers that use historical data generally have pre-programmed meteorological information. They are a relatively cheap option and, in most cases, reset the watering time to a monthly frequency, achieving considerable savings in water and energy.

Signal-based controllers obtain information regarding reference evapotranspiration by receiving data from a public meteorological station. These controllers generally have a service fee for data availability, but some public services provide this information free of charge, such as the *Instituto Português do Mar e da Atmosfera* – Portuguese Institute of the Sea and Atmosphere (IPMA) database. The advantage of these systems is that they do not require on-site sensing equipment. However, although they already allow for high savings, they may not have very high precision, as the data acquired can cover a large territory (an entire municipality, for example).

A solution that allows even greater savings is the use of these ET controllers connected to sensors strategically located along the land. The installation of mini meteorological stations is common, and they allow the controller to obtain data acquired on-site to make continuous calculations of evapotranspiration, automatically adjusting the amount of water required. It is the most accurate and effective option in this type of system, as it provides all the necessary information without large

margins of error, but it becomes more expensive due to the need for more expensive equipment [76].

## 2.6 Optimization and Resource Management Models

In the vast scientific and technological community, several solutions use most of the concepts covered in the previous chapters and that allow the optimization of productive efficiency in the agricultural sector.

In [77], the authors propose an intelligent energy management model that provides an increase in efficiency and autonomy through the use of renewable energy, namely photovoltaic and hydroelectric. The developed model and case studies are intended for agricultural fields close to rivers, where hydroelectric energy is used to power the water pumping system for a reservoir. Furthermore, for efficient energy management, decision trees are used to analyze and compare several variables, namely the cost–benefit of using the hydro generator or using energy from the electricity grid [78].

In the intelligent system developed in [79], an autonomous model uses the concept of mobile sprinkler irrigation (center pivot) that takes into account the water needs of plantations. Using data obtained from the ground, such as temperature, wind, soil humidity, and precipitation forecasts, the system can estimate the actual evapotranspiration of the plantation [80]. With this value, the model plans the irrigation processes taking into account the energy produced on site (through photovoltaic panels) and the cost of energy from the electricity grid.

In the dissertation [81], the authors used a network of humidity sensors based on the electrical resistance of the soil which allows constant monitoring of soil moisture. This relatively simple model defines a threshold that automatically manages the irrigation process [82]. Furthermore, an interesting innovation in this project was the implementation of a fire detection system, which allows an alarm to be issued in the event of a fire.

In [83], the authors carried out an intelligent approach using a database that contains the daily water needs of several plantations. With this database and taking into account data such as soil humidity and the time of day, the system can decide the amount of water needed for a given type of plantation. The results of the experiments carried out were satisfactory, and the authors valued the low cost of implementation, particularly in terms of the sensor network and access to the database.

Focusing more on the wine sector, the authors of publication [84] have developed a photovoltaic network to meet the energy demands of a winery's wastewater treatment plant and the pumping station of a vineyard's irrigation system. An interesting aspect of this article is the use of batteries as short-term storage, and with

the surplus energy, hydrogen is produced by electrolysis of water, which is used by a modified battery vehicle.

Some authors of the previous article have also published the scientific paper [85], where they characterize the energy demand of a vineyard and create a prototype of a photovoltaic network with a set of panels floating in an irrigation pond to avoid using land.

Additionally, the authors of the article [86] developed and tested an automatic management system, which involves the coordination of wireless sensors placed at strategic points on the land. All information obtained by the sensors is sent and interpreted by a controller that contains an intelligent decision-making model (Figure 2.12). The proposed system focuses mainly on the management and optimization of water resources and a reduction in human labor so that wine production costs can be minimized.

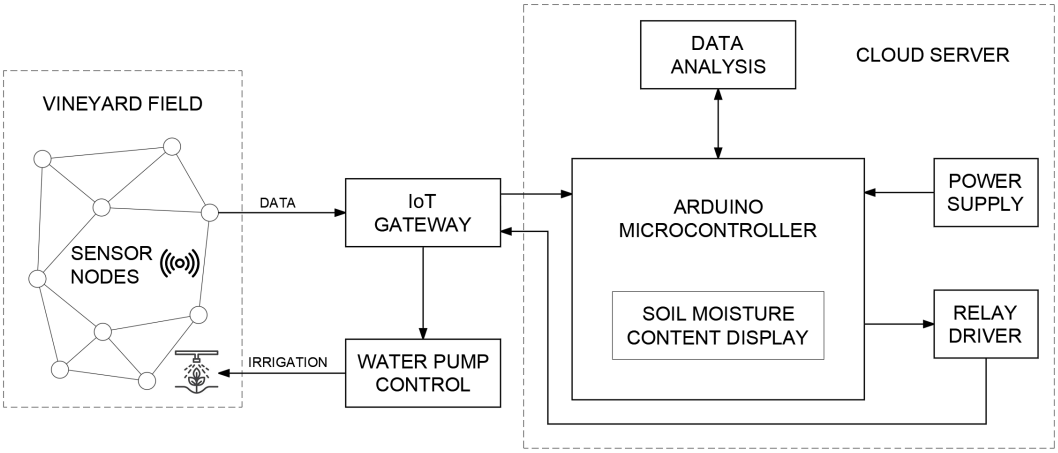


Figure 2.12: Authors' proposed wireless system architecture, adapted from [86].

# Chapter 3

# Methodology and Development of the Proposed Solution

With all the technologies that have been addressed in the previous chapters and with the knowledge obtained from them, the current idea is that all these techniques are dispersed across several isolated systems. In this sense, there is a lack of a resource management model that maximizes productive efficiency in the wine sector based on the largest number of compatible technologies and ideas mentioned previously. The purpose of this chapter is to explain a developed intelligent resource management system that implements multiple concepts simultaneously, with the option of a modular execution. The main final objective of the system is to output vital information that vineyard managers can incorporate on their farms, in order to guarantee the maximum sustainability and resource efficiency.

## 3.1 Resource Management System Architecture

The proposed system works with data obtained from multiple sources, namely weather stations that provide data such as temperature, humidity, wind speed, radiation, precipitation, as well as data from real electricity markets. Another important dataset is the renewable energy production, that can be obtained and processed via meters on site, or with multiple calculations with the provided information about the weather.

Of course, the quality of the data directly impacts the model performance, and the sources of data can vary according to the monetary resources provided by the vineyard. As an example, the model is certain to work more precisely with an on-site weather station, rather than a public weather Application Programming Interface (API) source. The energy meters can also provide more precise information about the production of renewable energy, rather than estimations obtained through weather data.

However, the model was constructed in a modular way, where the user can adapt the system to his data, as long as the information provided is in the same format. This offers the system the capacity to adapt to multiple vineyards, with multiple variables and equipment, and the more precise the data is, the more efficiently it performs. The high-level architecture of this system can be analyzed in Figure 3.1.

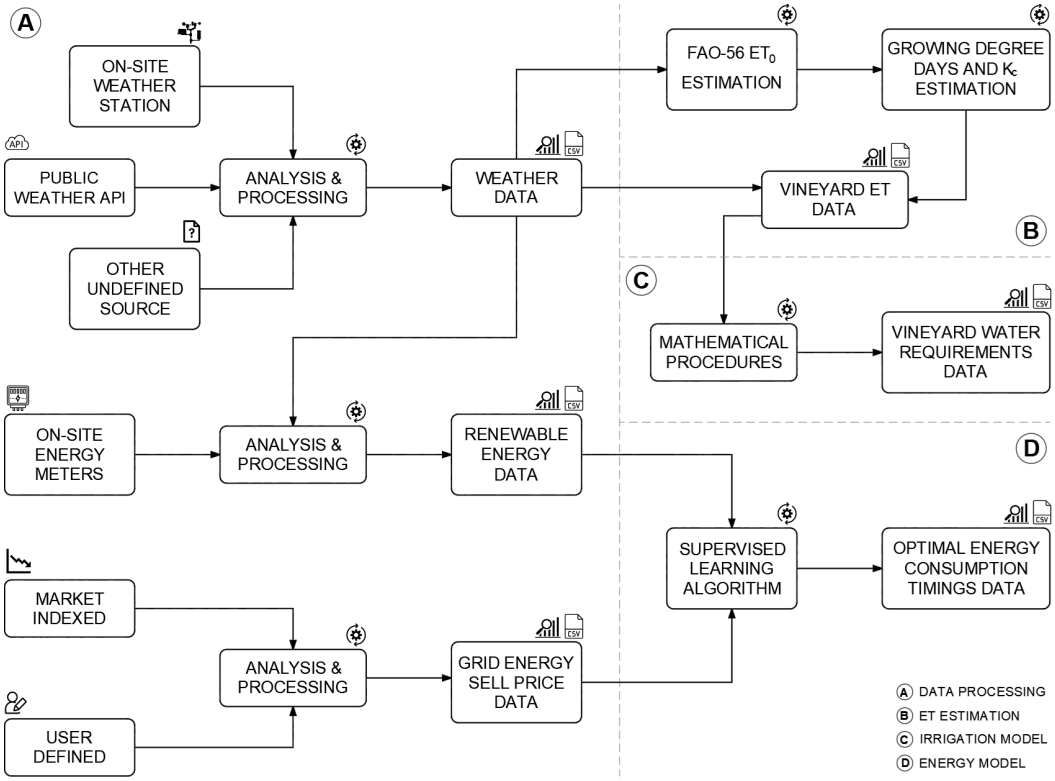


Figure 3.1: Methodology high-level architecture.

As seen in the high-level architecture, the system relies on four modules: data processing, evapotranspiration estimation, energy model, and irrigation model. Evidently, each module is dedicated to a particular set of operations or tasks, and together they generate multiple outputs such as information files in the format Comma-Separated Values (CSV) or graphical images in the format Portable Network Graphics (PNG). All this information is considered for past and future conditions, and it has the purpose of establishing the energy and water requirements for current

and following day. With this in mind, all the data is crossed regarding seven days prior and two days forecast, including current day.

The data processing module, represented in the schematic with letter A, is the main responsible for the system's data adaptability, because the sources of data can vary according to the availability of on-site resources. On-site weather station, public weather API, or even another undefined source such as a weather history logs, can all be data providers for the system, which analyses and interprets the information. The renewable energy data used by the system, can either be obtained by on-site energy meters or from the weather data previously acquired. As of grid energy sell price, this information can be derived by a market index source or in the form of a user defined value, since some energy contracts can have a fixed value throughout a certain period of time.

The remaining modules use the data prepared by the first one, and provide the desirable outputs. The evapotranspiration (ET) estimation module, symbolized with letter B, is responsible for estimating the water losses of the vineyard through a series of calculations. The data prepared by this module, alongside with precipitation derived from weather data, form a vineyard ET data containing the water losses and gains of the vineyard, without any sort of irrigation.

The irrigation model indicated with letter C, is responsible for interpreting and analysing the previous data and, with a series of mathematical procedures, it estimates the vineyard water requirements, ensuring high water sustainability.

Represented by letter D in the diagram, the energy model is responsible for implementing a supervised learning algorithm that uses information provided by the data processing module, namely the renewable energy production and grid energy sell price. With this algorithm, the system is able to output the optimal energy consumption timings, in order to guarantee energy cost savings.

In order to validate the solution, this model was built in Jupyter Lab [87], an advanced, web-based Interactive Development Environment (IDE) for working with Jupyter notebooks, code, and data. This IDE allows users to manage their entire data science workflow within one interface and provides a powerful and flexible environment for data science, scientific computing, and machine learning, enabling more effective analysis. This interface has the important advantage of allowing the development of multiple cells and view multiple outputs that can be user friendly such as graphical information. The platform also has cross-language support, offering a wide variety of programming languages through kernels [87]. Despite this cross-language support, the whole model was built using Python [88] language because of its strong readability, simplicity and versatility, as well as the availability of extensive libraries and frameworks, and powerful community support.

## 3.2 Data Processing Module

Starting of with the data processing module, its main objectives are processing data related to meteorologic conditions, estimate on-site photovoltaic and wind power production, and determine the grid energy sell price. This module is responsible for interpreting and processing the relevant data provided.

In this module, the system processes the meteorological conditions data, and builds a data frame that contains hourly information about multiple weather elements. Then, with the processed data frame about weather characteristics, the model creates another data frame containing renewable energy production values, that can either be photovoltaic, wind power, or both. As a final step, and for posterior implementation, the system generates another data frame that contains the information about grid energy sell price.

### 3.2.1 Meteorological Data Gathering

Since the prototype was built without on-site data, it was chosen to define the location of a supposed vineyard. However, the system is location-agnostic, and the meteorological data gathering can be done in any location, as long as the coordinates are provided. Since the nature of this work is related to Douro vineyards, the chosen location was Valença do Douro, Portugal, merely for testing and validation purposes. This region is known for windy steep terraced slopes and dry schist soils, which are characterized by a range of micro climates and often used for wine production.

With the prototype nature of the implementation, the weather conditions acquisition is done via public API sources, namely WeatherAPI [89] and EnsembleAPI [90]. The initial part of the code does a request to both API sources with the location and days of study required, and gets a response in the JavaScript Object Notation (JSON) format about the weather conditions. WeatherAPI is responsible for providing information about temperature, wind speed, air pressure, precipitation, and relative humidity. On the other hand, EnsembleAPI is responsible for providing solar radiation data, specifying it in Global Horizontal Irradiance (GHI), Diffuse Horizontal Irradiance (DHI) and Direct Normal Irradiance (DNI).

Since the model considers past conditions and it has the purpose of establishing the optimal energy consumption periods and water requirements for the current and following day, it has been decided to get a response regarding seven days prior and two days forecast including current day. All this information is provided in a very raw format with multiple variables that need to be filtered, but with some processing techniques, the output is a data frame with hourly timestamps. The desired output is available in a CSV file, that is generated when executing the program, as well as several graphics.

### 3.2.2 Estimation of Photovoltaic Energy Production

After successfully obtaining all the data required for the upcoming calculations, the next operation is to estimate the photovoltaic energy production. Once again, this step can be replaced by data obtained from on-site energy meters if available, however, since this prototype works without on-site data, there is a need to estimate all the renewable energy production values with the available weather data.

In order to correctly understand how this can be achieved, one needs to firstly understand how the different types of radiation that hit the earth influence the photovoltaic energy production. As seen previously, the radiation data obtained by EnsembleAPI is specified as GHI, DHI and DNI.

Starting with DNI, this value indicates the amount of solar radiation received by a surface that is always held perpendicular to the rays that come in a straight line from the direction of the sun at its current position. This value is of particular interest for solar thermal installations that concentrate the sun rays, or installations that track the position of the sun [91].

DHI is the amount of radiation received by a surface, without shadows, that does not arrive on a straight line from the sun, but has been scattered by molecules and particles in the atmosphere [91].

Finally, GHI is the total amount of shortwave radiation received by a surface horizontal to the ground. This value is particularly significant for photovoltaic installations, and features both DHI and DNI, and can be estimated by Equation 3.1 [91].

$$\mathrm{GHI} = \mathrm{DNI} \times \cos\theta + \mathrm{DHI} \tag{3.1}$$

where,

GHI — Global Horizontal Irradiance, or Shortwave Radiation [$\mathrm{W\,m^{-2}}$],
DNI — Direct Normal Irradiance [$\mathrm{W\,m^{-2}}$],
DHI — Diffuse Horizontal Irradiance [$\mathrm{W\,m^{-2}}$],
$\theta$ — solar zenith angle [rad],

With these considerations in mind, to begin the estimation of photovoltaic energy production, a widely used solar module is considered. The model chosen is the Canadian Solar CS6X-300M [92], with an estimated nominal peak power of 300 Wp in Standard Test Conditions (STC). This module was selected as a test object for experimentation and validation, and because it is available in the predefined database of Method B, which will be explained afterwards. All the relevant information about the 72 monocrystalline silicon cell with 1.92 $\mathrm{m^2}$ solar module can be seen in Table 3.1.

Table 3.1: Canadian Solar CS6X-300M specifications, adapted from [92].

| Parameter | Symbology | Value | Unit |
|---|---|---|---|
| STC Power Rating | $P_{max}$ | 300 | Wp |
| Peak Efficiency | $\eta_{STC}$ | 15.6 | % |
| Optimal Operating Current | $i_{mp}$ | 8.22 | A |
| Optimal Operating Voltage | $v_{mp}$ | 36.5 | V |
| Short Circuit Current | $i_{sc}$ | 8.74 | A |
| Open Circuit Voltage | $v_{oc}$ | 45 | V |
| Normal Operating Cell Temperature | $NOCT$ | 45 | °C |
| Temperature Coefficient of Power | $\gamma$ | -0.0045 | $°C^{-1}$ |

### Method A

After gathering the most relevant data about the solar module, the next step is to calculate the energy produced by the photovoltaic system. The generic formula present in Equation 3.2 takes into account key factors such as solar irradiance, the area of photovoltaic panel, and the efficiency of the system.

$$E = I_r \times A_{panel} \times \eta \tag{3.2}$$

where,

$E$ — energy produced [Wh],
$I_r$ — solar irradiance [$\mathrm{Wh\,m^{-2}}$],
$A_{panel}$ — area of the photovoltaic panel [$\mathrm{m^2}$],
$\eta$ — system efficiency.

From the previous equation, the algorithm assumes GHI for an hour as $I_r$, $\eta_{STC}$ as the system efficiency $\eta$, and $A_{panel}$ with a value of 1.92 $\mathrm{m^2}$, which are the specifications present in the manufacturer data sheet [92].

However, since the manufacturer of the solar module provides more efficiency characteristics such as Normal Operating Cell Temperature (NOCT) and temperature coefficient of power, the previous equation can be enhanced considering that the model also contains temperature data. A more reliable option is the formula present in Equation 3.3 that takes into consideration more factors that directly affect the energy production.

$$E = I_r \times A_{panel} \times \eta_{temp} \times (1 - f_{loss}) \tag{3.3}$$

where,

$E$ — energy produced [Wh],
$I_r$ — solar irradiance [$\mathrm{Wh\,m^{-2}}$],

$A_{panel}$ — area of the photovoltaic panel [$m^2$],
$\eta_{temp}$ — temperature corrected efficiency,
$f_{loss}$ — additional combined losses.

As seen in Equation 3.3, the new formula contains two new parameters. The value of $f_{loss}$ was determined 10 % to account for additional combined losses, mainly because of system degradation and inverter efficiency, and to calculate the parameter $\eta_{temp}$, Equation 3.4 was used.

$$\eta_{temp} = \eta_{STC} \times [1 + \gamma \times (T_c - T_{STC})] \tag{3.4}$$

where,
$\eta_{temp}$ — temperature corrected efficiency,
$\eta_{STC}$ — standard test condition efficiency,
$\gamma$ — temperature coefficient of power [$°C^{-1}$],
$T_c$ — cell temperature [°C],
$T_{STC}$ — standard test condition temperature, which is 25 °C.

From Equation 3.4, the value of $T_c$ is yet to be determined. The definition of NOCT is a common reference used to estimate photovoltaic cell temperature under standard conditions, and it is defined as the temperature of a photovoltaic module in the conditions of 20 °C, solar irradiance of 800 $W\,m^{-2}$, and wind speed of 1 $m\,s^{-1}$. With this in mind, one of the empirical formulas to estimate cell temperature $T_c$ is based on the NOCT and actual operating conditions, as seen in Equation 3.5.

$$T_c = T_{amb} + \left(\frac{\text{NOCT} - 20}{800}\right) \times I_r \tag{3.5}$$

where,
$T_c$ — cell temperature [°C],
$T_{amb}$ — ambient temperature [°C],
NOCT — Nominal Operating Cell Temperature [°C],
$I_r$ — solar irradiance [$Wh\,m^{-2}$].

In Equation 3.5, the process assumes GHI for an hour as $I_r$, and $T_{amb}$ as the ambient temperature, both present in the weather data frame processed in the meteorologic data gathering step from the previous subsection.

### Method B

Although the previous method for estimation of photovoltaic energy production is very accurate, another option for estimating the photovoltaic production is by using Python PVLib [93]. This library is used for simulating the performance of photovoltaic energy systems, and provides multiple tools to model an entire photovoltaic site considering the various aspects of photovoltaic systems, such as solar position, irradiance and module performance.

Considering the data obtained from the previous weather gathering step, some of the data requirements for the use of this library are already met. This part of the algorithm begins by retrieving necessary weather data from the weather data frame, including temperature, relative humidity, wind speed, atmospheric pressure, and solar irradiance.

Since the library has the ability to manage the multiple components of solar irradiance, such as GHI, DHI, and DNI, all these parameters are used for the calculation, which already makes a difference from the previous model that only considered GHI as the final solar radiation. All this data is organized into a structured format that can be used for the subsequent calculations.

For further calculations, latitude, longitude and altitude need to be defined. Using these values and the formatted weather data, the algorithm calculates solar position parameters such as zenith and azimuth angles, which are essential for determining how sunlight interacts with the panels at different times of the day.

After having this data ready, the physical and electrical characteristics of the photovoltaic system are defined. PVLib contains predefined databases, that include multiple types of solar modules and inverters. For this matter, and to directly compare with the previous method, the same solar module is chosen (Canadian Solar CS6X-300M) with the same specifications mentioned previously in Table 3.1.

With all these prerequisites established, the energy yield of the photovoltaic site can be estimated, by using multiple defined functions provided in the library.

The algorithm firstly computes additional factors that affect solar energy capture, such as extraterrestrial irradiance, air mass, and angle of incidence, which describes the angle at which sunlight strikes the photovoltaic panel surface. The total solar irradiance on the panel is calculated by combining the direct, diffuse, and reflected components of sunlight, that are then adjusted for the specific tilt and orientation of the panels.

As done in the previous method, this library also takes the cell temperature into consideration, which directly affects the output of the system. After accounting for all these factors, the algorithm proceeds to calculate the effective irradiance, which is the portion that directly contributes to electricity generation.

Finally, the Direct Current (DC) power output of photovoltaic modules based on the effective irradiance is estimated by using another function within the library.

Using a generic predefined inverter in the photovoltaic system, this DC power is then converted into Alternating Current (AC) power with another function, considering the inverter characteristics, which is also a difference compared to the previous method. The AC power output is calculated for each hour of the day and remains constant the whole hour, which means that the energy production for each hour can be considered as an hourly energy output in watt-hours (Wh).

### 3.2.3 Estimation of Wind Energy Production

To begin the estimation of wind energy production, a widely used wind turbine for small applications purposes is considered. The model chosen was the RyseEnergy E-5 Horizontal Axis Wind Turbine (HAWT), present in Figure 3.2, characterized by a rated power of 4 kW for a rated wind speed of 11 $\mathrm{m\,s^{-1}}$, and a rotor radius of 2.15 m [94]. This turbine was merely selected as a test object for experimentation and validation, and any other model would also work with this solution.

Figure 3.2: RyseEnergy E-5 HAWT model, adapted from [94].

The horizontal axis triple blade wind turbine, recommends that the rotor height should be installed between 6 m and 27 m, and the cut-in and cut-out speeds are 2 $\mathrm{m\,s^{-1}}$ and 60 $\mathrm{m\,s^{-1}}$, respectively. Since no turbine is 100 % efficient, the power coefficient is a measure of how efficiently a wind turbine converts the kinetic energy of wind into electrical energy. Considering that, the referred turbine has a power coefficient $\zeta_p$ of 0.40 [94].

Given that the installation of the rotor is done in a height above 10 meters, and since our weather data about wind is measured at 10 meters height, the adjusted wind speed at the height of the rotor must be calculated by using the logarithmic wind profile formula presented in Equation 3.6.

$$u_{rotor} = u_{ref} \frac{\ln\left(\frac{z}{z_0}\right)}{\ln\left(\frac{z_{ref}}{z_0}\right)} \tag{3.6}$$

where,

$u_{rotor}$ — wind speed at $z_{rotor}$ m height above the ground surface [$\mathrm{m\,s^{-1}}$],
$u_{ref}$ — measured wind speed at $z_{ref}$ m height above the ground surface [$\mathrm{m\,s^{-1}}$],
$z_0$ — surface roughness length [m].

Considering the previous definitions, and taking into account that the estimated surface roughness $z_0$ of vineyards is typically 0.25 m [95], and the height of the rotor $z_{rotor}$ is 25 m, the equation is able to successfully calculate the adjusted wind speed $u_{rotor}$.

### Method A

With the obtained data, the energy output of the turbine is finally estimated based on the previously calculated adjusted wind speed $u_{rotor}$. If the wind speed falls below the cut-in speed (2 $\mathrm{m\,s^{-1}}$) or exceeds the cut-out speed (60 $\mathrm{m\,s^{-1}}$), the turbine produces no power. For wind speeds between the cut-in and rated speeds (11 $\mathrm{m\,s^{-1}}$), the power output is calculated using the wind power as presented by Equation 3.7.

$$P = \frac{1}{2}\rho A u^3 \zeta_p \tag{3.7}$$

where,

$P$ — power output [W],
$\rho$ — air density, which is 1.225 $\mathrm{kg\,m^{-3}}$,
$A$ — rotor swept area [$\mathrm{m^2}$],
$u$ — adjusted wind speed, in this case $u_{rotor}$ [$\mathrm{m\,s^{-1}}$],
$\zeta_p$ — turbine power coefficient.

If the wind speed exceeds the rated speed, the power output is capped at the rated power of the turbine, which is 4 kW. As a representation of a loss factor, an availability factor is also defined, representing the proportion of time the turbine is operational (90 % in this case), that is then applied to the calculated power.

Considering that the power output is calculated for each hour of the day and remains constant the whole hour, the energy production for each hour can be derived, achieving the hourly energy output in watt-hours (Wh).

### Method B

Despite the previous method for estimation of wind energy production being very reliable, if a manufacturer provides a power curve of its equipment, the energy

produced can be estimated more accurately. Considering the same wind turbine (RyseEnergy E-5 HAWT) and that all of its respective parameters remain unchanged (including height of mounting), the manufacturer provides a power curve table that demonstrates the relationship between wind speed and the turbine's energy output, showing how efficiently it generates power with different wind conditions.

Once again, since the installation of the rotor is done in a height above the measured wind speed height, the adjusted wind speed at the height of the rotor $u_{rotor}$ still needs to be calculated by using the previous logarithmic wind profile in Equation 3.6. Furthermore, the algorithm also assumes that if this adjusted wind speed falls below the cut-in speed or exceeds the cut-out speed, the turbine produces no power.

However, instead of using the wind power formula previously mentioned in Equation 3.7 for wind speed values between cut-in and rated speeds, it is possible to estimate the power output from the equipment power curve in Table 3.2, which achieves a more precise methodology for this particular wind turbine. Like the previous method, if the wind speed exceeds the rated speed, the power output is capped at the rated power of the turbine, which is 4 kW.

Table 3.2: RyseEnergy E-5 HAWT power curve, adapted from [94].

| **Wind Speed** [$\mathrm{m\,s^{-1}}$] | **Power Output** [W] |
|---|---|
| 2 | 10 |
| 3 | 50 |
| 4 | 260 |
| 5 | 456 |
| 6 | 900 |
| 7 | 1400 |
| 8 | 2000 |
| 9 | 2800 |
| 10 | 3500 |
| 11 | 4000 |

Although the table provides all the wind speed values between cut-in and rated speeds, it is possible to observe that all these values are integers. This means that if the algorithm obtains a number with decimals that is between two integers (which is a recurrent situation), an error would occur because there would be no such value in the power curve table provided by the manufacturer. To solve this issue, the algorithm performs a process of linear interpolation to estimate the power output of a wind turbine at intermediate wind speeds using the given power curve.

To interpolate the power output for a wind speed between two known data points, the linear interpolation formula is used. For a wind speed $u$ between $u_1$ and $u_2$ with corresponding power outputs $P_1$ and $P_2$, the power output $P$ is given by Equation 3.8.

$$P = P_1 + \frac{(u - u_1)}{(u_2 - u_1)} \times (P_2 - P_1) \tag{3.8}$$

where,

$P$ — power output [W],
$u$ — adjusted wind speed, in this case $u_{rotor}$ [$\mathrm{m\,s^{-1}}$],
$u_1$, $u_2$ — power curve known wind speeds [$\mathrm{m\,s^{-1}}$],
$P_1$, $P_2$ — power outputs corresponding to $u_1$, $u_2$ [W].

As carried out in the previous method, after the power calculation, the availability factor of 90 % is applied to the calculated power. Considering that the power output is calculated for each hour of the day and remains constant the whole hour, the hourly energy output is also estimated in watt-hours (Wh).

### 3.2.4 Estimation of Energy Sell Price

When implementing sustainable irrigation systems for vineyards, and agriculture in general, a key factor that should be considered is the grid energy price. Since the multiple systems can vary, the irrigation processes of a farm might not have enough on-site power production to cover all the energy required. As irrigation processes often rely on electric pumps and other electrical machinery, fluctuations in energy prices can directly impact the effectiveness of irrigation operations.

To accurately determine the economic implications of energy consumption for irrigation, it is crucial to consider data of energy prices for planning and decision-making processes. This allows farmers and managers to evaluate the cost-efficiency of energy consumption, optimize its usage, and explore potential adjustments to reduce the costs.

In this context, the cost of grid electricity in Portugal is usually affected directly by *Operador do Mercado Ibérico de Energia* – Iberian Energy Market Operator (OMIE) [96], which impacts the final cost of electricity sold by the operators. OMIE database provides valuable insights about how electricity varies hourly throughout the day, and one can see that the renewable energy production by hydro, wind or photovoltaic sites, directly impacts its final reference value. By utilizing this data, it is possible to add another variable to make informed decisions about managing irrigation systems sustainably.

With this in mind, the developed algorithm gathers and processes information about energy price, and considers the electricity hourly prices of Portugal's daily market, available in OMIE database in the form of a CSV file [96]. Since the response time is high due to many requests from multiple sources, data files are stored locally to optimize the process for further executions. However, the algorithm always verifies and downloads the most recent prices, so that the system is always up to date.

Nevertheless, while the OMIE database provides essential data on electricity prices, it is important to consider that the actual cost of energy can be significantly higher due to additional charges. Seller management system costs, profit margins and grid access taxes, are usually charged by every seller, and directly impact the final cost of electricity [97]. As a result, while OMIE data offers a benchmark for understanding market prices, it is important to consider these extra charges in order to determine the true cost of electricity and their impact on sustainable irrigation processes. Considering this, Equation 3.9 establishes the true hourly grid energy sell price indexed to OMIE, with a real case scenario applied by a portuguese seller [98].

$$C_{grid} = (C_{omie} + C_{profit}) \times (1 + f_{loss}) + C_{tax} \tag{3.9}$$

where,

$C_{grid}$ — grid energy sell price [EUR kWh$^{-1}$],
$C_{omie}$ — OMIE energy sell price [EUR kWh$^{-1}$],
$C_{profit}$ — seller management system costs and profit margin [EUR kWh$^{-1}$],
$f_{loss}$ — grid loss factor,
$C_{tax}$ — grid access tax [EUR kWh$^{-1}$],

All these additional taxes are defined for a period of time (usually months), which means that $C_{grid}$ is affected hourly every day only by $C_{omie}$. For reference, the seller management system costs and grid access tax applied by the portuguese seller in August 2024, were 0.026 EUR kWh$^{-1}$ and 0.03 EUR kWh$^{-1}$, respectively, and the grid loss factor was fixed at 15 % [97, 98].

## 3.3 Evapotranspiration Estimation Module

After processing the various types of data, the module in the current section is responsible for estimating the ET of the vineyard. As stated previously in the literature review of this dissertation, ET is an extremely important parameter that can determine the water needs of any plantation.

To study this value, it is important to firstly determine $ET_0$ (reference evapotranspiration) and then $ET_c$ (crop evapotranspiration), using $K_c$ (crop coefficient). Considering what was explored in the literature review, the objective of this module is to estimate the crop evapotranspiration for each day available in the previous processed weather data, in order to determine the water needs for posterior implementation.

In this module, the system processes the weather data available in a CSV file, and with multiple calculations it estimates the reference ET. To determine the crop ET, the algorithm uses a relation between the Growing Degree Days (GDD) and $K_c$, that can be obtained with temperature data from the full growing season. Once again,

the weather data contained in the CSV file, can be replaced by on-site information from a weather station, as long as it has the same parameters and units.

### 3.3.1 Reference Evapotranspiration Estimation Procedure

As stated in the literature review, to determine $ET_0$, the FAO Penman–Moneith method, which includes the formula present in Equation 3.10, can be applied [61].

$$ET_0 = \frac{0.408\Delta(R_n - G) + \psi\frac{900}{T+273}u_2(e_s - e_a)}{\Delta + \psi(1 + 0.34u_2)} \tag{3.10}$$

where,

$ET_0$ — reference evapotranspiration [$\mathrm{mm\,day^{-1}}$],
$R_n$ — net radiation at the crop surface [$\mathrm{MJ\,m^{-2}\,day^{-1}}$],
$G$ — soil heat flux density [$\mathrm{MJ\,m^{-2}\,day^{-1}}$],
$T$ — mean daily air temperature at 2 m height [°C],
$u_2$ — wind speed at 2 m height [$\mathrm{m\,s^{-1}}$],
$e_s$ — saturation vapor pressure [kPa],
$e_a$ — actual vapor pressure [kPa],
$e_s - e_a$ — saturation vapor pressure deficit [kPa],
$\Delta$ — slope of saturation vapor pressure curve [$\mathrm{kPa\ °C^{-1}}$],
$\psi$ — psychrometric constant [$\mathrm{kPa\ °C^{-1}}$].

In order to estimate reference evapotranspiration, this method is based on the climatic data available, and the formula needs to be split into multiple parts giving its complexity. All these formulas were adapted from the FAO Irrigation and Drainage Paper 56 (FAO-56) [61] for the available weather data.

Starting off with a simple calculation, the mean daily temperature $T$ can be estimated by using Equation 3.11. For this calculation, the algorithm analyses all the hourly data in the weather data frame and determines the maximum and minimum temperature values for each day.

$$T = \frac{T_{max} + T_{min}}{2} \tag{3.11}$$

where,

$T$ — mean daily air temperature [°C],
$T_{max}$ — maximum daily air temperature [°C],
$T_{min}$ — minimum daily air temperature [°C].

Another simple calculation is the estimation of wind speed at the the FAO-56 standard height of 2 m ($u_2$). It is important to verify the height at which wind speed is measured, as wind speeds obtained at different heights above the soil surface are

different. Since our weather data concerning wind is measured at 10 meters height, the already known logarithm wind profile formula is applied in Equation 3.12.

$$u_2 = u_{ref} \frac{\ln\left(\frac{z}{z_0}\right)}{\ln\left(\frac{z_{ref}}{z_0}\right)} \tag{3.12}$$

where,

$u_2$ — wind speed at $z$ m height above the ground surface [$\mathrm{m\,s^{-1}}$],

$u_{ref}$ — measured wind speed at $z_{ref}$ m height above the ground surface [$\mathrm{m\,s^{-1}}$],

$z_0$ — surface roughness length [m].

For this calculation, the estimated surface roughness $z_0$ of vineyards is considered 0.25 m and the FAO-56 standard height $z$ is 2 m, which means the equation is able to successfully calculate the adjusted wind speed $u_2$.

As seen in Equation 3.10, for the estimation of reference evapotranspiration, the slope of saturation vapor pressure curve $\Delta$ is required. This value can be achieved by Equation 3.13, that requires simple data already obtained.

$$\Delta = \frac{4098\left(0.6108\exp\left(\frac{17.27\times T}{T+237.3}\right)\right)}{(T+237.3)^2} \tag{3.13}$$

where,

$\Delta$ — slope of saturation vapor pressure curve [kPa $^{\circ}\mathrm{C}^{-1}$],

$T$ — mean daily air temperature [°C],

exp — base of natural logarithm.

The psychrometric constant $\psi$ is also a required value that relates the partial pressure of water in air to the air temperature, and can be calculated by Equation 3.14.

$$\psi = 0.000665 \times p \tag{3.14}$$

where,

$\psi$ — psychrometric constant [kPa $^{\circ}\mathrm{C}^{-1}$],

$p$ — atmospheric pressure [kPa].

In order to determine saturation vapor pressure $e_s$, a more complex calculation is required. Saturation vapor pressure is related to air temperature, which means it can be calculated from the air temperature. For this matter, Equation 3.15 establishes the estimation of $e_s$ as the mean between the saturation vapor pressure at the daily maximum and minimum air temperature. Both of the temperatures are available in

the weather data frame, and the respective saturation vapor pressure values can be achieved by Equations 3.16 and 3.17, respectively.

$$e_s = \frac{e_{(T_{max})} + e_{(T_{min})}}{2} \tag{3.15}$$

$$e_{(T_{max})} = 0.6108 \exp\left(\frac{17.27 \times T_{max}}{T_{max} + 237.3}\right) \tag{3.16}$$

$$e_{(T_{min})} = 0.6108 \exp\left(\frac{17.27 \times T_{min}}{T_{min} + 237.3}\right) \tag{3.17}$$

where,

$e_s$—saturation vapor pressure [kPa],
$e_{(T_{max})}$—saturation vapor pressure at daily maximum air temperature [kPa],
$e_{(T_{min})}$—saturation vapor pressure at daily minimum air temperature [kPa],
$T_{max}$ — maximum daily air temperature [°C],
$T_{min}$ — maximum daily air temperature [°C].

To calculate the actual vapour pressure, FAO-56 presents multiple ways of deducing this value depending on the available data, but all of them consider the values of relative humidity [61]. However, the most accurate way of calculating this value is by using daily maximum and minimum values of relative humidity ($RH_{max}$ and $RH_{min}$, respectively). These are obtained in the algorithm, which analyses all the hourly data in the weather data frame and determines the maximum and minimum values for each day.

With the values of relative humidity, the actual vapour pressure $e_a$ is then calculated with the formula presented in Equation 3.18, that also requires values obtained previously in Equations 3.16 and 3.17.

$$e_a = \frac{e_{(T_{min})}\left[\frac{RH_{max}}{100}\right] + e_{(T_{max})}\left[\frac{RH_{min}}{100}\right]}{2} \tag{3.18}$$

where,

$e_a$ — actual vapour pressure [kPa],
$e_{(T_{min})}$ — saturation vapour pressure at daily minimum air temperature [kPa],
$e_{(T_{max})}$ — saturation vapour pressure at daily maximum air temperature [kPa],
$RH_{max}$ — maximum relative humidity [%],
$RH_{min}$ — minimum relative humidity [%].

Another parameter which can be easily calculated is soil heat flux density $G$, because it can be considered null for a daily estimation, which means that Equation 3.19 is also defined within the algorithm.

$$G = 0 \tag{3.19}$$

where,

$G$ — soil heat flux density [$\mathrm{MJ\,m^{-2}\,day^{-1}}$].

From all the previous equations, one can see that the only missing value to finally determine reference evapotranspiration $ET_0$ is net radiation at the crop surface $R_n$. From the FAO-56 this is by far one of the most complex values to estimate, because it considers a lot of factors that must be handled carefully as they can considerably impact the final value.

In order to estimate the value of net radiation at the crop surface $R_n$, a difference between the incoming net shortwave radiation $R_{ns}$ and the outgoing net longwave radiation $R_{nl}$ must be calculated, as shown in Equation 3.20.

$$R_n = R_{ns} - R_{nl} \tag{3.20}$$

where,

$R_n$ — net radiation at the crop surface [$\mathrm{MJ\,m^{-2}\,day^{-1}}$],
$R_{ns}$ — incoming net shortwave radiation [$\mathrm{MJ\,m^{-2}\,day^{-1}}$],
$R_{nl}$ — outgoing net longwave radiation [$\mathrm{MJ\,m^{-2}\,day^{-1}}$].

From Equation 3.20, the incoming net shortwave radiation $R_{ns}$ is the easiest parameter to calculate, according to Equation 3.21.

$$R_{ns} = (1 - a)R_s \tag{3.21}$$

where,

$R_{ns}$ — incoming net shortwave radiation [$\mathrm{MJ\,m^{-2}\,day^{-1}}$],
$R_s$ — incoming solar radiation [$\mathrm{MJ\,m^{-2}\,day^{-1}}$],
$a$ — albedo or canopy reflection coefficient.

The canopy reflection coefficient also known as albedo, has a fixed value of 0.23 for the hypothetical reference crop [61], which means the only required value is the incoming solar radiation $R_s$. Since data regarding solar radiation is available in the weather data frame, the values only need to be converted to the correct unit.

Considering that the weather data frame typically contains hourly information about solar radiation in $\mathrm{W\,m^{-2}}$, we can assume that this represents the power received per square meter during that hour. From this assumption, the incoming solar radiation for the whole day converted to the required units, can be calculated with Equation 3.22.

$$R_s = \sum_{h=1}^{24} \left( R_{s[\mathrm{W\,m^{-2}}]} \times \frac{3600}{10^6} \right) \tag{3.22}$$

where,

$R_s$ — incoming solar radiation [$\mathrm{MJ\,m^{-2}\,day^{-1}}$],

$R_{s[\mathrm{W\,m^{-2}}]}$ — incoming solar radiation [$\mathrm{W\,m^{-2}}$].

The last parameter needed to complete the formula in Equation 3.20 is the outgoing net longwave radiation, represented by Equation 3.23, which presents a lot of variables that need to be carefully estimated.

$$R_{nl} = \sigma \left[ \frac{(T_{max[K]})^4 + (T_{min[K]})^4}{2} \right] (0.34 - 0.14\sqrt{e_a}) \left( 1.35 \frac{R_s}{R_{so}} - 0.35 \right) \tag{3.23}$$

where,

$R_{nl}$ — outgoing net longwave radiation [$\mathrm{MJ\,m^{-2}\,day^{-1}}$],

$\sigma$ — Stefan-Boltzmann constant, which is 4.903 $\times 10^{-9}$ $\mathrm{MJ\,K^{-4}\,m^{-2}\,day^{-1}}$,

$T_{max[K]}$ — maximum daily air temperature [K = °C + 273.16],

$T_{min[K]}$ — minimum daily air temperature [K = °C + 273.16],

$e_a$ — actual vapor pressure [kPa],

$R_s$ — incoming solar radiation [$\mathrm{MJ\,m^{-2}\,day^{-1}}$],

$R_{so}$ — clear sky solar radiation [$\mathrm{MJ\,m^{-2}\,day^{-1}}$],

As seen in Equation 3.23, some of the parameters were already calculated by the routine such as $R_s$, $e_a$, and maximum and minimum temperatures after their conversion to absolute temperatures. However, the one missing value is the clear sky solar radiation $R_{so}$, that can be obtained from altitude and extraterrestrial radiation, as shown in Equation 3.24.

$$R_{so} = (0.00002H + 0.75)R_a \tag{3.24}$$

where,

$R_{so}$ — clear sky radiation [$\mathrm{MJ\,m^{-2}\,day^{-1}}$],

$R_a$ — extraterrestrial radiation [$\mathrm{MJ\,m^{-2}\,day^{-1}}$],

$H$ — elevation above sea level [m].

The value of elevation above sea level $H$ should be defined previously and must differ from vineyard to vineyard but, in this particular case, it is considered to be 250 m. Regarding extraterrestrial radiation $R_a$, this value can be estimated with Equation 3.25.

$$R_a = \left(\frac{24 \times 60}{\pi}\right) G_{sc} d_r \left[\omega_s \sin(\phi)\sin(\delta) + \cos(\phi)\cos(\delta)\sin(\omega_s)\right] \tag{3.25}$$

where,

$R_a$ — extraterrestrial radiation [MJ m$^{-2}$ day$^{-1}$],
$G_{sc}$ — solar constant, which is 0.0820 MJ m$^{-2}$ min$^{-1}$,
$d_r$ — inverse relative distance between earth and sun,
$\delta$ = solar declination [rad],
$\omega_s$ — sunset hour angle [rad],
$\phi$ = latitude [rad].

The missing values in the previous equation can be estimated by the following Equations 3.26, 3.27 and 3.28. The following equations apply defined values that can be obtained by the routine itself, such as the day of the year $J$, and latitude $\phi$, which can be defined by the user or obtained from the API request.

$$d_r = 1 + 0.033 \cos\left(\frac{2\pi}{365} J\right) \tag{3.26}$$

$$\delta = 0.409 \sin\left(\frac{2\pi}{365} J - 1.39\right) \tag{3.27}$$

$$\omega_s = \arccos\left[-\tan(\phi)\tan(\delta)\right] \tag{3.28}$$

where,

$d_r$ — inverse relative distance between earth and sun,
$\delta$ — solar declination [rad],
$\omega_s$ — sunset hour angle [rad],
$\phi$ — latitude [rad],
$J$ — number of the day in the year between 1 and 365 (or 366 in a leap year).

With the values obtained from all the previous equations, the process of determining net radiation at the crop surface $R_n$ is completed, and the algorithm can finally determine reference evapotranspiration $ET_0$ with the previously stated Equation 3.10 from the FAO Penman–Moneith method.

### 3.3.2 Crop Coefficient Determination

As previously mentioned, in order to determine crop evapotranspiration $ET_c$, the crop coefficient $K_c$ of the vineyards must be estimated. In cases where a plantation requires more water than grass (which is the reference crop for $ET_0$), the value of $K_c$ is bigger than 1. In the opposite case, where the crop requires less water, $K_c$ is less

than 1. Generally speaking, the $K_c$ of vineyards is typically less than 0.8, meaning that they require less water than grass. However, this value is not constant, and varies throughout the growing season and stage of the crops [99].

A parameter that is used to estimate the growth and development of certain crops during the growing season, is GDD that can be calculated with Equation 3.29 [100].

$$\text{GDD} = \frac{T_{max} + T_{min}}{2} - T_{base} \quad \text{with} \quad \text{GDD} \geq 0 \tag{3.29}$$

where,

GDD — growing degree days [corresponding to °C],
$T_{max}$ — maximum daily temperature [°C],
$T_{min}$ — minimum daily temperature [°C],
$T_{base}$ — base temperature [°C].

As seen in this equation, the mean daily temperature is calculated as GDD and includes a minimum development threshold that must be exceeded for growth to occur, referred to as the base temperature $T_{base}$. This means that if the mean temperature is below $T_{base}$, GDD must be considered null. For the simulation location, which is in a Douro Valley, the base temperature $T_{base}$ is typically considered as 10 °C, and the growing season usually begins on April 1$^{st}$ [101].

In order to determine the GDD of the vineyard, temperature data is required, and similarly to what has been done previously in the meteorological data gathering set of operations in data processing module, the first part of the code does a request to WeatherAPI. Since the only concern are daily temperatures, the request is done differently, in order to get a response exclusively with the maximum and minimum temperatures for the requested days. This information is then processed into a data frame, similarly to the previous modules.

With the data frame of maximum and minimum temperatures, Equation 3.29 is applied to estimate the GDD per day, and Accumulated Growing Degree Days (AGDD) is also determined for every day using a cumulative sum function, explained by Equation 3.30

$$\text{AGDD}_k = \sum_{i=1}^{k} \text{GDD}_i \tag{3.30}$$

Washington State University provided a varying-rate $K_c$ that is dependent on AGDD, which serves as an estimator of canopy and fruit development [99]. This means that the vineyard will have a $K_c$ that changes throughout the growing season, as seen in Figure 3.3.

However, since the data provided by Washington State University considered a base temperature of 50 °F, a conversion to °C is required. The base temperature can be considered the same, as 50 °F is equivalent to 10 °C. Regarding the GDD, as stated by [102], 9 GDD calculated using Fahrenheit are equal to 5 GDD using Celsius, which means Equation 3.31 is applied for this conversion.

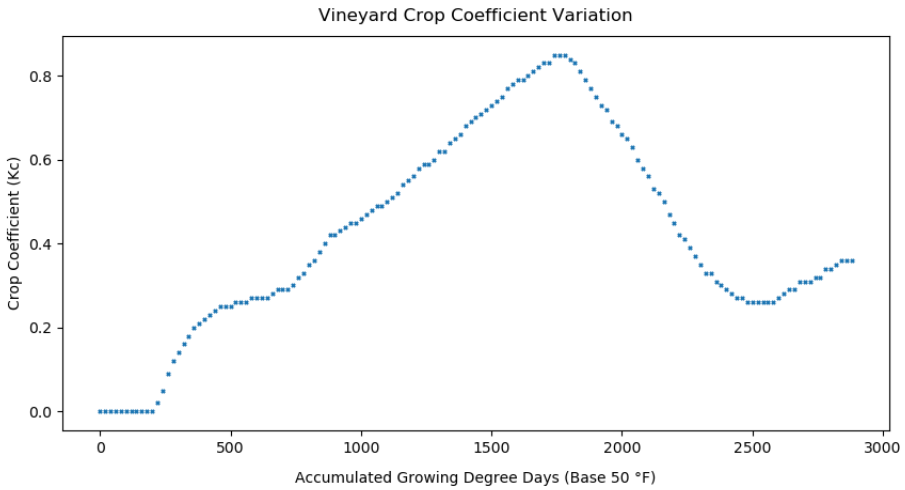


Figure 3.3: Variation of $K_c$ with AGDD, adapted from [99].

$$\mathrm{GDD}_{[^\circ\mathrm{C}]} = \frac{9}{5} \times \mathrm{GDD}_{[^\circ\mathrm{F}]} \tag{3.31}$$

where,

$\mathrm{GDD}_{[^\circ\mathrm{C}]}$ — growing degree days [corresponding to °C],
$\mathrm{GDD}_{[^\circ\mathrm{F}]}$ — growing degree days [corresponding to °F].

Despite the previous data already containing lots of points for multiple AGDD and $K_c$, there is only a relation for every 20 $GDD_{[^\circ\mathrm{F}]}$ or 11.11 $GDD_{[^\circ\mathrm{C}]}$. This means that if the routine gets an AGDD number that is between two relation values (which is a common situation), an error would occur because there would be no corresponding $K_c$. To solve this issue, the algorithm performs a process of linear interpolation, and the crop coefficient $K_c$ is successfully estimated.

As stated in Chapter 2, after determining the value of $K_c$, in order to estimate the crop evapotranspiration $ET_c$, Equation 3.32 is applied using reference evapotranspiration $ET_0$ obtained previously.

$$ET_c = K_c \times ET_0 \tag{3.32}$$

where,

$ET_c$ — crop evapotranspiration [$\mathrm{mm\,day^{-1}}$],
$K_c$ — crop coefficient,
$ET_0$ — reference evapotranspiration [$\mathrm{mm\,day^{-1}}$].

## 3.4 Irrigation Model

With the determination of crop evapotranspiration $ET_c$, the following system module is responsible for estimating the vineyard's water requirements. Using all the data available from evapotranspiration parameters and weather (mainly precipitation), the purpose of this module is to output the amount of water required per day for irrigation systems, considering the previous data available in multiple CSV files.

As previously stated in the literature review chapter, drip irrigation is one of the most efficient methods to water a vineyard field. However, this module can take into account multiple irrigation methods, as long as a value of irrigation efficiency is provided. If the dimensions of row and vine spacing are defined, the algorithm is also able to estimate the water requirements per vine, which can give a better perception of how much water every plant needs per day to achieve its optimal state.

The first parameter to be discussed is precipitation, which is of great importance in irrigation systems. This value directly impacts the amount of water required by the irrigation system, since it can partially or fully satisfy the water needs of a vineyard field. However, precipitation is not fully effective for irrigation purposes and, for this matter, Equation 3.33 defines the effective precipitation $\Gamma_e$.

$$\Gamma_e = \Gamma \times f_{Pe} \tag{3.33}$$

where,

$\Gamma_e$ — effective precipitation [$\mathrm{mm\,day^{-1}}$],
$\Gamma$ — total precipitation [$\mathrm{mm\,day^{-1}}$],
$f_{Pe}$ — effective precipitation factor.

As seen in the previous equation, this parameter is simply calculated by defining an effective precipitation factor that can vary according to the type of terrain, soil drainage, plantation, and other variables [103]. Food and Agriculture Organization (FAO) Training Manual No. 3 [104], which is related to irrigation water management, defines this value as 60 % for months when precipitation is lower than 75 $\mathrm{mm\,month^{-1}}$, and 80 % for the opposite scenario. For simplicity, this algorithm assumes the value as 70 %, which is a considerate median value. However, after implementation, vineyard managers should adapt this value as their needs, since the terrain might need more or less water on rainy days.

With the determination of effective precipitation $\Gamma_e$, the Net Irrigation Requirement (NIR) is then calculated by subtracting the effective precipitation $\Gamma_e$ from the estimated crop evapotranspiration $ET_c$. An additional condition must be defined, because the value of NIR can never be below zero, as Equation 3.34 shows.

$$\mathrm{NIR} = ET_c - \Gamma_e \quad \text{with} \quad \mathrm{NIR} \geq 0 \tag{3.34}$$

where,

NIR — net irrigation requirement [mm day$^{-1}$],
$ET_c$ — crop evapotranspiration [mm day$^{-1}$],
$\Gamma_e$ — effective precipitation [mm day$^{-1}$].

To obtain the Gross Irrigation Requirement (GIR), which can be considered as the water needs of the vineyard for the day, an effective irrigation factor $f_{Ie}$ is applied, as seen in Equation 3.35.

$$\mathrm{GIR} = \frac{\mathrm{NIR}}{f_{Ie}} \tag{3.35}$$

where,

NIR — net irrigation requirement [mm day$^{-1}$],
GIR — gross irrigation requirement [mm day$^{-1}$],
$f_{Ie}$ — effective irrigation factor.

The effective irrigation factor $f_{Ie}$ must be a previously defined value, according to the efficiency of the irrigation system being used in the vineyard. Considering one of the most effective methods, which is drip irrigation, a value of 85 % is assumed for this matter.

As vineyards typically tend to have areas in the order of hectares (ha), the total water requirement in liters per hectare per day $\mathrm{GIR}_{ha}$ is calculated. This is achievable because 1 mm day$^{-1}$ amount of water is equivalent to 1 L m$^{-2}$ day$^{-1}$, which means that Equation 3.36 easily manages this conversion.

$$\mathrm{GIR}_{ha} = \mathrm{GIR} \times 10^4 \tag{3.36}$$

where,

$\mathrm{GIR}_{ha}$ — gross irrigation requirement per hectare [L ha$^{-2}$ day$^{-1}$],
GIR — gross irrigation requirement [mm day$^{-1}$],

For a better perception of how much irrigation is needed by each grapevine, an approximation of the the total water requirement in liters per grapevine per day $\mathrm{GIR}_{gv}$ can also be estimated, if row spacing $L_r$ and vine spacing $L_v$ are provided, as seen in Equation 3.37.

$$\mathrm{GIR}_{gv} = \mathrm{GIR} \times (L_r \times L_v) \tag{3.37}$$

where,

$\mathrm{GIR}_{gv}$ — gross irrigation requirement per grapevine [L day$^{-1}$],
GIR — gross irrigation requirement [mm day$^{-1}$],

$L_r$ — vineyard row spacing [m],
$L_v$ — vineyard vine spacing [m].

Further calculations can also be executed, such as the amount of time that irrigation needs to be turned on in each row of grapevines per day, if the irrigation system flow rate is provided. Considering a row containing $N$ grapevines and a flow rate of $Q$, the time of irrigation for the vineyard row can be estimated using Equation 3.38.

$$t = \frac{N \times \mathrm{GIR}_{gv}}{Q} \tag{3.38}$$

where,
$t$ — irrigation time [$\mathrm{s\,day^{-1}}$],
$Q$ — irrigation flow rate [$\mathrm{L\,s^{-1}}$],
$N$ — number of grapevines in the row,
$\mathrm{GIR}_{gv}$ — gross irrigation requirement per vine [$\mathrm{L\,day^{-1}}$].

To implement or analyze all the previously obtained data, a CSV file containing all the metrics is generated, as well as a visual graphic with the most important values. With these considerations, vital information is acquired and vineyard managers can incorporate this data on their systems, in order to guarantee the maximum sustainability and resource efficiency, specially in terms of water savings.

## 3.5 Energy Model

The last module of the intelligent system is the energy model, which contains a set of operations that can estimate the optimal energy consumption timings. This algorithm can be applied not only for irrigation purposes, since it can estimate the best timings to power water pumps, flow pumps or valves, but also for the multiple electric devices that a vineyard warehouse can have [105, 106].

With multiple series of data processing and analysis steps to estimate optimal energy consumption timings, this module is based on electricity grid prices previously estimated, and renewable energy production, such as wind and solar. Given the modular nature of this system, this routine can use data sourced from different places, such as multiple CSV files, that can be either formed by the previous data processing module, or directly inserted by the user.

Starting of with the data processing, this module reads the information contained in the CSV files, such as the grid price and renewable energy production. All this information is merged considering the date and time of the information, in order to ensure that the data is in a consistent format for further processing.

Since this module does not require the source of renewable energy production, all the solar and wind energy is combined to a single value that displays the total amount of energy production. Once again, given the modular nature of the algorithm, the vineyard can have multiple sources of renewable energy production, or none.

Given that the optimal energy consumption timings should be considered per day, the algorithm then applies a normalization per day and all the values range between 0 and 1, for further model training. This process is characterized by scaling all numerical values in a dataset to a common range, in order to ensure that all features contribute equally to a model which denies domination of features with larger ranges compared to smaller ones.

The decision of normalization per day was applied for three main reasons: daily fluctuations, model stability and comparative analysis. Since data such as grid price and renewable energy can fluctuate significantly over a day, by normalizing these values within each day, the model can better distinguish changes within the day rather than being influenced by absolute values. This will ensure the achievement of better model stability, since it is not biased by differences in overall energy production or prices between days. These steps further allow a more meaningful comparison of values on a relative scale, rather than an absolute one.

In energy management systems, users often want to optimize their energy usage to minimize costs while maximizing the use of renewable energy sources. However, given the availability and fluctuation of these parameters, an heuristic approach combines these factors into a single score that reflects the most favorable times for energy consumption. Given the data normalization, the next step of the algorithm is to define the heuristic calculation for the most optimal moments. This is estimated using a weighted combination of the grid price and renewable energy, where the formula incorporates predefined weights, and the score is then normalized between 0 and 1.

The heuristic of the model is defined in Equation 3.39, which clearly evidences that the optimal score is calculated by combining the two main factors of energy grid price $C$ and renewable energy production $E$, where lower grid prices are preferred for minimizing costs and higher renewable energy availability is preferred for maximizing the use of clean energy.

$$S^* = \alpha \times (1 - C) + \beta \times E \tag{3.39}$$

where,

$S^*$ — normalized optimal score $[0 \leq S^* \leq 1]$,

$C$ — normalized grid price $[0 \leq C \leq 1]$,

$E$ — normalized renewable energy production $[0 \leq E \leq 1]$,

$\alpha$ — grid energy price weight,

$\beta$ — renewable energy production weight.

As seen in Equation 3.39, there are two predefined weights $\alpha$ and $\beta$, that are set to 1 and 1.5, respectively, since the model wants to value more the renewable energy production. However, these weights can be changed accordingly to user preferences.

With the previous straightforward approach to determine the best times for energy consumption, the significance of low grid prices and importance of high renewable energy availability are balanced. This score helps identify the most cost-effective and environmentally friendly times to use energy, which will then guide decision-making, help reduce costs and achieve better energy sustainability.

In order to extract more features from the data, the normalized hour adjusted to renewable energy is also calculated by multiplying the hour of the day in a cyclical format by renewable energy production, as seen in Equation 3.40. This feature captures the interaction between the hour of day and renewable energy production, since it often follows a daily pattern, particularly in photovoltaic energy production. This feature, along with the previous heuristic defined, helps the model understand how energy availability changes throughout the day and identify patterns.

$$F_h = \sin^2\left(\frac{2\pi \times h}{24}\right) \times E \tag{3.40}$$

where,

$F_h$ — hour adjusted to renewable energy feature $[0 \leq F_h \leq 1]$,

$h$ — hour of the day $[0 \leq h \leq 23]$,

$E$ — normalized renewable energy production $[0 \leq E \leq 1]$,

After defining the features, which are the grid energy sell price $C$ and renewable energy production $E$, as well as the adjusted hour of the day $F_h$, the next step is the model definition.

Characterized by providing a discrete or continuous output, high interpret ability and a good non-linearity handling, a Decision Tree model was chosen. This supervised learning algorithm is used for classification, regression and decision-making tasks, which aligns with the the intended objective. It works by recursively splitting the dataset into subsets based on the most significant features, creating a structure similar to a tree. This type of model is intuitive, and can show how decisions are made based on the input features. It is also capable of well handling noisy or irrelevant information, and the amount of data typically needed for the model to perform well is low, meaning the training time of this model is usually fast [107, 108].

Since the purpose is to predict continuous numerical values and not categorical labels or classes, the Decision Tree Regressor is chosen, instead of the Decision Tree Classifier. One downside of this model is that it can be prone to over fitting, especially with very complex trees. To mitigate this issue, a more complex method named Random Forest is typically used [109, 110]. However, since our tree is not

very complex and has a small amount of data, the Decision Tree Regressor model performed well after a few comparison tests.

Before training the model, which is a critical phase in the machine learning workflow where an algorithm learns from the training data to make predictions or decisions, the data must be prepared and split into training and test set. Using $scikit-learn$ [111], which is an open-source machine learning library utilized in Phyton, the features and labels are defined. The features are the input variables the model uses to learn, and the labels are the values that the model predicts. In this case, the features are the ones previously stated, and the label is the normalized optimal score $S^*$ defined by the heuristic in Equation 3.39, that defines the optimal energy consumption timings.

After the definition of features and labels, that data is then split into a training and test set, where the training set is used to train the model, while the test set is used to evaluate its performance. The proportion of the dataset to be used for testing, which is defined as the test size, is established as 20 %, and a random state is defined to control the randomness of the data splitting process. The random state definition is a good practice, because every time the algorithm is executed, the same train-test split occurs, which is useful for consistency and debugging.

With the previous settings, the model is ready to be trained and make predictions, using multiple functions provided by the $scikit-learn$ library, such as the model $fit$ and $predict$ ones. After some processing and formatting, all the predicted information and features weights are then stored in a CSV file, and a graphical image is generated containing the predicted score $S_p^*$ for optimal energy consumption. All this information can be used to guide decision-making in energy management systems, ensuring the highest level of sustainability and resource efficiency.

# Chapter 4

# Results and Discussion

With the methodology of the developed intelligent resource management explained, the purpose of the current chapter is to present the findings and results derived from the methods and calculations in the previous chapter, in order to validate the system. The outcomes are analyzed and discussed to evaluate their significance, implications, and alignment with the objectives of this study, to provide a comprehensive understanding of all achieved results. The chapter explores potential explanations for the observed trends, as well as providing multiple simulations of realistic conditions with multiple interchanging variables. All the system information outputs can also be analyzed in Appendix A, which contains the log file of the system.

## 4.1 Test Scenario

In order to experiment and validate the system, a test scenario was defined, which has the objective to host the system and present the findings and results obtained from the methods clarified in the previous chapter. With this purpose, some assumptions need to be accounted for and, once again, they can be adapted according to user preferences and vineyard specifications. As stated previously, since the model is a prototype built without on-site data, the simulation location chosen was Valença do Douro, Portugal, whose coordinates are 41°10'23.4"N, 7°32'54.1"W, merely for test purposes.

As a reminder, the solar module used for this simulation was Canadian Solar CS6X-300M, and it was considered that the photovoltaic site has 4 units, totalling to

a theoretic maximum of 1200 Wp. The number of units can be changed according to user preferences, in order to possibly match the vineyard's installed equipment. The chosen wind turbine for the simulation was RyseEnergy E-5 HAWT, characterized by a rated power of 4 kW for a rated wind speed of 11 $\mathrm{m\,s^{-1}}$. Once again, similarly to the photovoltaic simulation, the user can define the number of wind turbines installed on-site but, for simplicity, the number of units for the current simulation was considered to be 1. Row spacing and vine spacing are also predefined values that can always be changed and, for this test scenario, these values were defined as 2 m and 1.1 m, respectively, in order to obtain gross irrigation requirements per vine.

The system began running on August 13$^{\mathrm{th}}$, 2024, at approximately 03:50, with the data processing module, which means all the results extend from August 6$^{\mathrm{th}}$ to August 14$^{\mathrm{th}}$. As earlier outlined, the system considers historical conditions to identify patterns and has the purpose of establishing the optimal energy consumption periods and water requirements for current and following day.

## 4.2 Data Processing Module Results

As explained in the previous chapter, after processing the raw information from the WeatherAPI and EnsembleAPI responses, the output will be a CSV file containing all the following hourly meteorological data: temperature, wind speed, air pressure, precipitation, relative humidity, and solar radiation data (specified in GHI, DHI and DNI). As an example of the output, an excerpt of the Comma-Separated Values (CSV) file can be seen in Listing 4.1.

```
datetime,temp_c,wind_ms,pressure_mb,precip_mm,humidity,ghi,dhi,dni
06/08/2024T00:00,19.1,1.65,1014.0,0.0,68,0.0,0.0,0.0
06/08/2024T01:00,18.7,1.44,1014.0,0.0,69,0.0,0.0,0.0
# data ommited for brevity
14/08/2024T18:00,29.5,3.85,1014.0,0.0,17,320.0,57.0,723.8867
14/08/2024T19:00,26.6,2.75,1015.0,0.0,23,128.0,39.0,507.17822
14/08/2024T20:00,24.2,1.99,1016.0,0.0,29,9.0,5.0,52.405167
14/08/2024T21:00,22.9,1.65,1017.0,0.0,32,0.0,0.0,0.0
14/08/2024T22:00,22.1,1.44,1017.0,0.0,34,0.0,0.0,0.0
14/08/2024T23:00,21.6,2.32,1017.0,0.0,34,0.0,0.0,0.0
```

Listing 4.1: Processed climate data included in the CSV file.

However, as mentioned in the methodology Chapter 3, the system also automatically outputs graphical information in Portable Network Graphics (PNG) format. The following Figures 4.1 to 4.6 display the same information that is present in the CSV file, but in a more intuitive way.

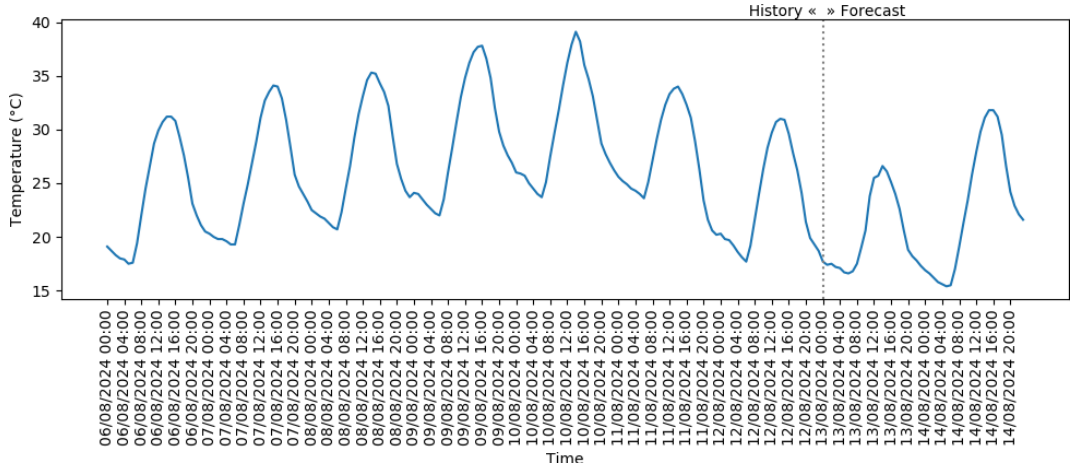


Figure 4.1: Processed climate data regarding temperature.

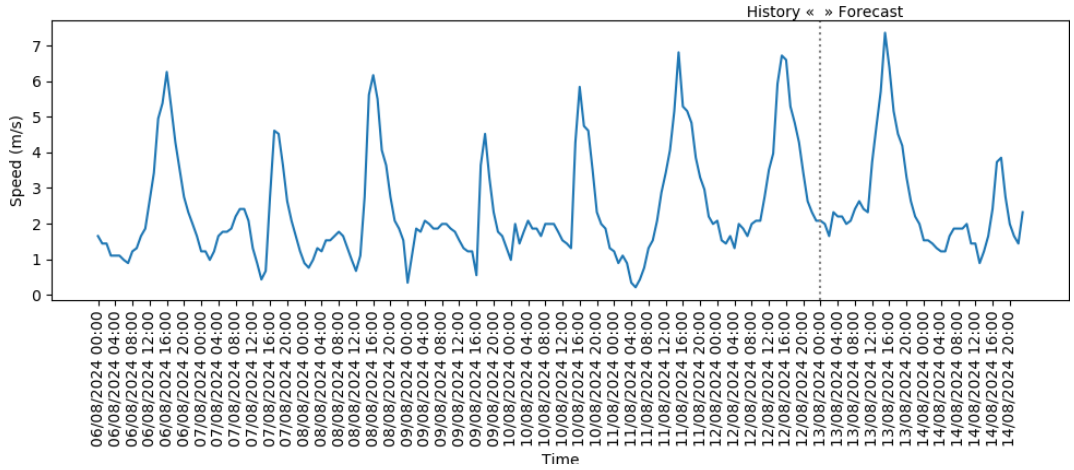


Figure 4.2: Processed climate data regarding wind speed.

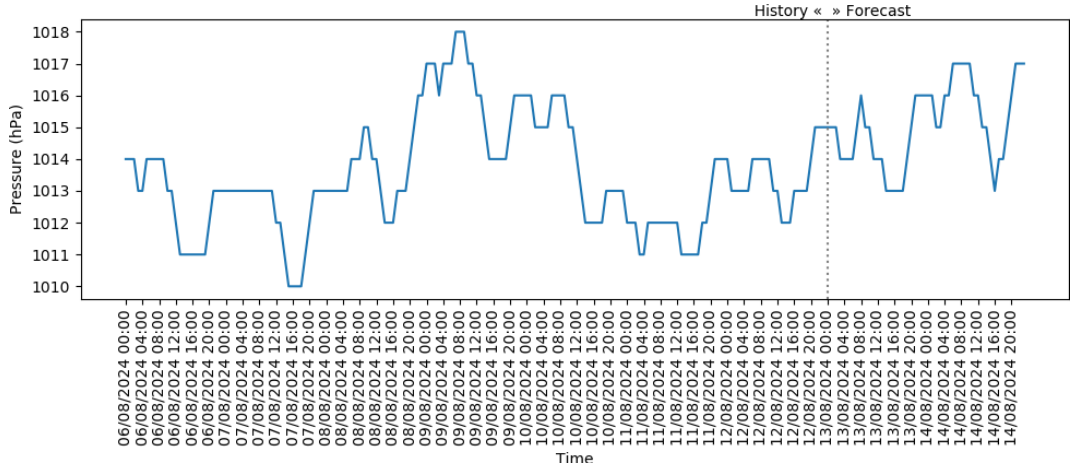


Figure 4.3: Processed climate data regarding air pressure.

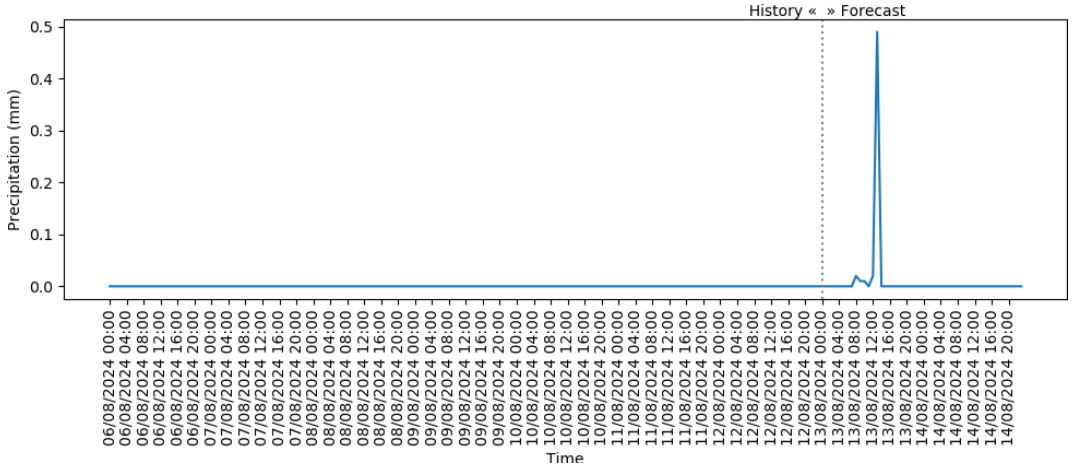


Figure 4.4: Processed climate data regarding precipitation.

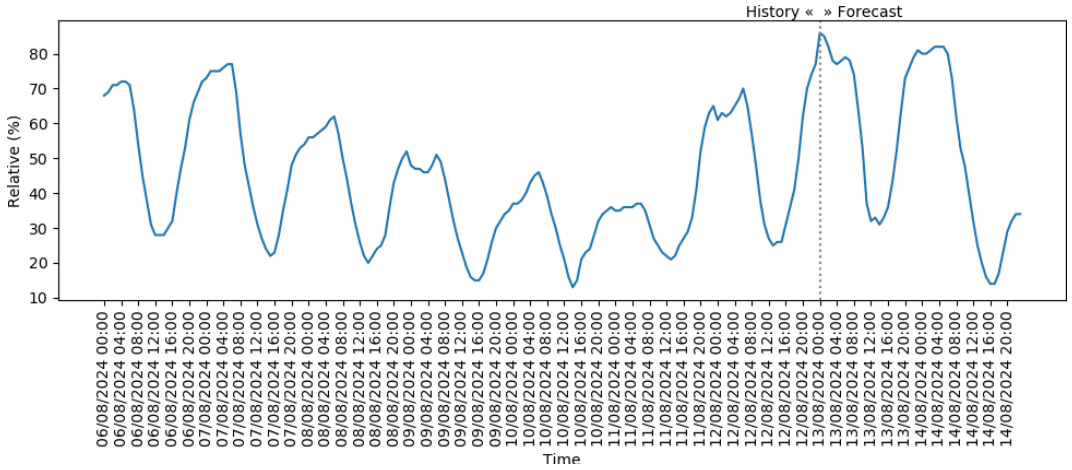


Figure 4.5: Processed climate data regarding relative humidity.

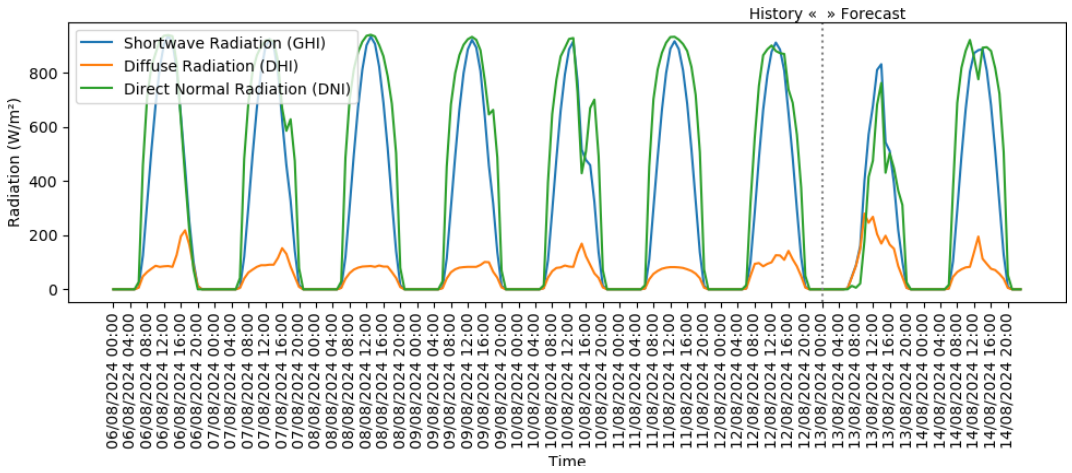


Figure 4.6: Processed climate data regarding solar radiation.

As a short discussion of the previous meteorological data, one can see that the days in study were quite hot, with minimum temperatures exceeding 20 °C, and maximum temperatures reaching almost 40 °C, as observed in Figure 4.1. Regarding wind speed, it is visible in Figure 4.2 that, in average, the days had a light breeze, with stronger winds generally in the afternoon. It is also noticeable that on August $14^{\text{th}}$, the winds are quite low compared to the previous days, which suggests that the wind energy production will be very poor for that day. By analysing air pressure in Figure 4.3, the relationship between this value and air temperature is visible, because when air temperature increases, the air expands and becomes less dense, which leads to a decrease in air pressure.

Evidenced in Figure 4.4, the days were very clear in terms of precipitation, with a small chance of rain for August $13^{\text{th}}$, which means the irrigation model should consider this value. In Figure 4.5, relative humidity value tends to be dry to moderate during the day, with an increase in its value as the night approaches. In regard to solar radiation, one can see that the days were very similar, except on August $13^{\text{th}}$ because of the predicted precipitation which usually means clouds. This event becomes evident given the increase of DHI value, as the radiation tends to get scattered by molecules and particles in the atmosphere, as seen in Figure 4.6.

Considering the processed meteorological data, the next operation of the module was to estimate the photovoltaic energy production using the two previously explained methods. Both methods generate a CSV file containing the energy produced hourly in kWh and, as an example of the output, an excerpt of the file regarding Method A can be analyzed in Listing 4.2.

```
1  datetime,pv_energy
2  06/08/2024T00:00,0.0
3  06/08/2024T01:00,0.0
4  # data ommited for brevity
5  14/08/2024T18:00,0.32253272064000005
6  14/08/2024T19:00,0.1345407418368
7  14/08/2024T20:00,0.0097271018208
8  14/08/2024T21:00,0.0
9  14/08/2024T22:00,0.0
10 14/08/2024T23:00,0.0
```

Listing 4.2: Estimated hourly photovoltaic energy production included in the CSV file, for Method A.

Similarly to the processed climate data, this part of the algorithm also generates a graphic for both methods, where one can analyse the estimated hourly photovoltaic energy production for each method, as seen in Figures 4.7 and 4.8.

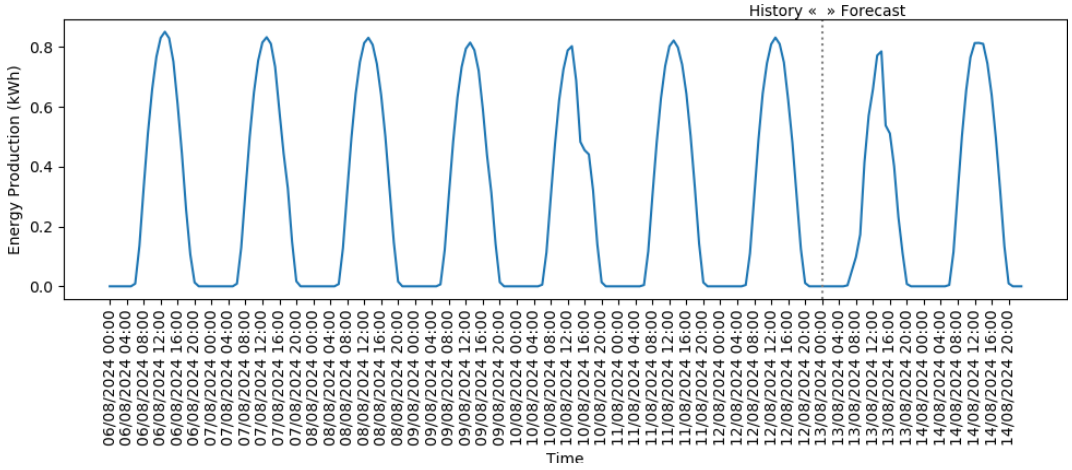


Figure 4.7: Estimated hourly photovoltaic energy production, applying Method A.

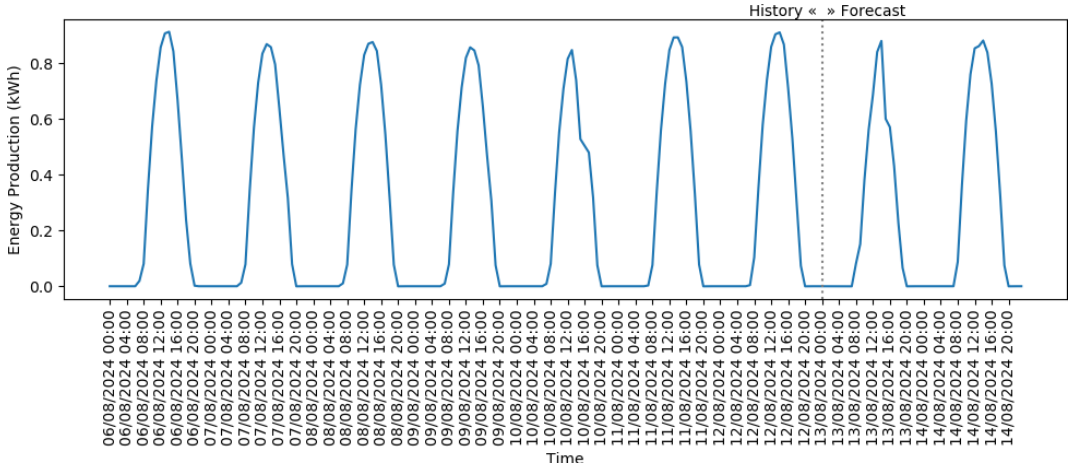


Figure 4.8: Estimated hourly photovoltaic energy production, applying Method B.

As seen in the previous graphics, the estimated values appear to be similar to each other. However, in order to highlight the differences between the two methods, the total energy output per day is also estimated and can be seen in the result log of the system and in Table 4.1.

With Table 4.1, the differences between both methods are more noticeable and, as one can see, Method B tends to estimate lower values than Method A. This can be explained because PVLib uses more parameters for the calculation that directly influence the efficiency values for multiple variables, such as different types of radiation, altitude, relative humidity, wind speed, atmospheric pressure and many other parameters. Further extended analysis can also detect that August 13$^{th}$ was the day with the lowest amount of photovoltaic energy production because of precipitation and consequent increase in scattered radiation in the atmosphere, defined by Diffuse Horizontal Irradiance (DHI).

Table 4.1: Total estimated daily photovoltaic energy production.

| Day | Method A [kWh] | Method B [kWh] |
|---|---|---|
| August 6$^{th}$ | 7.11 | 6.72 |
| August 7$^{th}$ | 7.08 | 6.59 |
| August 8$^{th}$ | 7.17 | 6.80 |
| August 9$^{th}$ | 6.90 | 6.50 |
| August 10$^{th}$ | 6.37 | 5.99 |
| August 11$^{th}$ | 7.07 | 6.89 |
| August 12$^{th}$ | 7.04 | 6.94 |
| August 13$^{th}$ | 5.33 | 5.48 |
| August 14$^{th}$ | 7.14 | 6.93 |

Having successfully estimated the photovoltaic yield for the days in study, the next task executed by the system was the estimation of wind energy production. From the previously explained approaches in methodology Chapter 3, both methods generate a CSV file containing the wind energy produced in kWh. As an example, a small excerpt of the file regarding Method B, which was the process that considered the turbine power curve, can be seen in Listing 4.3.

```
datetime,wind_energy
06/08/2024T00:00,0.01409035035127231
06/08/2024T01:00,0.0
# data ommited for brevity
14/08/2024T18:00,0.40979967234954684
14/08/2024T19:00,0.15254056557363277
14/08/2024T20:00,0.02997563466607995
14/08/2024T21:00,0.01409035035127231
14/08/2024T22:00,0.0
14/08/2024T23:00,0.047066949865755575
```

Listing 4.3: Estimated hourly wind energy production included in the CSV file, for Method B.

Once again, similarly to estimated photovoltaic energy production, the algorithm also generates a graphic for both methods, where one can analyse the estimated hourly wind energy production for each one, as seen in Figures 4.9 and 4.10.

The graphics look nearly identical, with small differences being noticed in daily curves and at the maximum values, with an accentuation particularly on Method B. This suggests that the method that considers the turbine power curve might have higher daily production values. Similarly to whats been done previously, in order to highlight the methods differences, the total energy output per day is also estimated and showcased in Table 4.2.

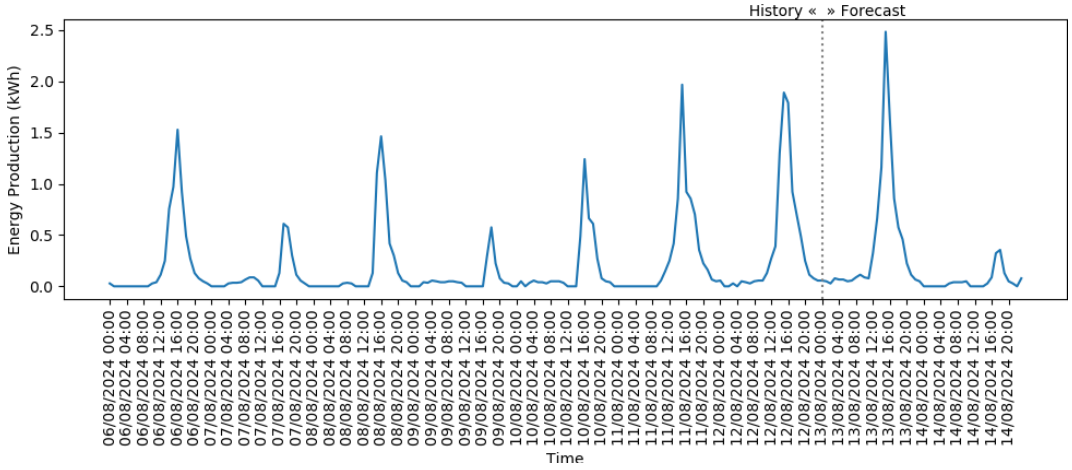


Figure 4.9: Estimated hourly wind energy production, applying Method A.

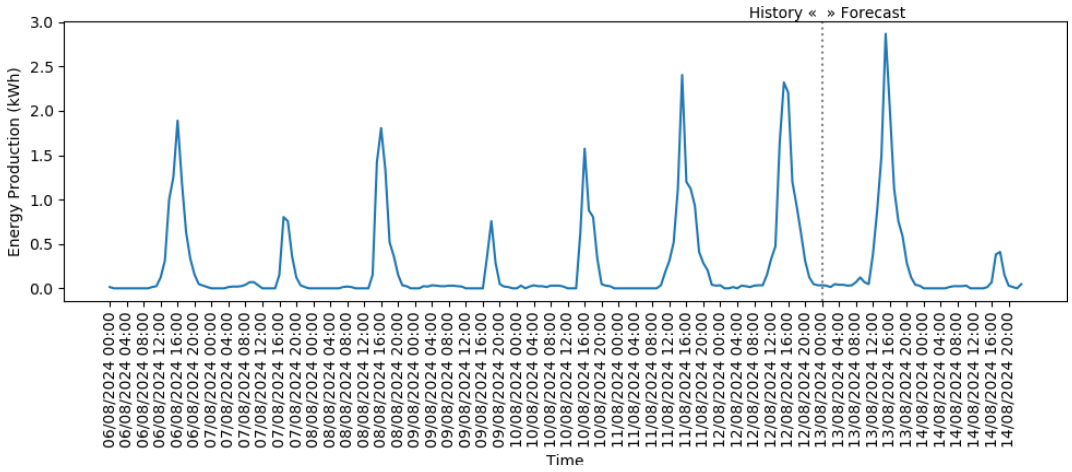


Figure 4.10: Estimated hourly wind energy production, applying Method B.

Table 4.2: Total estimated daily wind energy production.

| **Day** | **Method A [kWh]** | **Method B [kWh]** |
|---|---|---|
| August 6$^{\text{th}}$ | 5.68 | 7.04 |
| August 7$^{\text{th}}$ | 2.25 | 2.53 |
| August 8$^{\text{th}}$ | 4.77 | 5.85 |
| August 9$^{\text{th}}$ | 1.67 | 1.74 |
| August 10$^{\text{th}}$ | 3.87 | 4.57 |
| August 11$^{\text{th}}$ | 7.03 | 8.79 |
| August 12$^{\text{th}}$ | 8.74 | 10.61 |
| August 13$^{\text{th}}$ | 9.41 | 11.14 |
| August 14$^{\text{th}}$ | 1.28 | 1.23 |

As suspected, Method B tends to have greater values than Method A, specially on windier days. This can be explained because this method considers the power curve of the turbine, which already contains multiple defined efficiency factors provided by the manufacturer. Further analysis also showcases that August $14^{\text{th}}$ was the day with the lowest wind energy production, confirming the assumption done in the climate analysis where winds were predicted to be quite low.

With the estimation of photovoltaic and wind energy production accomplished, as stated in the methodology chapter, it is crucial to consider data of energy prices for planning and decision making processes. For this matter, the next step executed in the module is the gathering and processing of information provided in OMIE database, whose values are used to generate a CSV file after processing and a graphic visible in Figure 4.11.

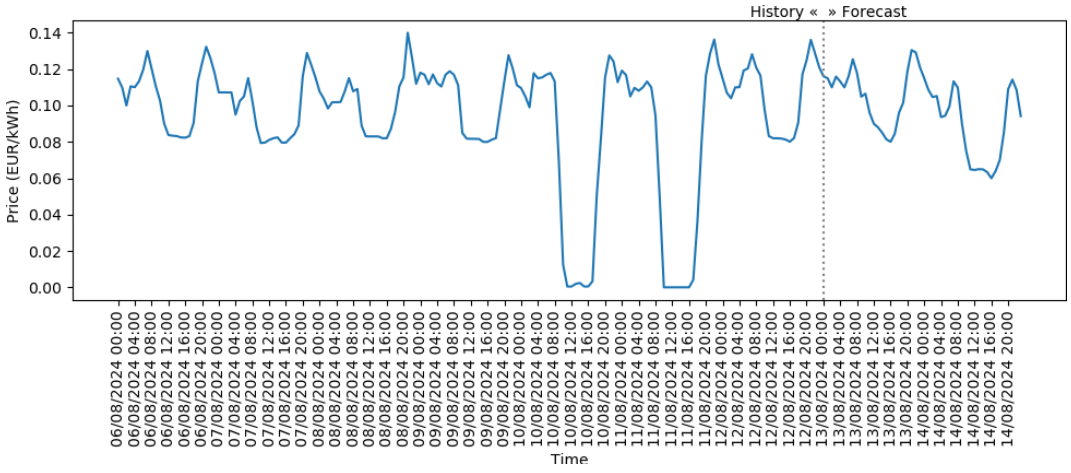


Figure 4.11: OMIE daily market energy price.

However, as explained previously, it is vital to consider additional charges such as seller management costs, profit margins and grid access taxes. Considering the prior information about OMIE daily market energy price, the algorithm outputs another CSV file, containing the final price of electricity used from the grid in $\text{EUR}\,\text{kWh}^{-1}$. Comparably to previous results, an excerpt of the output can be seen in Listing 4.4 and the full graphic in Figure 4.12.

```
datetime,grid_price
06/08/2024T00:00,0.191874
06/08/2024T01:00,0.186239
# data ommited for brevity
14/08/2024T18:00,0.14038849999999997
14/08/2024T19:00,0.15825949999999997
14/08/2024T20:00,0.185273
14/08/2024T21:00,0.19129899999999997
14/08/2024T22:00,0.18472100000000002
14/08/2024T23:00,0.168207
```

Listing 4.4: Estimated grid energy sell price included in the CSV file.

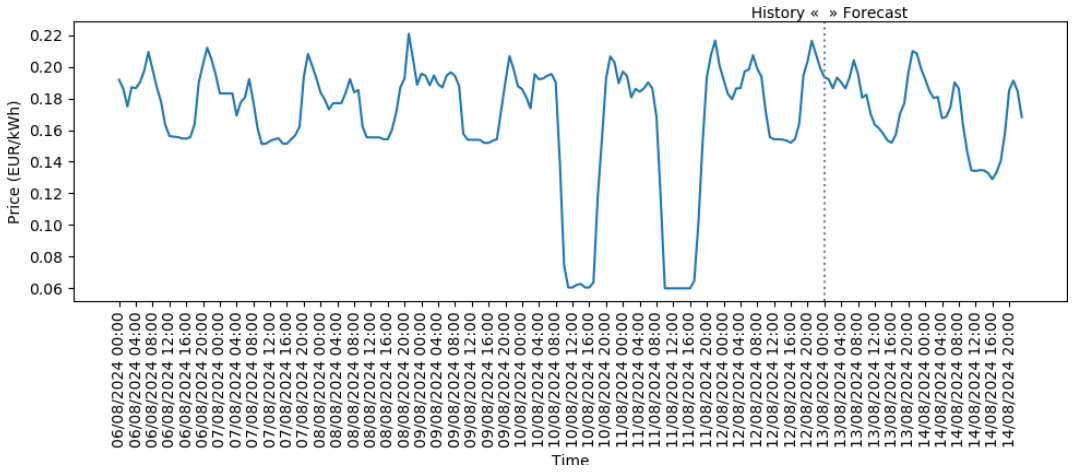


Figure 4.12: Estimated grid energy sell price.

By comparing Figures 4.11 and 4.12, we can see that the curves follow the same pattern, but with higher values. This can be justified due to the fact that grid energy sell price is always indexed to OMIE price, after summing up all the taxes.

## 4.3 Evapotranspiration Estimation Module Results

After processing and estimating the multiple types of data in the previous module, the following results are relative to the evapotranspiration estimation module. As previously stated, this module can accurately estimate reference $ET_0$ and vineyard $ET_c$ using crop coefficient $K_c$, that can be derived from the AGDD.

The beginning of the module is responsible for estimating reference evapotranspiration by using all the previous methods discussed and data from data processing module. The algorithm firstly produces a CSV file containing the $ET0$ values for the considered days, and gathers precipitation data that is required for the further irrigation model. The full CSV can be analysed in Listing 4.5, as well as the graphic provided by the algorithm in Figure 4.13, equally to all the previous processes.

```
1  date,total_precip,estimated_et0
2  06/08/2024,0.0,5.752915019212967
3  07/08/2024,0.0,5.890384031468934
4  08/08/2024,0.0,6.232368943678565
5  09/08/2024,0.0,6.218157581462105
6  10/08/2024,0.0,6.041552355754466
7  11/08/2024,0.0,6.124280404176885
8  12/08/2024,0.0,5.7824340792510025
9  13/08/2024,0.55,4.219663638646137
10 14/08/2024,0.0,5.727710981291331
```

Listing 4.5: Estimated reference evapotranspiration in comparison to total precipitation, included in the CSV file.

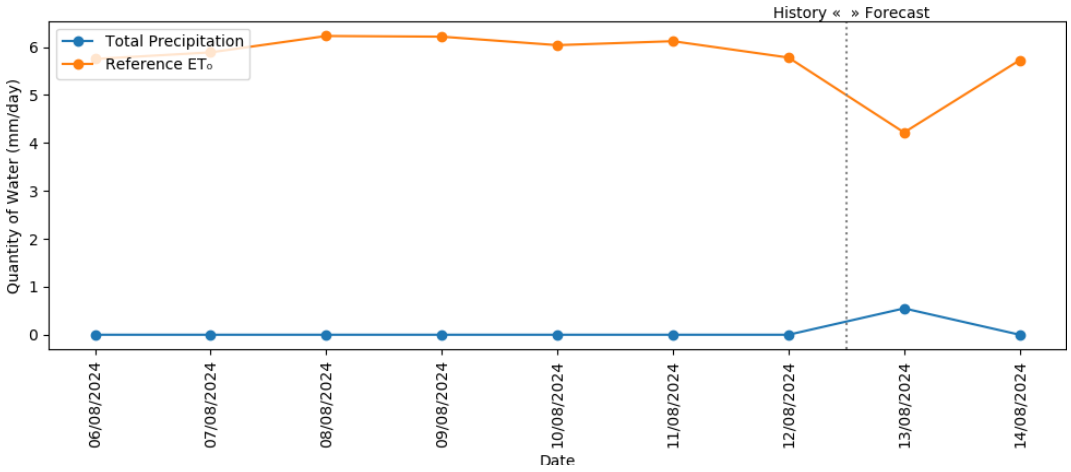


Figure 4.13: Estimated reference evapotranspiration in comparison to total precipitation.

As one can see from the prior listing and graphic, reference evapotranspiration had a similar value throughout the days, which makes sense since the climatic conditions were similar. However, on August 13$^{\text{th}}$, a decrease in evapotranspiration can be spotted, specially because of the lowering of radiation values due to precipitation.

With the determination of reference evapotranspiration $ET_0$ achieved, the following step is to estimate the crop evapotranspiration $ET_c$, by using the Accumulated Growing Degree Days (AGDD) calculated from the temperatures gathered in the growing season. An extensive CSV file is produced, since it is considered that the growing season starts on April 1$^{\text{st}}$, and an excerpt of it is exposed in Listing 4.6.

```
1  date,max_temp_c,min_temp_c,gdd,cumsum_gdd,kc
2  01/04/2024,9.7,4.3,0.0,0.0,0.0
3  02/04/2024,8.2,5.3,0.0,0.0,0.0
4  03/04/2024,17.1,7.6,2.350,2.350,0.0
5  # data ommited for brevity
6  06/08/2024,31.2,17.5,14.350,1075.949,0.722
7  07/08/2024,34.1,19.3,16.700,1092.649,0.687
8  08/08/2024,35.3,20.7,18.0,1110.649,0.661
9  09/08/2024,37.8,22.0,19.9,1130.550,0.635
10 10/08/2024,39.1,23.7,21.4,1151.950,0.586
11 11/08/2024,34.0,20.2,17.1,1169.050,0.553
12 12/08/2024,31.0,17.7,14.350,1183.3999999999999,0.524
13 13/08/2024,26.6,16.6,11.600,1194.9999999999998,0.509
14 14/08/2024,31.8,15.4,13.600,1208.599,0.476
```

Listing 4.6: Estimated grid energy sell price included in the CSV file.

Similarly to the previous modules, this set of operations also produces graphical information that can showcase the values fluctuations in a more intuitive way, as seen in Figures 4.14 and 4.15.

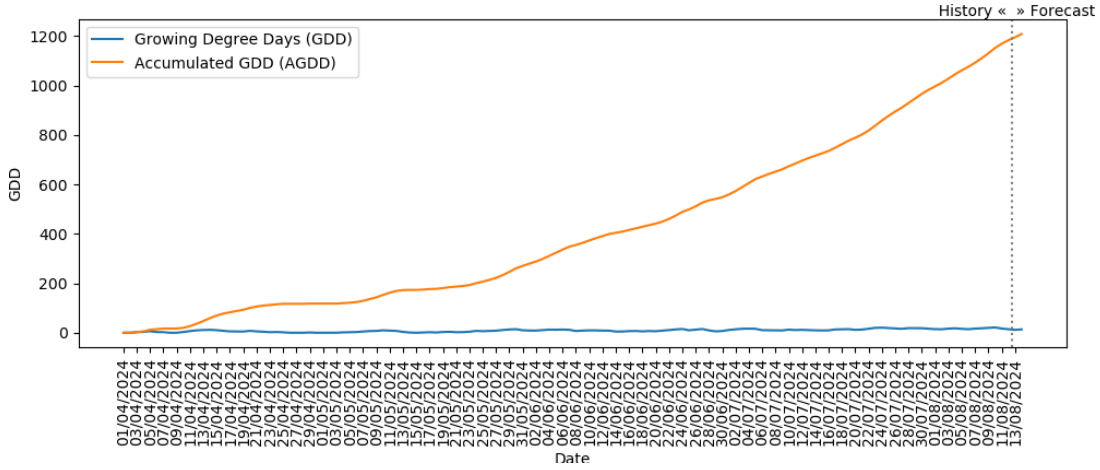


Figure 4.14: Estimated daily Growing Degree Days (GDD) and AGDD.

The graphic showcases that on the first days of growing season the AGDD value remains particularly constant, with small increases. This can be explained since the average temperatures on these days are typically low, and they might not be enough to surpass the base temperature of 10 °C, which results in a null value of daily GDD in some cases. Once the temperatures start to increase at the end of May, their average begins to easily surpass the base temperature, and a rapid increase in AGDD is visible with a constant escalation until the forecast days of study.

Using the vineyard crop coefficient variation with AGDD explained in the methodology chapter, the value of $K_c$ can finally be determined, as shown in Figure 4.15.

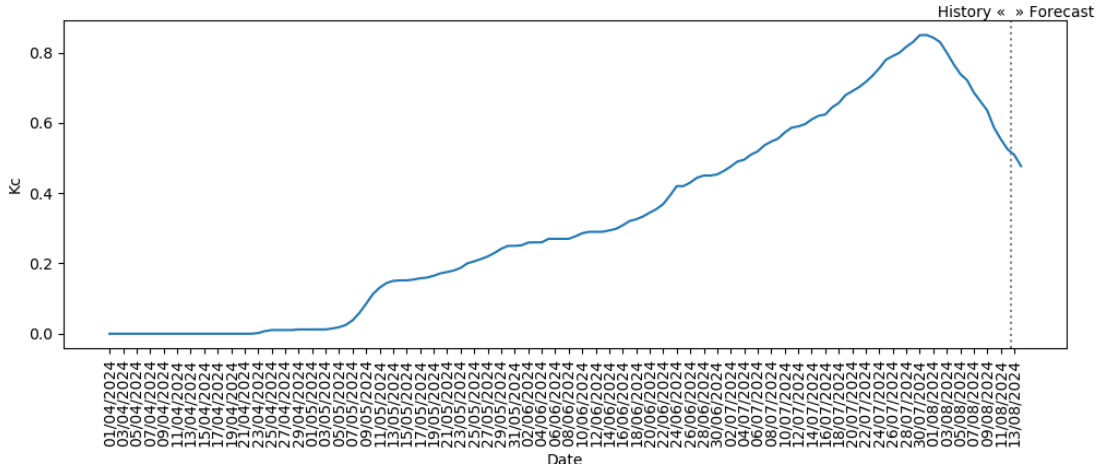


Figure 4.15: Estimated crop coefficient.

By analysing the previous graphic, multiple conclusions can be drawn from it. The value of $K_c$ is partially parallel to the AGDD and a pattern can be seen between the two values. However, at the beginning of August, the value of $K_c$ stops following the trend of AGDD and starts to decrease.

As previously stated, this coefficient varies depending on the growth stage of the grapevine, environmental conditions, and the specific practices in the vineyard. At the beginning of the graph, the value of $K_c$ is minimal, as the canopy is still small, which is considered the bud break phase of the vineyard. Once the vineyard has a shoot development around the beginning of May, the value of $K_c$ starts increasing, as the canopy expands and the vine enters a more active growth phase, reaching flowering around June. From the flowering to fruit set, the value keeps increasing, but in a moderate way, as the vine is actively growing and setting fruit [112].

In the middle of June towards the beginning of July, we can see another rapid increase in the crop coefficient due to the large canopy and significant fruit development as the vineyard is likely reaching the *véraison* phase. The graph shows that the $K_c$ value reaches its highest point around beginning of August, when the water demand is at its peak, because the grapes are rapidly developing and ripening. After this peak, the crop coefficient should decline slightly as the vines begin preparing for harvest and reduce their water uptake, because grapes approach full ripeness. Not only that, $K_c$ value is initially high from *véraison* to harvest phases, but it tends to decrease as deficit irrigation is used to concentrate flavors of the grapes to provide flavorful wines [112].

## 4.4 Irrigation Model Results

With all the previous results, particularly crop evapotranspiration $ET_c$, the following module is responsible for estimating the vineyard water requirements, as explained in the methodology chapter. As a reminder, if row spacing $L_r$ and vine spacing $L_v$ are provided, the algorithm can also estimate the water requirement in liters per grapevine. Once again, like the previous modules, this algorithm also generates a CSV file containing all information (Listing 4.7), and a graphic containing the most relevant values for the system (Figure 4.16).

```
1  date,total_precip,estimated_et0,kc,estimated_etc,Pe,NIR,GIR,
       irrigation_l_per_ha,irrigation_l_per_vine
2  06/08/2024,0.0,5.752,0.721,4.151,0.0,4.151,4.884,48841.910,10.745
3  07/08/2024,0.0,5.890,0.686,4.044,0.0,4.044,4.758,47581.482,10.467
4  08/08/2024,0.0,6.232,0.660,4.118,0.0,4.118,4.845,48453.369,10.659
5  09/08/2024,0.0,6.218,0.635,3.948,0.0,3.948,4.645,46454.026,10.219
6  10/08/2024,0.0,6.041,0.586,3.543,0.0,3.543,4.168,41686.004,9.170
7  11/08/2024,0.0,6.124,0.553,3.390,0.0,3.390,3.988,39884.556,8.774
8  12/08/2024,0.0,5.782,0.524,3.035,0.0,3.035,3.571,35710.952,7.856
9  13/08/2024,0.55,4.22,0.509,2.147,0.385,1.762,2.073,20738.926,4.562
10 14/08/2024,0.0,5.727,0.476,2.730,0.0,2.730,3.212,32127.741,7.068
```

Listing 4.7: Irrigation water requirements values in the CSV file.

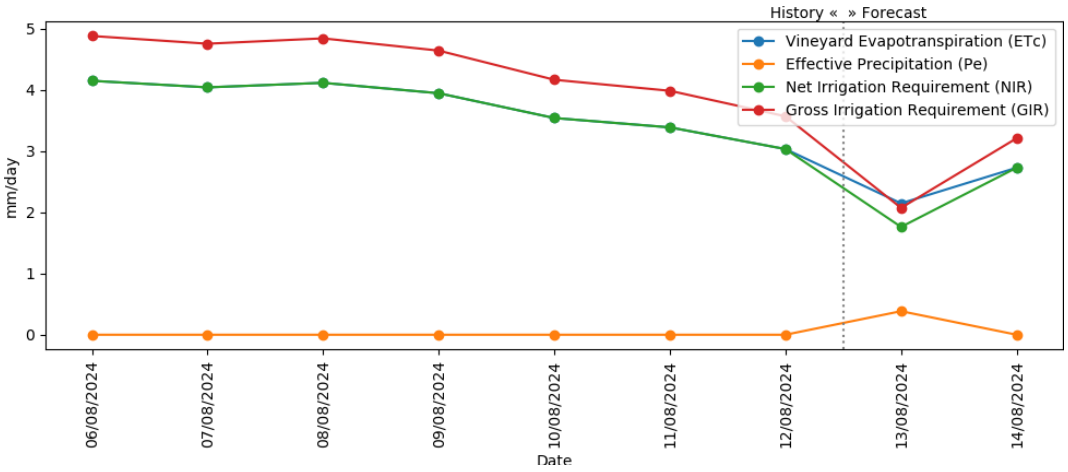


Figure 4.16: Irrigation model water requirements.

From this graphic we can conclude that the information contained in the CSV file is more intuitive to analyse. As one can see, when there is no precipitation occurrence, the NIR line aligns with $ET_c$ line, which makes sense since there is no compensation for the water requirement by effective precipitation $\Gamma_e$. When precipitation occurs, as seen on August 13$^{\text{th}}$, the effective precipitation can partially satisfy some of the vineyard evapotranspiration, which causes the NIR value to lower. Considering the effectiveness of the irrigation system, which is drip irrigation, the value of GIR is always higher than NIR, which is also clearly evident in the graphic.

Given that row spacing and vine spacing are provided, the water requirement in liters per grapevine $\text{GIR}_{gv}$ can be estimated, in comparison to the Gross Irrigation Requirement (GIR) in $\text{mm}\,\text{day}^{-1}$ and water requirement in liters per hectare $\text{GIR}_{ha}$, as seen in Table 4.3, which resumes the information output by the system.

Table 4.3: Irrigation water requirements in multiple formats.

| **Day** | **GIR** $[\text{mm}\,\text{day}^{-1}]$ | $\textbf{GIR}_{ha}$ $[\text{L}\,\text{ha}^{-2}\,\text{day}^{-1}]$ | $\textbf{GIR}_{gv}$ $[\text{L}\,\text{day}^{-1}]$ |
|---|---|---|---|
| August 6$^{\text{th}}$ | 4.88 | 48841.91 | 10.75 |
| August 7$^{\text{th}}$ | 4.76 | 47581.48 | 10.47 |
| August 8$^{\text{th}}$ | 4.85 | 48453.37 | 10.66 |
| August 9$^{\text{th}}$ | 4.65 | 46454.03 | 10.22 |
| August 10$^{\text{th}}$ | 4.17 | 41686.00 | 9.17 |
| August 11$^{\text{th}}$ | 3.99 | 39884.56 | 8.77 |
| August 12$^{\text{th}}$ | 3.57 | 35710.95 | 7.86 |
| August 13$^{\text{th}}$ | 2.07 | 20738.93 | 4.56 |
| August 14$^{\text{th}}$ | 3.21 | 32127.74 | 7.07 |

By analyzing this table, it is clear that the amount of water required by the vineyard begins to lower because of the decrease in the crop coefficient value as the vineyard is approaching the harvesting phase. On August 13$^{\text{th}}$, the amount of water required is even lower because of the precipitation prediction. With these results,

vital data is provided and vineyard managers can incorporate it on their irrigation systems, to ensure maximum sustainability regarding water efficiency.

## 4.5 Energy Model Results

As explained in the methodology chapter, the last module of the intelligent system is the energy model, which contains a set of operations that can estimate the optimal energy consumption timings. Like the previous modules, a CSV file and a graphic containing the most relevant value is also generated, which is the optimal energy consumption score. As inputs, the module requires the grid energy sell price and renewable energy production files. As a prototype in evaluation, Method B previous estimations for photovoltaic and wind energy were used as input data, along with the grid energy sell price indexed to OMIE. Listing 4.8 displays an example of the output, with an excerpt of the CSV generated file, that contains the normalized features values and predicted optimal score for every hour of the study.

```
datetime,grid_price,renewable_energy,hour,predicted_optimal_score
06/08/2024T00:00,0.648,0.005,0.0,0.124
06/08/2024T01:00,0.550,0.0,0.0,0.149
# data ommited for brevity
14/08/2024T19:00,0.464,0.242,0.256,0.339
14/08/2024T20:00,0.890,0.035,0.0354,0.052
14/08/2024T21:00,0.986,0.015,0.017,0.000
14/08/2024T22:00,0.8827,0.0,0.0,0.039
14/08/2024T23:00,0.621,0.050,0.064,0.161
```

Listing 4.8: Optimal energy consumption scores in the CSV file.

Like previously described, the model calculates a score normalized between 0 and 1, where 0 represents the less optimal hour to consume energy, and 1 represents the most optimal hour. To estimate this score, the model uses a Decision Tree Regressor algorithm, that considers three features: grid energy price, renewable energy production, and hour of the day. However, the algorithm receives two inputs, since the hour of the day is adjusted by renewable energy. Given this, to evaluate the model performance and features' importance in multiple scenarios, a list of case studies, that follows a complexity order, was implemented, as seen in Table 4.4.

Table 4.4: Summary of energy model case studies.

| Case Study | Grid Energy Sell Price | Renewable Energy Production |
|---|---|---|
| A | Considered | None Considered |
| B | Considered | Only Photovoltaic Considered |
| C | Considered | Only Wind Considered |
| D | Considered | Photovoltaic and Wind Considered |

### 4.5.1 Case Study A

As seen in Table 4.4 the system must have at least one input in order to generate a result and, in this case, the grid energy sell price is always considered. Starting from the lowest complexity Case Study A, this feature is the only considered input parameter of the system, and Figures 4.17 and 4.18 display the output graphics of the module.

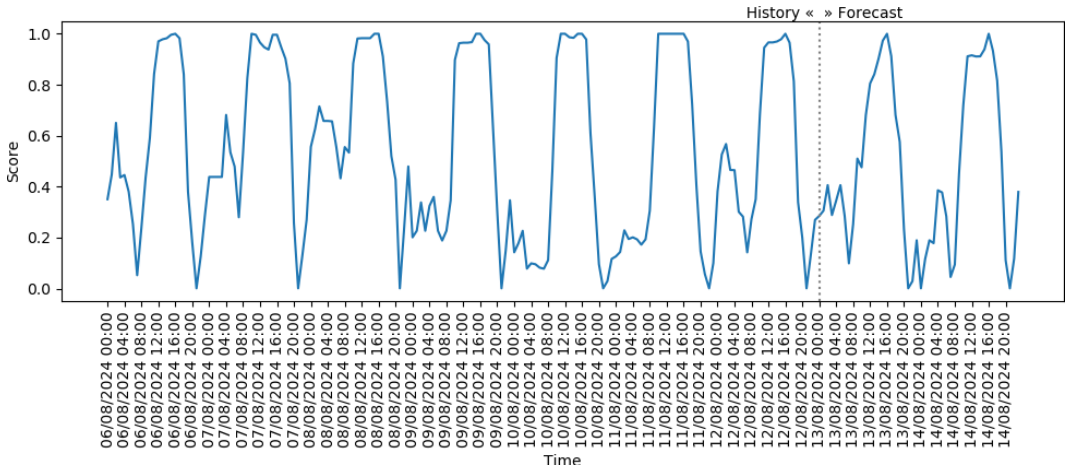


Figure 4.17: Optimal energy consumption, for Case Study A.

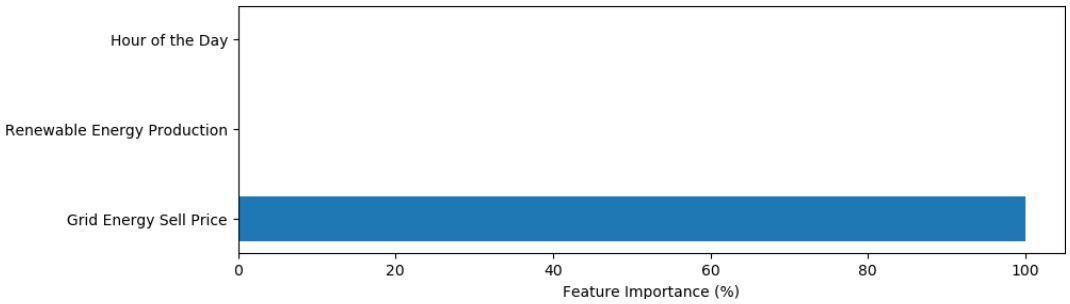


Figure 4.18: Energy model features' importance, for Case Study A.

From the previous figures analysis, it is no surprise that the most optimal timings typically follow the daily estimated grid energy sell prices, where the most optimal time to consume electricity is the hour with lower price. This is also confirmed in the model features' importance, where grid energy sell price has an importance of 100 % compared to the null importance of the other variables.

### 4.5.2 Case Study B

The following Case Study B, considers a vineyard that has the ability to produce photovoltaic energy. For this matter, the model evaluates the contribution of grid energy sell price and photovoltaic production, outputting the graphics visible in Figures 4.19 and 4.20.

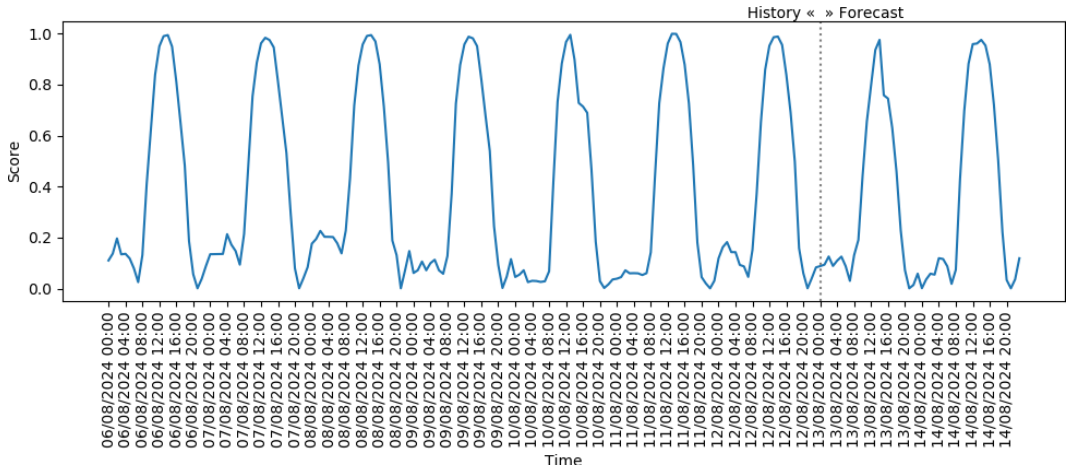


Figure 4.19: Optimal energy consumption, for Case Study B.

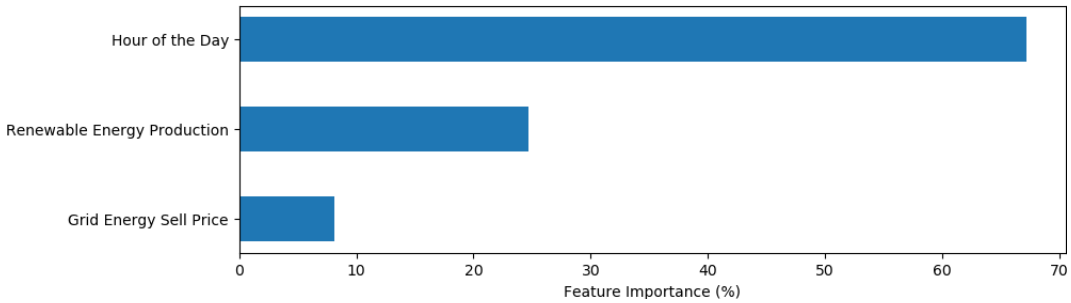


Figure 4.20: Energy model features' importance, for Case Study B.

From the optimal energy consumption graphic, it is possible to analyse differences in the score relatively to the last case study. This happens because the model is now considering two input variables, and gives particular importance to renewable energy production. When comparing the typical energy yield curve of a photovoltaic system, similarities can be seen alongside this graphic, although some small spikes appear at night time regarding the grid energy price. However, from the features' importance figure, one can see that the most important feature for the model was hour of the day. This means that the model can effectively predict the major part of the score by only considering the hour of the day. This makes sense since the only type of renewable energy considered is photovoltaic, and effective energy production hours from these systems are typically consistent each day, corresponding to sunlight hours.

### 4.5.3 Case Study C

In order to confirm that the model is working properly and the major importance given on hour of the day was not a model formulation error, the Case Study C considers wind energy as the only renewable energy production input, for a direct

confrontation of the previous case study. Once again, the model predicted optimal scores and features' importance can be seen in Figures 4.21 and 4.22.

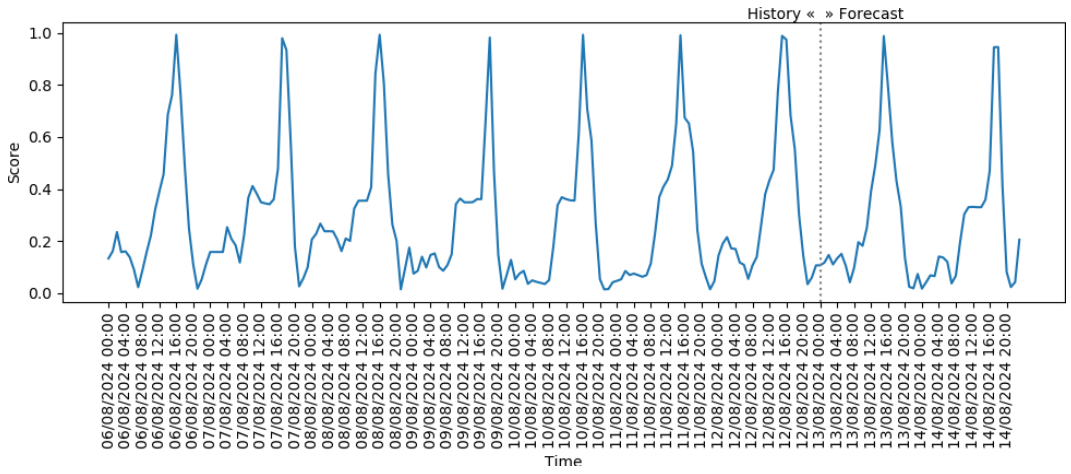


Figure 4.21: Optimal energy consumption, for Case Study C.

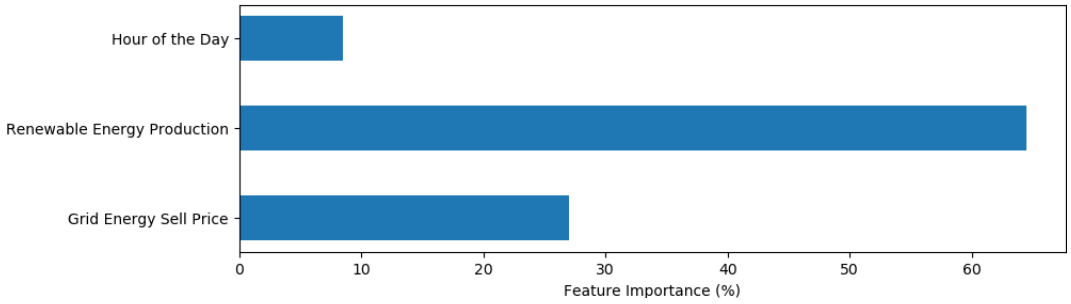


Figure 4.22: Energy model features' importance, for Case Study C.

In this case, the model cannot predict any major relationship with the hour of day so its importance has a lower value. This can be explained since the production of wind energy does not have any relation to a specific hour of the day, contrary to photovoltaic energy. Since wind speeds are typically random, the model gives more importance to the renewable energy production and grid energy sell price, and the graphic presents correspondences to the wind energy yield.

### 4.5.4 Case Study D

To determine the model performance for a vineyard that contains multiple types of renewable energy sources, Case Study D showcases what happens when the renewable energy production comes either from wind energy or photovoltaic energy. Once again, grid energy price is always considered for all case studies, and Figures 4.23 and 4.24 display the results of the model.

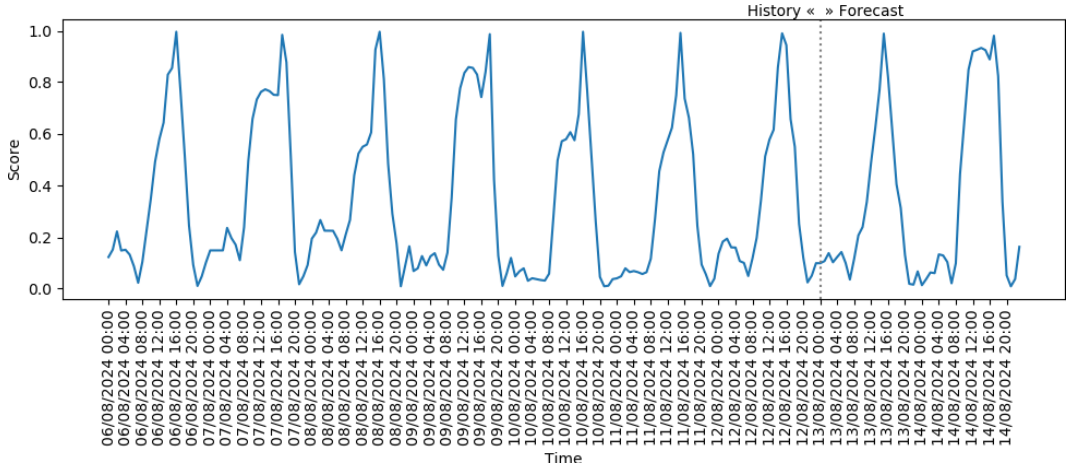


Figure 4.23: Optimal energy consumption, for Case Study D.

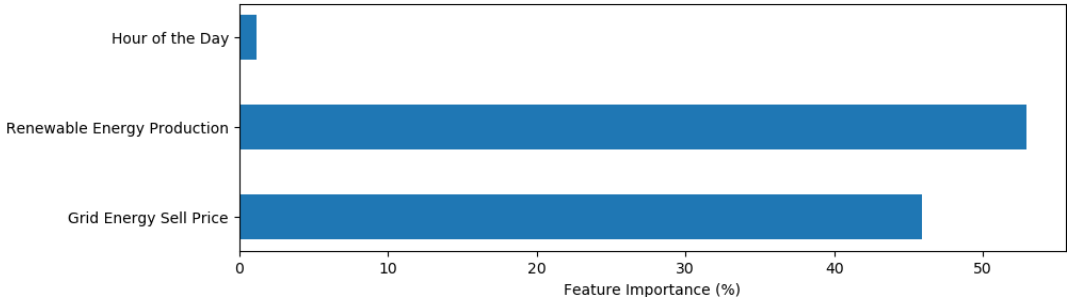


Figure 4.24: Energy model features' importance, for Case Study D.

This score graphic is more complex than the ones shown before, and contains multiple similarities with all the previous case studies, because it considers all the electricity sources. When it comes to features' importance, the model works as expected, by giving more relevance to renewable energy production in contrast to grid energy sell price. As previously stated, since photovoltaic energy is now just a small part of all the inputs considered, the model gives almost null importance to the hour of the day. This predicted optimal score is recognized as the most efficient, since it considers multiple renewable energy sources. To further extend the analysis of this case study, Table 4.5 provides the predicted optimal scores for all the hours on forecast days, which are August $13^{\text{th}}$ and $14^{\text{th}}$.

As seen in Table 4.5, the columns contain the hourly scores for both days in a color scheme, where green represents the most optimal window to consume energy, and red the least optimal. With all this information, these values can be used to guide decision-making in energy management systems, promoting top-tier sustainability in terms of energy resources.

Table 4.5: Predicted optimal scores, for Case Study D.

| Hour | August 13$^{th}$ | August 14$^{th}$ |
|---|---|---|
| 00:00 | 0.099 | 0.017 |
| 01:00 | 0.107 | 0.039 |
| 02:00 | 0.136 | 0.064 |
| 03:00 | 0.102 | 0.061 |
| 04:00 | 0.123 | 0.130 |
| 05:00 | 0.140 | 0.127 |
| 06:00 | 0.099 | 0.103 |
| 07:00 | 0.038 | 0.020 |
| 08:00 | 0.115 | 0.098 |
| 09:00 | 0.204 | 0.456 |
| 10:00 | 0.237 | 0.648 |
| 11:00 | 0.331 | 0.844 |
| 12:00 | 0.479 | 0.918 |
| 13:00 | 0.622 | 0.923 |
| 14:00 | 0.767 | 0.930 |
| 15:00 | **1.000** | 0.923 |
| 16:00 | 0.822 | **1.000** |
| 17:00 | 0.612 | 0.884 |
| 18:00 | 0.414 | 0.818 |
| 19:00 | 0.311 | 0.339 |
| 20:00 | 0.133 | 0.052 |
| 21:00 | 0.022 | **0.000** |
| 22:00 | **0.000** | 0.039 |
| 23:00 | 0.066 | 0.161 |

### 4.5.5 Case Studies Discussion

From the previous case studies, it is noticeable that the energy model can adapt to the variables in study, such as the types of renewable energies and grid energy prices, with the features' importance varying depending on the case. Case Study A served mostly as a baseline scenario, where no renewable energies were considered, making it only vulnerable to fluctuations in grid energy prices. On the other hand, the other case studies provided a more complex approach with the addition of renewable energy sources, reducing dependency on grid energy but offering more exposure to weather conditions, such as solar radiation and wind speeds. From a comparative point of view, Case Study D displayed the most efficient results in terms of sustainability, since it combines two renewable energy sources. This confirms that the energy model is based on the interaction between renewable energy sources and the impact of grid energy sell prices, which supports the system's adaptive nature.

# Chapter 5

# Conclusions

## 5.1 Main Findings

All the research carried out within the scope of literature review highlights numerous intelligent solutions and models that significantly increase productive efficiency in sustainable agriculture worldwide. From the most effective irrigation methods to smart sensors, actuators, and decision-making models, many solutions enable optimal efficiency.

In most agricultural activities, water and energy are not dissociated, and there is a close link between these resources, which is why the analysis of the water-energy nexus deserves special attention. The definition of solutions that allow the identification of these resources' consumption, interconnection, forecasting, and control, particularly through monitoring, management, and decision support systems, allows greater efficiency.

The studies in this area highlight the importance of using renewable energy as a source of clean energy for irrigation processes, which solves problems generated by the adversity of the most common terrains in vineyards, such as the unavailability of energy on-site. By encouraging the use of renewable sources, vineyards can also reduce their carbon footprint and dependence on non-renewable energy.

Smart irrigation techniques, such as precision irrigation and automated systems, ensure efficient water and energy use, minimizing waste, allowing resource optimization, and enhancing crop growth. Furthermore, using intelligent management systems for irrigation processes in conjunction with green energy such as photovoltaic

or wind, a very efficient ecological footprint towards more sustainable agriculture can be achieved.

After determining one of the best and most efficient irrigation methods for vineyards, which is drip irrigation, it is clear that using intelligent solutions to manage irrigation processes brings considerable advantages. Solutions based on measuring soil moisture with sensors or solutions based on measuring evapotranspiration end up delivering a huge benefit in terms of efficiency compared to more traditional irrigation methods, namely the ones based on a schedule.

The scientific community has created numerous solutions that allow the use of the concepts covered throughout this work. From simpler to more complex projects that consider many variables, these solutions allow the achievement of excellent levels of efficiency and sustainability. However, the current idea is that all these techniques are dispersed across several isolated systems, and there is a lack of a resource management model that maximizes productive efficiency in the wine sector.

For this matter, and considering all the technologies and systems addressed in the literature review, an intelligent resource management system that implements multiple concepts was developed. Modularity is an important aspect of the system, and different types of vineyards with different types of systems and equipment can effectively use the intelligent system. All the modules, considered as the main core tenets of the system, work in a modular way, and together they can achieve the maximum sustainability of resources.

Multiple concepts and methodologies are addressed along the explanation of the model, and various mathematical formulas are considered. The main objective of the system, is the output of utmost important information that vineyard farms can implement, specially regarding energy and water resources. With user preferences defined, the system can adapt to a specific farm and different types of renewable energy production or irrigation methods can be considered by the model. Evapotranspiration was used as the main parameter to calculate vineyard water needs, and a supervised learning algorithm was implemented to estimate the most optimal window for energy consumption.

In order to validate the proposed model, multiple results are provided for the various methodologies of the system, and realistic examples are provided. As a prototype built without on-site data, the data processing module uses public information from climate databases, and estimates photovoltaic and wind energy yield for realistic scenarios. Evapotranspiration is also estimated using open access data, and irrigation water requirements are estimated in multiple formats. As for the supervised learning algorithm, which is a Decision Tree Regressor model, four case studies are analysed and their scientific results are addressed and explained.

With this system, vital metrics are acquired and vineyard farms can collect essential data to make informed decisions regarding resource management. These

considerations can be used to guide irrigation systems, by ensuring that water is used efficiently and only when necessary, and a better energy management can also be achieved, by identifying opportunities to optimize energy consumption, reducing costs and promoting maximum efficiency. Overall, the resource management system is able to boost the environmental sustainability of the wine sector operations and enhance productivity of vineyards.

## 5.2 Contributions

This work contributes to the scientific community by developing an intelligent resource management system in vineyards that integrates renewable energy, smart irrigation techniques, and decision-making models. Some methodologies were proposed to optimize water use, energy consumption, and overall resource sustainability in vineyard operations. Accordingly, the system performs the management of efficient irrigation with weather and evapotranspiration data, and a supervised learning model carries out the optimization in energy consumption.

The experiments and tests on different renewable energy sources have been performed on different case studies. Using public climate data in combination with photovoltaic and wind energy estimations, the results obtained were proficient, confirming the effectiveness of the system. The results allow vineyards to achieve better productivity and sustainability, and form a basis for further work to refine the model using on-site data.

Given the impact of the study carried out in this work, the research presented in the literature review was published in a special issue of Multidisciplinary Digital Publishing Institute (MDPI) *electronics* journal, named "Sustainable Irrigation Systems in Vineyards: A Literature Review on the Contribution of Renewable Energy Generation and Intelligent Resource Management Models". Submitted to revisions from international authors, this article was funded by Vine and Wine Portugal-Driving Sustainable Growth Through Smart Innovation Mobilizing Agenda, whose project identifier is C644866286-011. The proposed resource management system is also in preparation for another article and getting arranged for submission soon. The provisional title of this journal article is "Sustainable Irrigation Systems in Vineyards: Resource Management System for Optimizing Production Efficiency", and will provide a direct correlation to the previous article. Together, both articles are set to contribute to the advancement in the area and to the identification of new promising paths in this field.

## 5.3 Limitations and Future Work

Given the infeasibility of data access in real vineyards, due to bureaucratic situations that could not be resolved within a reasonable time, one of the limitations that occurred was the impossibility of testing the system in a large-scale real environment. For future work, it would be interesting to see the system behaving on this type of application, with on-site data acquired from a meteorological station and renewable energy production meters. All the processed data from this on-site information would run on the multiple modules of the system, and the outputs could be operating together with the multiple components of a irrigation system, namely the irrigation valves and water pumps. Although the simulations already provided excellent results, this type of insight would further accentuate the importance of this resource management system.

## 5.4 Final Considerations

As a final reflection, it is important to note that all the work carried out required a high level of planning and organization, as well as extensive knowledge in the field of Electrical Engineering, particularly in Autonomous Systems. It was a challenging project, proving to have great potential for study and inevitably allowed to learn and explore various concepts and technologies that are used in this context. Despite all the difficulties naturally encountered by a project in this area of engineering, it is concluded that the proposed objectives were successfully met, achieving a good design and positive results for a resource management system for optimizing production efficiency in the wine sector.

# References


[1] S. Heller, "Improving Agriculture: 7 Techniques To Make Farming Less Destructive," *Emagazine.com*, May 2020. Available online: https://emagazine.com/improving-agriculture-7-techniques/ (accessed on 13 April 2024). [Cited on page 1]

[2] A. D. Jones and G. Ejeta, "A new global agenda for nutrition and health: the importance of agriculture and food systems.," *Bulletin of the World Health Organization*, vol. 94, pp. 228–229, March 2016. Available online: https://doi.org/10.2471/BLT.15.164509 (accessed on 13 April 2024). [Cited on page 1]

[3] S. Wensley, "Global Threats to Agriculture," 2020. Available online: https://farmtogether.com/learn/blog/global-threats-on-agriculture (accessed on 13 April 2024). [Cited on page 1]

[4] European Parliamentary Research Service, "Russia's war on Ukraine: Impact on global food security and EU response," 2022. Available online: https://www.europarl.europa.eu/RegData/etudes/BRIE/2022/733667/EPRS_BRI(2022)733667_EN.pdf (accessed on 13 April 2024). [Cited on page 2]

[5] J. Beckman and A. M. Countryman, "The Importance of Agriculture in the Economy: Impacts from COVID-19," *American Journal of Agricultural Economics*, vol. 103, no. 5, pp. 1595–1611, 2021. Available online: https://doi.org/10.1111/ajae.12212 (accessed on 13 April 2024). [Cited on page 2]

[6] Food and Agriculture Organization of The United Nations, "FAO Food Price Index and World Food Situation," 2023. Available online: https://www.fao.org/worldfoodsituation/foodpricesindex/en/ (accessed on 13 April 2024). [Cited on pages vii and 2]

[7] C. Matos, I. Bentes, S. Pereira, A. M. Gonçalves, D. Faria, and A. Briga-Sá, "Which are the factors that may explain the differences in water and energy consumptions in urban and rural environments?," *Science of The Total Environment*, vol. 642, pp. 421–435, November 2018. Available online: https://doi.org/10.1016/j.scitotenv.2018.06.062 (accessed on 13 April 2024). [Cited on page 2]

[8] C. Matos, A. Briga-Sá, S. Pereira, and A. Silva-Afonso, "Water and energy consumption in urban and rural households," in *Proceedings of the 39th International Symposium CIB W062 on Water Supply and Drainage for Buildings, Nagano, Japan*, pp. 17–20, 2013. Available online: https://www.researchgate.net/publication/263069488 (accessed on 13 April 2024). [Cited on page 2]

[9] H. Ritchie and M. Roser, "Land Use," *Our World in Data*, 2013. Available online: https://ourworldindata.org/land-use (accessed on 13 April 2024). [Cited on page 2]

[10] P. Baweja, S. Kumar, and G. Kumar, "Fertilizers and Pesticides: Their Impact on Soil Health and Environment," in *Soil Health* (B. Giri and A. Varma, eds.), Soil Biology, pp. 265–285, Cham: Springer International Publishing, 2020. Available online: https://doi.org/10.1007/978-3-030-44364-1_15 (accessed on 13 April 2024). [Cited on page 2]

[11] Food and Agriculture Organization of The United Nations, "Water Scarcity – One of the greatest challenges of our time," 2019. Available online: https://www.fao.org/newsroom/story/Water-Scarcity-One-of-the-greatest-challenges-of-our-time/en (accessed on 13 April 2024). [Cited on page 2]

[12] E. Melchiors and F. B. Freire, "Winery Wastewater Treatment: a Systematic Review of Traditional and Emerging Technologies and Their Efficiencies," *Environmental Processes*, vol. 10, p. 43, September 2023. Available online: https://www.doi.org/10.1007/s40710-023-00657-4 (accessed on 13 April 2024). [Cited on page 2]

[13] S. Ray and S. Majumder, *Water Management in Agriculture: Innovations for Efficient Irrigation*, pp. 169–185. International Books & Periodical Supply Service, July 2024. Available online: https://www.researchgate.net/publication/381867727 (accessed on 13 April 2024). [Cited on page 2]

[14] E. Bonamente, F. Scrucca, S. Rinaldi, M. C. Merico, F. Asdrubali, and L. Lamastra, "Environmental impact of an Italian wine bottle: Carbon and water footprint assessment," *Science of The Total Environment*, vol. 560-561, pp. 274–283, August 2016. Available online: https://www.doi.org/10.1016/j.scitotenv.2016.04.026 (accessed on 13 April 2024). [Cited on page 2]

[15] World Population Review, "Wine Producing Countries," 2024. Available online: https://worldpopulationreview.com/country-rankings/wine-producing-countries (accessed on 13 April 2024). [Cited on page 2]

[16] Governo da República Portuguesa, "Sucesso do setor vitivinícola contribui para «crescimento nacional»," 2020. Available online: https://www.portugal.gov.pt/pt/gc22/comunicacao/noticia?i=sucesso-do-setor-vitivinicola-contribui-para-crescimento-nacional (accessed on 13 April 2024). [Cited on page 3]

[17] University of Massachusetts Amherst, "Water Quality for Crop Production," April 2015. Available online: https://ag.umass.edu/greenhouse-floriculture/greenhouse-best-management-practices-bmp-manual/water-quality-for-crop (accessed on 13 April 2024). [Cited on page 3]

[18] E. Aivazidou and N. Tsolakis, "A Water Footprint Review of Italian Wine: Drivers, Barriers, and Practices for Sustainable Stewardship," *Water*, vol. 12, p. 369, February 2020. Available online: https://www.doi.org/10.3390/w12020369 (accessed on 13 April 2024). [Cited on page 3]

[19] E. Borsato, E. Giubilato, A. Zabeo, L. Lamastra, P. Criscione, P. Tarolli, F. Marinello, and L. Pizzol, "Comparison of Water-focused Life Cycle Assessment and Water Footprint Assessment: The case of an Italian wine," *Science of The Total Environment*, vol. 666, pp. 1220–1231, May 2019. Available online: https://www.doi.org/10.1016/j.scitotenv.2019.02.331 (accessed on 13 April 2024). [Cited on page 3]

[20] R. Branquinho, A. Briga-Sá, S. Ramos, C. Serôdio, and T. Pinto, "Sustainable irrigation systems in vineyards: A literature review on the contribution of renewable energy generation and intelligent resource management models," *Electronics*, vol. 13, no. 12, 2024. Available online: https://www.mdpi.com/2079-9292/13/12/2308 (accessed on 13 June 2024). [Cited on page 5]

[21] Food and Agriculture Organization of the United Nations, "Fao aquastat," 2024. Available online: https://data.apps.fao.org/aquastat/ (accessed on 13 April 2024). [Cited on pages vii, 5, 6, and 7]

[22] European Comission, "Eurostat," 2024. Available online: https://ec.europa.eu/eurostat (accessed on 13 April 2024). [Cited on pages vii, 5, 6, and 7]

[23] Elsevier B.V., "Scopus," 2024. Available online: https://www.scopus.com (accessed on 13 April 2024). [Cited on page 7]

[24] X. Dong, M. C. Vuran, and S. Irmak, "Autonomous precision agriculture through integration of wireless underground sensor networks with center pivot irrigation systems," *Ad Hoc Networks*, vol. 11, pp. 1975–1987, September

2013. Available online: https://doi.org/10.1016/j.adhoc.2012.06.012 (accessed on 13 April 2024). [Cited on page 8]

[25] Y. Kim, R. G. Evans, and W. M. Iversen, "Remote Sensing and Control of an Irrigation System Using a Distributed Wireless Sensor Network," *IEEE Transactions on Instrumentation and Measurement*, vol. 57, pp. 1379–1387, July 2008. Available online: https://doi.org/10.1109/TIM.2008.917198 (accessed on 13 April 2024). [Cited on page 9]

[26] M. M. Rahman, I. Khan, D. L. Field, K. Techato, and K. Alameh, "Powering agriculture: Present status, future potential, and challenges of renewable energy applications," *Renewable Energy*, vol. 188, pp. 731–749, 2022. Available online: https://doi.org/10.1016/j.renene.2022.02.065 (accessed on 13 April 2024). [Cited on pages vii, 9, and 12]

[27] T. Fellmann, P. Witzke, F. Weiss, B. Van Doorslaer, D. Drabik, I. Huck, G. Salputra, T. Jansson, and A. Leip, "Major challenges of integrating agriculture into climate change mitigation policy frameworks," *Mitigation and Adaptation Strategies for Global Change*, vol. 23, pp. 451–468, March 2018. Available online: https://doi.org/10.1007/s11027-017-9743-2 (accessed on 13 April 2024). [Cited on page 9]

[28] European Comission, "The European Green Deal," July 2021. Available online: https://commission.europa.eu/strategy-and-policy/priorities-2019-2024/european-green-deal_en (accessed on 13 April 2024). [Cited on page 9]

[29] LUT University, "New Study: Global Energy System based on 100% Renewable Energy," *Energy Watch Group*, April 2019. Available online: https://energywatchgroup.org/wp/en/2019/04/12/new-study-global-energy-system-based-100-renewable-energy/ (accessed on 13 April 2024). [Cited on page 9]

[30] N. K. M. A. Alrikabi, "Renewable Energy Types," *Journal of Clean Energy Technologies*, pp. 61–64, 2014. Available online: https://doi.org/10.7763/JOCET.2014.V2.92 (accessed on 13 April 2024). [Cited on page 10]

[31] Wines of Portugal, "Porto e Douro," 2022. Available online: https://www.winesofportugal.com/pt/descobrir/regioes-vitivinicolas/porto-e-douro/ (accessed on 13 April 2024). [Cited on page 10]

[32] Grape to Glass, "Flat vs Sloping Vineyards," 2022. Available online: https://grape-to-glass.com/index.php/flat-slope-vineyards/ (accessed on 13 April 2024). [Cited on page 10]

[33] N. García-Casarejos, P. Gargallo, and M. M. B. Cabanés, "A multi-level approach to analyze the effects of renewable energy in the wine sector," *Energy Procedia*, vol. 136, pp. 374–379, October 2017. Available online: `https://www.doi.org/10.1016/j.egypro.2017.10.264` (accessed on 13 April 2024). [Cited on page 10]

[34] J. L. Bernal-Agustín, R. Dufo-López, J. Carroquino-Oñate, J. S. Artal-Sevil, J. A. Domínguez-Navarro, A. A. Bayod-Rújula, and J. Yago-Loscos, "Profitable small-scale renewable energy systems in agrifood industry and rural areas: demonstration in the wine sector," *Renewable Energy and Power Quality Journal*, vol. 1, pp. 774–777, April 2017. Available online: `https://www.doi.org/10.24084/repqj15.461` (accessed on 13 April 2024). [Cited on page 10]

[35] Y. W. Wong and K. Sumathy, "Solar thermal water pumping systems: a review," *Renewable and Sustainable Energy Reviews*, vol. 3, pp. 185–217, June 1999. Available online: `https://doi.org/10.1016/S1364-0321(98)00018-5` (accessed on 13 April 2024). [Cited on page 10]

[36] M. Aliyu, G. Hassan, S. A. Said, M. U. Siddiqui, A. T. Alawami, and I. M. Elamin, "A review of solar-powered water pumping systems," *Renewable and Sustainable Energy Reviews*, vol. 87, pp. 61–76, May 2018. Available online: `https://doi.org/10.1016/j.rser.2018.02.010` (accessed on 13 April 2024). [Cited on pages vii, 10, and 11]

[37] M. A. Hossain, M. S. Hassan, M. A. Mottalib, and M. Hossain, "Feasibility of solar pump for sustainable irrigation in Bangladesh," *International Journal of Energy and Environmental Engineering*, vol. 6, pp. 147–155, June 2015. Available online: `https://doi.org/10.1007/s40095-015-0162-4` (accessed on 13 April 2024). [Cited on page 10]

[38] Z. Xu and X. Chen, "Optimization of the Coupling between Water and Energy Consumption in a Smart Integrated Photovoltaic Pumping Station System," *Water*, vol. 16, p. 1493, January 2024. Available online: `https://www.mdpi.com/2073-4441/16/11/1493` (accessed on 13 April 2024). [Cited on page 10]

[39] L. Pluschke, "Solar-Powered Irrigation Systems: A clean-energy, low-emission option for irrigation development and modernization," 2017. Available online: `https://www.fao.org/3/bt437e/bt437e.pdf` (accessed on 13 April 2024). [Cited on page 10]

[40] S. A. Vargas, G. R. T. Esteves, P. M. Maçaira, B. Q. Bastos, F. L. Cyrino Oliveira, and R. C. Souza, "Wind power generation: A review and a research agenda," *Journal of Cleaner Production*, vol. 218, pp. 850–870, May

2019. Available online: https://doi.org/10.1016/j.jclepro.2019.02.015 (accessed on 13 April 2024). [Cited on page 11]

[41] NetZero S.A.S, "NetZero - For climate and people, now," 2024. Available online: https://netzero.green/en/ (accessed on 13 April 2024). [Cited on page 11]

[42] Fonseca Porto, "Geography of the Douro Valley Vineyards," 2022. Available online: https://www.fonseca.pt/en/vineyards-and-douro/douro-valley/geography (accessed on 13 April 2024). [Cited on page 12]

[43] R. Morris, "Understanding Wind, an Underappreciated Part of Wine," May 2020. Available online: https://www.winemag.com/2020/05/14/wind-wine-vineyard/ (accessed on 13 April 2024). [Cited on page 12]

[44] T. Pinto, S. Ramos, T. M. Sousa, and Z. Vale, "Short-term wind speed forecasting using Support Vector Machines," in *2014 IEEE Symposium on Computational Intelligence in Dynamic and Uncertain Environments (CIDUE)*, pp. 40–46, December 2014. Available online: https://doi.org/10.1109/CIDUE.2014.7007865 (accessed on 13 April 2024). [Cited on page 12]

[45] M. Armand, P. Axmann, D. Bresser, M. Copley, K. Edström, C. Ekberg, D. Guyomard, B. Lestriez, P. Novák, M. Petranikova, W. Porcher, S. Trabesinger, M. Wohlfahrt-Mehrens, and H. Zhang, "Lithium-ion batteries – Current state of the art and anticipated developments," *Journal of Power Sources*, vol. 479, p. 228708, December 2020. Available online: https://doi.org/10.1016/j.jpowsour.2020.228708 (accessed on 13 April 2024). [Cited on page 12]

[46] J. C. Intriago Zambrano, J. Michavila, E. Arenas Pinilla, J. C. Diehl, and M. W. Ertsen, "Water Lifting Water: A Comprehensive Spatiotemporal Review on the Hydro-Powered Water Pumping Technologies," *Water*, vol. 11, p. 1677, August 2019. Available online: https://www.mdpi.com/2073-4441/11/8/1677 (accessed on 13 April 2024). [Cited on page 13]

[47] United States Geological Survey, "Evapotranspiration and the Water Cycle | U.S. Geological Survey," 2018. Available online: https://www.usgs.gov/special-topics/water-science-school/science/evapotranspiration-and-water-cycle (accessed on 13 April 2024). [Cited on page 13]

[48] Agricultura e Mar, "Principais métodos de rega utilizados na agricultura," January 2019. Available online: https://agriculturaemar.com/

principais-metodos-de-rega-utilizados-na-agricultura/ (accessed on 13 April 2024). [Cited on page 13]

[49] H. Jamal, "Surface Irrigation Methods - Advantages and Disadvantages," 2017. Available online: https://www.aboutcivil.org/surface-irrigation-methods.html (accessed on 13 April 2024). [Cited on pages vii and 13]

[50] OrnaW, "Irrigation Sprinklers Agriculture - Free photo on Pixabay," 2022. Available online: https://pixabay.com/photos/irrigation-sprinklers-agriculture-6986021/ (accessed on 13 April 2024). [Cited on pages vii and 14]

[51] Breanna, "Increase Yield Performance with Subsurface Drip Irrigation," July 2020. Available online: https://southernirrigation.com/2020/07/27/increase-yield-performance-with-subsurface-drip-irrigation/ (accessed on 13 April 2024). [Cited on pages vii and 15]

[52] J. Hernandez, "Best Practices for Drip Irrigation System Management in Vineyards," 2019. Available online: https://www.vineyardteam.org/files/resources/4.%20LIT_REVIEW_BMPS_for_Vineyard_Drip_Irrigation_Systems.pdf (accessed on 13 April 2024). [Cited on page 15]

[53] Y. Wang, S. Li, Y. Cui, S. Qin, H. Guo, D. Yang, and C. Wang, "Effect of Drip Irrigation on Soil Water Balance and Water Use Efficiency of Maize in Northwest China," *Water*, vol. 13, p. 217, January 2021. Available online: https://www.mdpi.com/2073-4441/13/2/217 (accessed on 13 April 2024). [Cited on page 15]

[54] J. Carroquino, R. Dufo-López, and J. L. Bernal-Agustín, "Sizing of off-grid renewable energy systems for drip irrigation in Mediterranean crops," *Renewable Energy*, vol. 76, pp. 566–574, April 2015. Available online: https://www.doi.org/10.1016/j.renene.2014.11.069 (accessed on 13 April 2024). [Cited on page 15]

[55] V. Phogat, J. Cox, D. Mallants, P. Petrie, D. Oliver, and T. Pitt, "Historical and future trends in evapotranspiration components and irrigation requirement of winegrapes," *Australian Journal of Grape and Wine Research*, vol. 26, no. 4, pp. 312–324, 2020. Available online: https://doi.org/10.1111/ajgw.12446 (accessed on 13 April 2024). [Cited on page 16]

[56] M. A. Youssef, R. T. Peters, M. El-Shirbeny, A. M. Abd-ElGawad, Y. M. Rashad, M. Hafez, and Y. Arafa, "Enhancing irrigation water management based on ETo prediction using machine learning to mitigate climate change,"

*Cogent Food & Agriculture*, vol. 10, p. 2348697, December 2024. Available online: https://doi.org/10.1080/23311932.2024.2348697 (accessed on 13 April 2024). [Cited on page 16]

[57] V. Sadras, P. Petrie, and M. Moran, "Effects of elevated temperature in grapevine. II juice pH, titratable acidity and wine sensory attributes," *Australian Journal of Grape and Wine Research*, vol. 19, no. 1, pp. 107–115, 2013. Available online: https://doi.org/10.1111/ajgw.12001 (accessed on 13 April 2024). [Cited on page 16]

[58] T. Kizildeniz, I. Juan José, I. Pascual, and F. Morales, "Simulating the impact of climate change (elevated CO 2 and temperature, and water deficit) on the growth of red and white Tempranillo grapevine in three consecutive growing seasons (2013–2015)," *Agricultural Water Management*, vol. 202, February 2018. Available online: https://doi.org/10.1016/j.agwat.2018.02.006 (accessed on 13 April 2024). [Cited on page 16]

[59] L. Lamastra, N. A. Suciu, E. Novelli, and M. Trevisan, "A new approach to assessing the water footprint of wine: An Italian case study," *Science of The Total Environment*, vol. 490, pp. 748–756, August 2014. Available online: https://www.doi.org/10.1016/j.scitotenv.2014.05.0631 (accessed on 13 April 2024). [Cited on page 16]

[60] F. J. Villalobos, L. Testi, and E. Fereres, "Calculation of Evapotranspiration and Crop Water Requirements," in *Principles of Agronomy for Sustainable Agriculture* (F. J. Villalobos and E. Fereres, eds.), pp. 119–137, Cham: Springer International Publishing, 2016. Available online: https://doi.org/10.1007/978-3-319-46116-8_10 (accessed on 13 April 2024). [Cited on page 16]

[61] Allen, R.G.; Pereira, L.S.; Raes, D.; Smith, M., *Crop Evapotranspiration-Guidelines for Computing Crop Water Requirements-FAO Irrigation and Drainage Paper 56*, vol. 56. January 1998. Available online: https://www.fao.org/3/x0490e/x0490e00.htm (accessed on 13 April 2024). [Cited on pages 16, 36, 38, and 39]

[62] R. D. Rosa, P. Paredes, G. C. Rodrigues, I. Alves, R. M. Fernando, L. S. Pereira, and R. G. Allen, "Implementing the dual crop coefficient approach in interactive software. 1. Background and computational strategy," *Agricultural Water Management*, vol. 103, pp. 8–24, January 2012. Available online: https://doi.org/10.1016/j.agwat.2011.10.013 (accessed on 13 April 2024). [Cited on page 17]

[63] R. G. Allen, L. S. Pereira, M. Smith, D. Raes, and J. L. Wright, "*FAO-56* Dual Crop Coefficient Method for Estimating Evaporation from Soil and Application Extensions," *Journal of Irrigation and Drainage Engineering*, vol. 131, pp. 2–13, February 2005. Available online: `https://doi.org/10.1061/(ASCE)0733-9437(2005)131:1(2)` (accessed on 13 April 2024). [Cited on page 17]

[64] H. Ojeda and N. Saurin, "L'irrigation de précision de la vigne : méthodes, outils et stratégies pour maximiser la qualité et les rendements de la vendange en économisant de l'eau," *Innovations Agronomiques*, vol. 38, p. 97, 2014. Available online: `https://www.doi.org/10.17180/n4p2-pr93` (accessed on 13 April 2024). [Cited on page 18]

[65] A. Glória, C. Dionísio, G. Simões, J. Cardoso, and P. Sebastião, "Water Management for Sustainable Irrigation Systems Using Internet-of-Things," *Sensors (Basel, Switzerland)*, vol. 20, p. 1402, March 2020. Available online: `https://doi.org/10.3390/s20051402` (accessed on 13 April 2024). [Cited on page 18]

[66] National Association of Landscape Professionals, "Shopping for a Smart Irrigation System?," 2019. Available online: `https://www.loveyourlandscape.org/expert-advice/water-smart-landscaping/smart-irrigation/shopping-for-a-smart-irrigation-system/` (accessed on 13 April 2024). [Cited on page 18]

[67] Hydro Point, "What Is Smart Irrigation?," 2020. Available online: `https://www.hydropoint.com/what-is-smart-irrigation/` (accessed on 13 April 2024). [Cited on page 18]

[68] L. Buchen, "3 Types of Soil Moisture Sensors - Which is Best For You?," 2022. Available online: `https://mytrellis.com/blog/smstypes` (accessed on 13 April 2024). [Cited on page 19]

[69] J. C. Songara and J. N. Patel, "Calibration and comparison of various sensors for soil moisture measurement," *Measurement*, vol. 197, p. 111301, June 2022. Available online: `https://doi.org/10.1016/j.measurement.2022.111301` (accessed on 13 April 2024). [Cited on page 19]

[70] B. Li, C. Wang, X. Gu, X. Zhou, M. Ma, L. Li, Z. Feng, T. Ding, X. Li, T. Jiang, X. Li, and X. Zheng, "Accuracy calibration and evaluation of capacitance-based soil moisture sensors for a variety of soil properties," *Agricultural Water Management*, vol. 273, p. 107913, November 2022. Available online: `https://doi.org/10.1016/j.agwat.2022.107913` (accessed on 13 April 2024). [Cited on page 19]

[71] C. Briciu-Burghina, J. Zhou, M. I. Ali, and F. Regan, "Demonstrating the Potential of a Low-Cost Soil Moisture Sensor Network," *Sensors*, vol. 22, p. 987, January 2022. Available online: https://www.mdpi.com/1424-8220/22/3/987 (accessed on 13 April 2024). [Cited on page 20]

[72] A. G. N. Bandara, B. M. A. N. Balasooriya, H. G. I. W. Bandara, K. S. Buddhasiri, M. A. V. J. Muthugala, A. G. B. P. Jayasekara, and D. P. Chandima, "Smart irrigation controlling system for green roofs based on predicted evapotranspiration," in *2016 Electrical Engineering Conference (EECon)*, pp. 31–36, December 2016. Available online: https://doi.org/10.1109/EECon.2016.7830931 (accessed on 13 April 2024). [Cited on page 20]

[73] M. D. Cahn, L. F. Johnson, and S. D. Benzen, "Evapotranspiration Based Irrigation Trials Examine Water Requirement, Nitrogen Use, and Yield of Romaine Lettuce in the Salinas Valley," *Horticulturae*, vol. 8, p. 857, October 2022. Available online: https://www.mdpi.com/2311-7524/8/10/857 (accessed on 13 April 2024). [Cited on page 20]

[74] V. Sharma, "Evapotranspiration-based irrigation scheduling or water-balance method," 2023. Available online: https://extension.umn.edu/irrigation/evapotranspiration-based-irrigation-scheduling-or-water-balance-method (accessed on 13 April 2024). [Cited on page 20]

[75] GardenSoft, "Weather Based and Smart Irrigation Controllers," 2019. Available online: https://www.ladwp.cafriendlylandscaping.com/Garden-Resources/SmartControllers.php (accessed on 13 April 2024). [Cited on page 20]

[76] M. Gotcher, S. Taghvaeian, and J. Q. Moss, "Smart Irrigation Technology: Controllers and Sensors - Oklahoma State University," January 2017. Available online: https://extension.okstate.edu/fact-sheets/smart-irrigation-technology-controllers-and-sensors.html (accessed on 13 April 2024). [Cited on page 21]

[77] O. Abrishambaf, P. Faria, Z. Vale, and J. M. Corchado, "Energy Scheduling Using Decision Trees and Emulation: Agriculture Irrigation with Run-of-the-River Hydroelectricity and a PV Case Study," *Energies*, vol. 12, p. 3987, January 2019. Available online: https://www.mdpi.com/1996-1073/12/20/3987 (accessed on 13 April 2024). [Cited on page 21]

[78] M. Amayri and S. Ploix, *Decision tree and Parametrized classifier for Estimating occupancy in energy management.* 2018. Available online: https://www.doi.org/10.1109/CoDIT.2018.8394848 (accessed on 13 April 2024). [Cited on page 21]

[79] O. Abrishambaf, P. Faria, L. Gomes, and Z. Vale, "Agricultural irrigation scheduling for a crop management system considering water and energy use optimization," *Energy Reports*, vol. 6, pp. 133–139, February 2020. Available online: `https://www.doi.org/10.1016/j.egyr.2019.08.031` (accessed on 13 April 2024). [Cited on page 21]

[80] J. Boobalan, V. Jacintha, J. Nagarajan, K. Thangayogesh, and S. Tamilarasu, *An IOT Based Agriculture Monitoring System*. 2018. Available online: `https://www.doi.org/10.1109/ICCSP.2018.8524490` (accessed on 13 April 2024). [Cited on page 21]

[81] O. Rahman, M. N. Islam, M. Z. Haque, and J. Islam, *Design and Implementation of a Smart Irrigation System*. Thesis, Sonargaon University (SU), August 2022. Available online: `http://suspace.su.edu.bd/handle/123456789/289` (accessed on 13 April 2024). [Cited on page 21]

[82] B. Cardenas, M. Dukes, and G. Miller, "Sensor-based automation of irrigation on bermudagrass during dry weather conditions," *Journal of Irrigation and Drainage Engineering-asce - J IRRIG DRAIN ENG-ASCE*, vol. 136, 03 2010. Available online: `https://www.doi.org/10.1061/(ASCE)IR.1943-4774.0000153` (accessed on 13 April 2024). [Cited on page 21]

[83] M. S. Munir, I. S. Bajwa, M. A. Naeem, and B. Ramzan, "Design and Implementation of an IoT System for Smart Energy Consumption and Smart Irrigation in Tunnel Farming," *Energies*, vol. 11, p. 3427, December 2018. Available online: `https://www.mdpi.com/1996-1073/11/12/3427` (accessed on 13 April 2024). [Cited on page 21]

[84] J. Carroquino, V. Roda, R. Mustata, J. Yago, L. Valiño, A. Lozano, and F. Barreras, "Combined production of electricity and hydrogen from solar energy and its use in the wine sector," *Renewable Energy*, vol. 122, pp. 251–263, July 2018. Available online: `https://www.doi.org/10.1016/j.renene.2018.01.106` (accessed on 13 April 2024). [Cited on page 21]

[85] J. Carroquino, N. García-Casarejos, P. Gargallo, F.-J. García-Ramos, and J. Yago, "Renewable energy and hydrogen on-site generation for irrigation and mobility in vineyards," *BIO Web of Conferences*, vol. 9, p. 01005, 2017. Available online: `https://www.doi.org/10.1051/bioconf/20170901005` (accessed on 13 April 2024). [Cited on page 22]

[86] J. D. F. Selvaraj, P. M. Paul, and I. D. J. Jingle, "Automatic Wireless Water Management System (AWWMS) for Smart Vineyard Irrigation using IoT Technology," 2019. Available online: `http://www.ripublication.com/`

ijoo19/ijoov13n1_17.pdf (accessed on 13 April 2024). [Cited on pages vii and 22]

[87] Jupyter, "Project Jupyter," 2024. Available online: https://jupyter.org (accessed on 13 April 2024). [Cited on page 25]

[88] Phyton Software Foundation, "Phyton," 2024. Available online: https://www.python.org/ (accessed on 13 April 2024). [Cited on page 25]

[89] Weather API, "JSON and XML Weather API and Geolocation Developer API," 2024. Available online: https://www.weatherapi.com/ (accessed on 13 April 2024). [Cited on page 26]

[90] Open-Meteo, "Ensemble API," 2024. Available online: https://open-meteo.com/en/docs/ensemble-api (accessed on 13 April 2024). [Cited on page 26]

[91] S. Vashishtha, "Differentiate between the DNI, DHI and GHI?," 2012. Available online: https://firstgreenconsulting.wordpress.com/2012/04/26/differentiate-between-the-dni-dhi-and-ghi/ (accessed on 13 April 2024). [Cited on page 27]

[92] Canadian Solar, "CS6X-300M (300W) Solar Panel Specification Data Sheet," 2019. Available online: http://www.solardesigntool.com/components/module-panel-solar/Canadian-Solar/3847/CS6X-300M/specification-data-sheet.html (accessed on 13 April 2024). [Cited on pages ix, 27, and 28]

[93] W. F. Holmgren, C. W. Hansen, and M. A. Mikofski, "PVLib Python: a python package for modeling solar energy systems," *Journal of Open Source Software*, vol. 3, p. 884, September 2018. Available online: https://www.doi.org/10.21105/joss.00884 (accessed on 13 April 2024). [Cited on page 30]

[94] Ryse Energy, "E-5 HAWT Small Wind Turbine," 2024. Available online: https://www.ryse.energy/5kw-wind-turbines/ (accessed on 13 April 2024). [Cited on pages vii, ix, 31, and 33]

[95] J. G. Alfieri, W. P. Kustas, H. Nieto, J. H. Prueger, L. E. Hipps, L. G. McKee, F. Gao, and S. Los, "Influence of wind direction on the surface roughness of vineyards," *Irrigation Science*, vol. 37, pp. 359–373, May 2019. Available online: https://doi.org/10.1007/s00271-018-0610-z (accessed on 13 April 2024). [Cited on page 32]

[96] OMI, Polo Español S.A., "OMIE," 2024. Available online: https://www.omie.es/pt (accessed on 13 April 2024). [Cited on page 34]

[97] ERSE - Entidade Reguladora dos Serviços Energéticos, "Tarifas e Preços Regulados," 2024. Available online: https://www.erse.pt/atividade/regulacao/tarifas-e-precos-eletricidade/ (accessed on 10 August 2024). [Cited on page 35]

[98] MEO Energia, "Tarifa Variável - Fórmula de cálculo do preço da energia," 2024. Available online: https://conteudos.meo.pt/meoenergia/Documentos/formula-calculo-preco-tarifa-variavel-meo-energia.pdf (accessed on 13 September 2024). [Cited on page 35]

[99] M. Moyer and L. Mills, "Grapevine Crop Coefficient (Kc)," *Washington State University Viticulture and Enology Program*, 2017. Available online: https://s3-us-west-2.amazonaws.com/sites.cahnrs.wsu.edu/wp-content/uploads/sites/66/2017/07/CropCoefficient-2017.pdf (accessed on 13 April 2024). [Cited on pages vii, 42, and 43]

[100] Z. Curtis, "Understanding Growing Degree Days," 2023. Available online: https://extension.psu.edu/understanding-growing-degree-days (accessed on 13 April 2024). [Cited on page 42]

[101] G. Jones, "Climate Assessement for the Douro Wine Region - An Examination for the Past, Present and Future Conditions for Wine Production," 2012. Available online: https://www.advid.pt/en/climate-evaluation-in-the-douro-region (accessed on 13 April 2024). [Cited on page 42]

[102] BC Wine, "Growing Degree Days (GDD) Calculator," 2020. Available online: https://www.bc-winery.com/calculators/Growing-Degree-Days.php (accessed on 13 April 2024). [Cited on page 43]

[103] T. Prichard, "Winegrape Irrigation Scheduling Using Deficit Irrigation Techniques," 2021. Available online: https://cesanjoaquin.ucanr.edu/files/35706.pdf (accessed on 13 April 2024). [Cited on page 44]

[104] C. Brouwer and M. Heibloem, *Irrigation Water Management: Training Manual No. 3: Irrigation water needs*. Rome, Italy: FAO, 1985. Available online: http://hdl.handle.net/10919/67227 (accessed on 13 April 2024). [Cited on page 44]

[105] E. Vinagre, T. Pinto, S. Ramos, Z. Vale, and J. M. Corchado, "Electrical Energy Consumption Forecast Using Support Vector Machines," in *2016 27th International Workshop on Database and Expert Systems Applications (DEXA)*, pp. 171–175, September 2016. Available online: https://doi.org/10.1109/DEXA.2016.046 (accessed on 13 April 2024). [Cited on page 46]

[106] M. Cordeiro-Costas, D. Villanueva, P. Eguía-Oller, M. Martínez-Comesaña, and S. Ramos, "Load Forecasting with Machine Learning and Deep Learning Methods," *Applied Sciences*, vol. 13, p. 7933, January 2023. Available online: https://doi.org/10.3390/app13137933 (accessed on 13 April 2024). [Cited on page 46]

[107] S. Suthaharan, *Decision Tree Learning*, pp. 237–269. Boston, MA: Springer US, 2016. Available online: https://doi.org/10.1007/978-1-4899-7641-3_10 (accessed on 13 April 2024). [Cited on page 48]

[108] T. Pinto, I. Praça, Z. Vale, and J. Silva, "Ensemble learning for electricity consumption forecasting in office buildings," *Neurocomputing*, vol. 423, pp. 747–755, January 2021. Available online: 10.1016/j.neucom.2020.02.124 (accessed on 13 April 2024). [Cited on page 48]

[109] E. Helmud, F. Fitriyani, and P. Romadiana, "Classification comparison performance of supervised machine learning random forest and decision tree algorithms using confusion matrix," *Jurnal Sisfokom*, vol. 13, no. 1, p. 92–97, 2024. Available online: https://doi.org/10.32736/sisfokom.v13i1.1985 (accessed on 13 April 2024). [Cited on page 48]

[110] Q. Xiaokun and H. Tian, "Analysis and Prediction of Energy Consumption in Neural Networks Based on Machine Learning," *Academic Journal of Computing & Information Science*, vol. 7, no. 4, 2024. Available online: https://doi.org/10.25236/AJCIS.2024.070412 (accessed on 13 April 2024). [Cited on page 48]

[111] F. Pedregosa, G. Varoquaux, A. Gramfort, V. Michel, B. Thirion, O. Grisel, M. Blondel, P. Prettenhofer, R. Weiss, V. Dubourg, J. Vanderplas, A. Passos, D. Cournapeau, M. Brucher, M. Perrot, and E. Duchesnay, "Scikit-learn: Machine learning in Python," *Journal of Machine Learning Research*, vol. 12, pp. 2825–2830, 2011. Available online: https://scikit-learn.org/stable/ (accessed on 13 April 2024). [Cited on page 49]

[112] C. Roussey, X. Delpuech, F. Amardeilh, S. Bernard, and C. Jonquet, "Semantic description of plant phenological development stages, starting with grapevine," in *Metadata and Semantic Research*, pp. 257–268, Springer International Publishing, 2021. Available online: https://doi.org/10.1007/978-3-030-71903-6_25 (accessed on 13 April 2024). [Cited on page 63]

# Appendix A

# System Log File

The following listing displays the log file of the resource management system implemented and discussed in the previous chapters. This log contains information regarding the timestamps and the sequence of operations executed. In addition, some results are also displayed, regarding the multiple outputs of the system.

```
1  [2024-08-13 03:51:59.005136] WeatherAPI history request for
       2024-08-12 successfully fetched.
2  [2024-08-13 03:51:59.111757] WeatherAPI history request for
       2024-08-11 successfully fetched.
3  [2024-08-13 03:51:59.236589] WeatherAPI history request for
       2024-08-10 successfully fetched.
4  [2024-08-13 03:51:59.348839] WeatherAPI history request for
       2024-08-09 successfully fetched.
5  [2024-08-13 03:51:59.474934] WeatherAPI history request for
       2024-08-08 successfully fetched.
6  [2024-08-13 03:51:59.596181] WeatherAPI history request for
       2024-08-07 successfully fetched.
7  [2024-08-13 03:51:59.712617] WeatherAPI history request for
       2024-08-06 successfully fetched.
8  [2024-08-13 03:51:59.723682] Data has been successfully processed.
9  [2024-08-13 03:51:59.733659] EnsembleAPI history request for the
       past 7 days successfully fetched.
10 [2024-08-13 03:51:59.739224] Data has been successfully processed.
11 [2024-08-13 03:51:59.860289] WeatherAPI forecast request for
       current and following day successfully fetched.
```

```
12 [2024-08-13 03:51:59.867378] Data has been successfully processed.
13 [2024-08-13 03:51:59.878194] EnsembleAPI forecast request for
       current and following day successfully fetched.
14 [2024-08-13 03:51:59.882556] Data has been successfully processed.
15 [2024-08-13 03:52:03.622016] IPMA API evapotranspiration request
       successfully fetched.
16 [2024-08-13 03:52:03.679006] Data has been successfully processed.
17 [2024-08-13 03:52:03.864800] Estimating hourly photovoltaic energy
        production using history and forecast weather.
18 [2024-08-13 03:52:03.867401] Hourly photovoltaic energy production
        has been successfully estimated, with Method A.
19 /> Total Estimated Photovoltaic Energy Production for 06/08/2024:
       7.11 kWh
20 /> Total Estimated Photovoltaic Energy Production for 07/08/2024:
       7.08 kWh
21 /> Total Estimated Photovoltaic Energy Production for 08/08/2024:
       7.17 kWh
22 /> Total Estimated Photovoltaic Energy Production for 09/08/2024:
       6.90 kWh
23 /> Total Estimated Photovoltaic Energy Production for 10/08/2024:
       6.37 kWh
24 /> Total Estimated Photovoltaic Energy Production for 11/08/2024:
       7.07 kWh
25 /> Total Estimated Photovoltaic Energy Production for 12/08/2024:
       7.04 kWh
26 /> Total Estimated Photovoltaic Energy Production for 13/08/2024:
       5.33 kWh
27 /> Total Estimated Photovoltaic Energy Production for 14/08/2024:
       7.14 kWh
28 [2024-08-13 03:52:04.331978] Estimating hourly photovoltaic energy
        production using history and forecast weather.
29 [2024-08-13 03:52:04.385460] Hourly photovoltaic energy production
        has been successfully estimated, with Method B.
30 Total Estimated Photovoltaic Energy Production for 06/08/2024:
       6.72 kWh
31 Total Estimated Photovoltaic Energy Production for 07/08/2024:
       6.59 kWh
32 Total Estimated Photovoltaic Energy Production for 08/08/2024:
       6.80 kWh
33 Total Estimated Photovoltaic Energy Production for 09/08/2024:
       6.50 kWh
34 Total Estimated Photovoltaic Energy Production for 10/08/2024:
       5.99 kWh
35 Total Estimated Photovoltaic Energy Production for 11/08/2024:
       6.89 kWh
36 Total Estimated Photovoltaic Energy Production for 12/08/2024:
       6.94 kWh
37 Total Estimated Photovoltaic Energy Production for 13/08/2024:
       5.48 kWh
```

```
38 Total Estimated Photovoltaic Energy Production for 14/08/2024:
       6.93 kWh
39 [2024-08-13 03:52:04.849807] Estimating hourly wind energy
       production using history and forecast weather.
40 [2024-08-13 03:52:04.852227] Hourly wind energy production has
       been successfully estimated, with Method A.
41 /> Total Estimated Wind Energy Production for 06/08/2024: 5.68 kWh
42 /> Total Estimated Wind Energy Production for 07/08/2024: 2.25 kWh
43 /> Total Estimated Wind Energy Production for 08/08/2024: 4.77 kWh
44 /> Total Estimated Wind Energy Production for 09/08/2024: 1.67 kWh
45 /> Total Estimated Wind Energy Production for 10/08/2024: 3.87 kWh
46 /> Total Estimated Wind Energy Production for 11/08/2024: 7.03 kWh
47 /> Total Estimated Wind Energy Production for 12/08/2024: 8.74 kWh
48 /> Total Estimated Wind Energy Production for 13/08/2024: 9.41 kWh
49 /> Total Estimated Wind Energy Production for 14/08/2024: 1.28 kWh
50 [2024-08-13 03:52:05.315685] Estimating hourly wind energy
       production using history and forecast weather.
51 [2024-08-13 03:52:05.327475] Hourly wind energy production has
       been successfully estimated, with Method B.
52 /> Total Estimated Wind Energy Production for 06/08/2024: 7.04 kWh
53 /> Total Estimated Wind Energy Production for 07/08/2024: 2.53 kWh
54 /> Total Estimated Wind Energy Production for 08/08/2024: 5.85 kWh
55 /> Total Estimated Wind Energy Production for 09/08/2024: 1.74 kWh
56 /> Total Estimated Wind Energy Production for 10/08/2024: 4.57 kWh
57 /> Total Estimated Wind Energy Production for 11/08/2024: 8.79 kWh
58 /> Total Estimated Wind Energy Production for 12/08/2024: 10.61
       kWh
59 /> Total Estimated Wind Energy Production for 13/08/2024: 11.14
       kWh
60 /> Total Estimated Wind Energy Production for 14/08/2024: 1.23 kWh
61 [2024-08-13 03:52:06.470544] Local file not found for day
       20240814. Attempting to download.
62 [2024-08-13 03:52:11.015755] File for day 20240814 downloaded.
       Respective data has been successfully fetched.
63 [2024-08-13 03:52:11.018092] Local file not found for day
       20240813. Attempting to download.
64 [2024-08-13 03:52:15.275363] File for day 20240813 downloaded.
       Respective data has been successfully fetched.
65 [2024-08-13 03:52:15.277551] Local file not found for day
       20240812. Attempting to download.
66 [2024-08-13 03:52:19.757993] File for day 20240812 downloaded.
       Respective data has been successfully fetched.
67 [2024-08-13 03:52:19.760370] Local file not found for day
       20240811. Attempting to download.
68 [2024-08-13 03:52:24.282416] File for day 20240811 downloaded.
       Respective data has been successfully fetched.
69 [2024-08-13 03:52:24.284644] Local file found for day 20240810.
       Respective data has been successfully fetched.
```

```
70 [2024-08-13 03:52:24.286059] Local file found for day 20240809.
       Respective data has been successfully fetched.
71 [2024-08-13 03:52:24.287386] Local file found for day 20240808.
       Respective data has been successfully fetched.
72 [2024-08-13 03:52:24.288691] Local file found for day 20240807.
       Respective data has been successfully fetched.
73 [2024-08-13 03:52:24.290044] Local file found for day 20240806.
       Respective data has been successfully fetched.
74 [2024-08-13 03:52:24.298404] OMIE data has been successfully
       processed.
75 [2024-08-13 03:52:24.653181] Estimating grid energy sell price.
76 [2024-08-13 03:52:24.814462] Grid energy sell price has been
       successfully estimated.
77 [2024-08-13 03:52:29.808173] Estimating daily reference
       evapotranspiration and total precipitation for 06/08/2024.
78 [2024-08-13 03:52:29.809631] Estimating daily reference
       evapotranspiration and total precipitation for 07/08/2024.
79 [2024-08-13 03:52:29.810852] Estimating daily reference
       evapotranspiration and total precipitation for 08/08/2024.
80 [2024-08-13 03:52:29.811808] Estimating daily reference
       evapotranspiration and total precipitation for 09/08/2024.
81 [2024-08-13 03:52:29.812637] Estimating daily reference
       evapotranspiration and total precipitation for 10/08/2024.
82 [2024-08-13 03:52:29.813562] Estimating daily reference
       evapotranspiration and total precipitation for 11/08/2024.
83 [2024-08-13 03:52:29.814372] Estimating daily reference
       evapotranspiration and total precipitation for 12/08/2024.
84 [2024-08-13 03:52:29.815185] Estimating daily reference
       evapotranspiration and total precipitation for 13/08/2024.
85 [2024-08-13 03:52:29.816020] Estimating daily reference
       evapotranspiration and total precipitation for 14/08/2024.
86 [2024-08-13 03:52:29.818260] Daily reference evapotranspiration
       have been successfully estimated.
87 /> Estimated Reference Evapotranspiration and Total Precipitation
       for 06/08/2024: 5.75 / 0.00 (mm/day)
88 /> Estimated Reference Evapotranspiration and Total Precipitation
       for 07/08/2024: 5.89 / 0.00 (mm/day)
89 /> Estimated Reference Evapotranspiration and Total Precipitation
       for 08/08/2024: 6.23 / 0.00 (mm/day)
90 /> Estimated Reference Evapotranspiration and Total Precipitation
       for 09/08/2024: 6.22 / 0.00 (mm/day)
91 /> Estimated Reference Evapotranspiration and Total Precipitation
       for 10/08/2024: 6.04 / 0.00 (mm/day)
92 /> Estimated Reference Evapotranspiration and Total Precipitation
       for 11/08/2024: 6.12 / 0.00 (mm/day)
93 /> Estimated Reference Evapotranspiration and Total Precipitation
       for 12/08/2024: 5.78 / 0.00 (mm/day)
94 /> Estimated Reference Evapotranspiration and Total Precipitation
       for 13/08/2024: 4.22 / 0.55 (mm/day)
```

```
95 /> Estimated Reference Evapotranspiration and Total Precipitation
       for 14/08/2024: 5.73 / 0.00 (mm/day)
96 [2024-08-13 03:52:33.932350] WeatherAPI history request for
       2024-08-12 successfully fetched.
97 [2024-08-13 03:52:43.370664] WeatherAPI history request for days
       between successfully fetched.
98 [2024-08-13 03:52:54.157956] WeatherAPI history request for
       2024-04-01 successfully fetched.
99 [2024-08-13 03:52:54.168811] Data has been successfully processed.
100 [2024-08-13 03:52:54.292978] WeatherAPI forecast request for
       current and following day successfully fetched.
101 [2024-08-13 03:52:54.296154] Data has been successfully processed.
102 [2024-08-13 03:52:54.301889] Estimating Growing Degree Days (GDD)
       with provided data.
103 [2024-08-13 03:52:54.303729] Growing Degree Days (GDD) have been
       successfully estimated.
104 /> Estimated Growing Degree Days for 13/08/2024: 11.60 GDD, which
       results in Accumulated 1195.00 GDD.
105 /> Estimated Growing Degree Days for 14/08/2024: 13.60 GDD, which
       results in Accumulated 1208.60 GDD.
106 [2024-08-13 03:52:54.143721] Estimating Crop Coefficient (Kc) with
        GDD relation.
107 [2024-08-13 03:52:54.867208] Crop Coefficient (Kc) has been
       successfully estimated.
108 /> Estimated Crop Coefficient for 13/08/2024: 0.51
109 /> Estimated Crop Coefficient for 14/08/2024: 0.48
110 [2024-08-13 03:53:08.150263] Estimating irrigation requirements
       with provided data.
111 [2024-08-13 03:53:08.159958] Irrigation requirements have been
       successfully estimated.
112 /> Irrigation Requirements for 06/08/2024: GIR is 4.88 mm/day or
       48841.91 l/ha/day, equivalent to 10.75 liters per grapevine (
       for Rs = 2, Vs = 1.1)
113 /> Irrigation Requirements for 07/08/2024: GIR is 4.76 mm/day or
       47581.48 l/ha/day, equivalent to 10.47 liters per grapevine (
       for Rs = 2, Vs = 1.1)
114 /> Irrigation Requirements for 08/08/2024: GIR is 4.85 mm/day or
       48453.37 l/ha/day, equivalent to 10.66 liters per grapevine (
       for Rs = 2, Vs = 1.1)
115 /> Irrigation Requirements for 09/08/2024: GIR is 4.65 mm/day or
       46454.03 l/ha/day, equivalent to 10.22 liters per grapevine (
       for Rs = 2, Vs = 1.1)
116 /> Irrigation Requirements for 10/08/2024: GIR is 4.17 mm/day or
       41686.00 l/ha/day, equivalent to 9.17 liters per grapevine (for
        Rs = 2, Vs = 1.1)
117 /> Irrigation Requirements for 11/08/2024: GIR is 3.99 mm/day or
       39884.56 l/ha/day, equivalent to 8.77 liters per grapevine (for
        Rs = 2, Vs = 1.1)
```

```
118 /> Irrigation Requirements for 12/08/2024: GIR is 3.57 mm/day or
        35710.95 l/ha/day, equivalent to 7.86 liters per grapevine (for
         Rs = 2, Vs = 1.1)
119 /> Irrigation Requirements for 13/08/2024: GIR is 2.07 mm/day or
        20738.93 l/ha/day, equivalent to 4.56 liters per grapevine (for
         Rs = 2, Vs = 1.1)
120 /> Irrigation Requirements for 14/08/2024: GIR is 3.21 mm/day or
        32127.74 l/ha/day, equivalent to 7.07 liters per grapevine (for
         Rs = 2, Vs = 1.1)
121 [2024-08-13 03:53:37.774695] Estimating optimal energy consumption
         timings with provided data.
122 [2024-08-13 03:53:37.868622] Optimal energy consumption timings
        have been successfully estimated.
```